



Fakultät für Mathematik  
Lehrstuhl für Mathematische Optimierung

# Stochastic Programming for Charging Stations Allocation Including Electricity Grid Constraints

Master's Thesis by Gen Li

Examiner: Prof. Dr. Michael Ulbrich

Advisor: Dr. Ing. Dominik Husarek

Submission Date: January 16, 2023



I hereby confirm that this is my own work, and that I used only the cited sources and materials.

München, January 16, 2023

---

Gen Li



## **Abstract**

The roll-out of charging infrastructures must sustain the rapid growth of electric vehicle markets to help decarbonize transport and eliminate the dependency on fossil fuels. Proactively considering grid connections before allocating charging infrastructures is critical since the already expensive cost of allocations depends on the locations selected and the local energy supply. This thesis proposes a multi-period two-stage stochastic mixed-integer optimization framework to assist the strategic decisions on the allocation planning of electric vehicle charging stations under imperfect grid information. The objective is to maximize the profit earned by satisfying the charging demand of electric vehicles while minimizing the expected cost of grid congestion due to uncertain grid connections between charging stations and substations. Correspondingly, a novel scenario generation algorithm is developed for sampling possible grid connection scenarios. This sampling algorithm considers the probability of grid connections being established between charging stations and secondary substations based on the distance between objects and the neighborhood grid connection status of charging stations. Furthermore, this study suggests a node-based approach to accurately represent the actual charging energy capacities of charging stations, which addresses the influences of (long) parking time, arrival frequency, and arrival state of charge of electric vehicles on the capacity representation. A case study is conducted in the German municipality Schutterwald with the optimization model implemented in the `Python` optimization modeling language `Pyomo`. Scenario-based Sample Average Approximation method is applied to solve the model with the commercial solver `CPLEX`.

## **Zusammenfassung**

Die Einführung von Ladeinfrastrukturen soll mit dem raschen Wachstum des E-Fahrzeugmarkts Schritt halten, um die Dekarbonisierung des Verkehrs voranzutreiben und die Abhängigkeit von fossilen Brennstoffen zu verringern. Dabei ist es unerlässlich, Netzanschlüsse vor der räumlichen Zuteilung der Ladeinfrastruktur zu berücksichtigen, da die ohnehin hohen Zuteilungskosten von den gewählten Standorten und der lokalen Energieversorgung abhängen. Die vorliegende Arbeit schlägt ein multiperiodisches, zweistufiges, stochastisches und gemischt-ganzzahliges Optimierungsverfahren vor, mit dem strategische Entscheidungen bei der Zuteilung von E-Fahrzeug-Ladestationen auch bei unvollständigen Netzinformationen verbessert werden können. Ziel ist einerseits die Gewinnmaximierung, indem der Ladebedarf von E-Fahrzeugen abgedeckt wird. Andererseits sollen die erwartbaren Kosten für Netzengpässe, die durch unzuverlässige Netzverbindungen zwischen Ladestationen und Umspannwerken entstehen, minimiert werden. Dafür wurde ein neuartiger Algorithmus zur Szenariengenerierung entwickelt, mithilfe dessen mögliche Szenarien beim Netzanschluss simuliert werden. Dabei wird die Wahrscheinlichkeit einer Netzverbindung zwischen Ladestationen und örtlichen Umspannwerken auf Grundlage der Entfernung zwischen den betreffenden Objekten und dem Netzstatus der Ladestationen in der Umgebung berücksichtigt. Darüber hinaus arbeitet diese Studie mit einem node-basierten Ansatz, der die tatsächlichen Ladekapazitäten von Ladestationen treffsicher wiedergibt. Dabei werden die Auswirkungen einer (längerer) Parkdauer, der Nutzungshäufigkeit und dem Ladestatus der Fahrzeuge zu Beginn des Ladenvorgangs auf die Ladeleistung berücksichtigt. Dazu wird eine Fallstudie in der Gemeinde Schutterwald (Baden-Württemberg) durchgeführt, bei der das Optimierungsmodell in "Pyomo", einer auf Python basierenden Programmiersprache zur Modelloptimierung, implementiert wird. Eine szenarienbasierte Sample-Average-Approximationsmethode dient der Lösung des Modells mithilfe des kommerziellen Solvers CPLEX.

## Acknowledgments

First and foremost, words cannot express my deepest gratitude and appreciation to my thesis advisor Dr. Ing. Dominik Husarek. Without his deep insights into e-mobility and energy systems, this study would have been impossible. His professional guidance helped me overcome countless difficulties, and his profound knowledge guided me to numerous research ideas, such as the charging demand representation and uncertainty of grid connection. His encouragement and patience during my unproductive periods gave me great faith in accomplishing this stochastic modeling project. Despite my imperfect information, I surely believe that I am one of the luckiest master's students to have such a perfect thesis advisor as Dr. Ing. Dominik Husarek.

Furthermore, I owe my sincerest thanks to my thesis supervisor Prof. Dr. Michael Ulbrich for his professional supervision in mathematical modeling. From the first seminar work to the linearization of the base model, from the resolution of stochastic programming to the analysis of computational results, I have benefited broadly from every fruitful discussion with him.

It is my great honor to work with my colleagues and friends at Siemens Infrastructure Design Research Group. Doctoral candidate Mr. Domenico Tomaselli provided me with insightful power grid knowledge and abundant research experience. Dr. Paul Stursberg and Doctoral candidate Ms. Sisi Bazan Santos helped me a lot in the modeling and data processing part. Moreover, I sincerely appreciate Dr. rer. nat. Hans Jörg Heger for all the great organizations and support.

Last but not least, I owe my deepest thanks to my parents. Without their selfless support, I will never make it today. In addition, I owe my thanks to all my friends and people who supported me during my master's study. Finally, I am grateful that I managed to make it. It was uneasy, but every day was meaningful, and I enjoyed it.



## Basic Terminology and Notation

Table of notations and terminologies

Term	Meaning	Term	Meaning
<b>EV</b>	Electric Vehicle	<b>CS</b>	Charging Station
<b>EVCSAP</b>	Electric Vehicle Charging Stations Allocation Planning	<b>FLP</b>	Facility Location Problem
<b>CD</b>	Charging Demand of EVs	<b>CC</b>	Charging (Energy) Capacity of CSs
<b>SP</b>	Stochastic Programming	<b>CI</b>	Charging Infrastructure
<b>CP</b>	Charging Point (Charger)	<b>POI</b>	Point of Interest
<b>DSO</b>	Distribution System Operator	<b>CSO</b>	Charging Stations Operator
<b>MILP</b>	Mixed-integer Linear Programming	<b>ABM</b>	Agent-based e-Mobility Model
<b>TESC</b>	Theoretical (Charging) Energy Supply Capability	<b>EESC</b>	Exogenous (Charging) Energy Supply Capability
<b>SS</b>	Secondary Substations (MV/LV transformers)	<b>MPSP</b>	Multi-Period Stochastic Programming
<b>2D-C-S-NET</b>	Distance Decayed CS-SS Connection Scenario Generation under Neighborhood Effect	<b>SW</b>	Schutterwald
<b>SAA</b>	Sample Average Approximation	<b>EF</b>	Extensive Form

**Table 1:** Table of Abbreviations

ID	Domain	Unit	Meaning
$\mathbb{R}$	-	-	Real Numbers
$\mathbb{Z}$	-	-	Integers
$I_0$	$\{\mathbb{R} \times \mathbb{R}\}^{ I_0 }$	-	Set of candidate locations with existing CSs to update.
$I_1$	$\{\mathbb{R} \times \mathbb{R}\}^{ I_1 }$	-	Set of candidate locations for opening potential new CSs.
$I$	$\{\mathbb{R} \times \mathbb{R}\}^{ I_0 \cup I_1 }$	-	Set of candidate locations for CSs, $I := I_0 \cup I_1$ .
$J$	$\{\mathbb{R} \times \mathbb{R}\}^{ J }$	-	Set of POIs with Charging Demand.
$T$	$\mathbb{Z}$	-	Set of periods of a day
$\Delta t$	$\mathbb{R}$	hour	Length of a period $t \in T$ , $\sum_{t \in T} \Delta t = 24$
$N_0$	$\mathbb{Z}$	-	Maximum amount of existing CSs the investors want to update.
$N_1$	$\mathbb{Z}$	-	Maximum amount of new CSs the investors want to open.
$N^x$	$\mathbb{Z}$	-	Maximum amount of existing or new CSs that the investors want to update or open. $N^x \leq N_0 + N_1$
$N^y$	$\mathbb{Z}$	-	Maximum amount of new CPs the investors want to install.
$\pi$	$\mathbb{R}$	kW	Power rating of a CP.
$\rho$	$\mathbb{R}$	hour	All new CSs must be at least $\rho$ walking distance away from each other and from existing CSs.
$\phi^{IJ}$	$\mathbb{R}$	hour	Maximum walking distance from a POI to a CS the drivers can tolerate to charge their EVs.

**Table 2:** Notations in **Base Model**

ID	Domain	Unit	Meaning
$d_{ij}$	$\mathbb{R}$	hour	Distance (in terms of walking time) between the location of candidate location $i \in I$ and the location of another node $j \in I \cup J$
$c_i^x$	$\mathbb{R}$	Euro/CS	Average annual cost of locating a CS at location $i \in I_1$ , or updating an opened CS at location $i \in I_0$ .
$c^y$	$\mathbb{R}$	Euro/CP	Average annual installation cost per CP.
$m_i$	$\mathbb{Z}$	-	The maximum number of extra CPs that can be installed at an opened or updated CS at $i \in I$ .
$n_i$	$\mathbb{Z}$	-	Number of CPs already sited in an opened CS $i \in I$ .
$\mathcal{A}_j^t$	$\mathbb{R}$	-	Number of EV arrivals with CD at POI $j \in J$ during $t \in T$
$\mathcal{T}_j^t$	$\mathbb{R}$	hour	Visit duration of an EV driver at POI $j \in J$ during $t \in T$
$\delta_j^t$	$\mathbb{R}$	-	Average arrival SOC of EV arrivals at POI $j \in J$ during $t \in T$
$\mathcal{A}_{ij}^t$	$\mathbb{Z}$	-	Number of price-scaled-distance-decayed EV arrivals with CD at POI $j \in J$ during $t \in T$ as defined in (3.4)
$\mathcal{T}_{ij}^t$	$\mathbb{R}$	hour	Average parking time of a CS recharging at $i \in I$ from a POI $j \in J$ during $t \in T$ as defined in (3.8)
$\mathcal{D}_{ij}^t$	$\mathbb{R}$	kWh	the Charging (energy) Demand of each EV visit to a POI $j \in J$ recharging at a CS $i \in I$ as defined in definition 3.4
$B_{cap}$	$\mathbb{R}$	kWh	Average battery capacity of EVs
$\tau_{ij}$	$\mathbb{R}$	-	Price-scaled-distance decay factor between a CS $i$ and a POI $j$ with CD as defined in (3.3).
$u_i$	$\mathbb{R}$	Euro/kWh	Energy price at an opened CS $i \in I$ .
$\mathbf{w}_i^t$	$\mathbb{R}$	kWh	EESC of a CS $i \in I$ during a $t \in T$ as defined in definition 3.6.
$\mathcal{T}_i^t$	$\mathbb{R}$	hour	TSC of a CS $i \in I$ during period $t \in T$ as defined in definition 3.5
$\mathbf{w}_{ij}^t$	$\mathbb{R}$	kWh	As defined in (3.13), which is exclusively used for setting lower bound on $\mathbf{z}_{ij}^t$ . And it can be understood as the estimated recharging energy of the EV arrivals from a POI $j \in J$ during period $t \in T$ that a CS $i \in I$ can cover.
$\psi_i^t(\mathbf{z}^t)$	$\mathbb{R}$	kWh	Total energy a CS $i \in I$ serves during period $t \in T$
$\mathcal{D}_j^t$	$\mathbb{R}$	kWh	Exclusively used for setting lower bound on $\mathbf{z}_{ij}^t$ in constraints B as illustrated in appendix B. Average CD of visits to the POI $j \in J$ during period $t \in T$ defined by , without considering walking time.
$\mathcal{M}^t$	$\mathbb{R}$	kWh	Big-M notations. Exclusively used for linearizing constraints (3.26) of setting lower bound on $\mathbf{z}_{ij}^t$ , as illustrated in appendix B.

**Table 3:** Parameters in Base Model

ID	Domain	Unit	Meaning
<b><i>CS and CD Decision Variables</i></b>			
$\mathbf{x}_i$	$\{0, 1\}$	-	1, if an existing CS at $i \in I_0$ will be updated, or a new CS will be open at candidate location $i \in I_1$ ; 0, otherwise.
$\mathbf{y}_i$	$\mathbb{Z}$	-	Number of CPs to be installed at an opened or updated CS $i \in I$ .
$\mathbf{z}_{ij}^t$	$[0, 1]$	-	The fraction of CD from POI $j \in J$ covered by a CS located in $i \in I$ during period $t \in T$ , if and only if a CS is located in $i$ .
<b><i>Auxiliary Decision Variables</i></b>			
$\mathbf{x}_{ij}$	$\{0, 1\}$	-	Exclusively used for Linearization of quadratic constraints ((3.26)) as defined in section 3.1.3
$\chi_j^t$	$\mathbb{R}$	kWh	Exclusively used for setting lower bound on $\mathbf{z}_{ij}^t$ according to section 3.1.3
$\varepsilon_j^t$	$\{0, 1\}$	-	Exclusively used for setting lower bound on $\mathbf{z}_{ij}^t$ according to section 3.1.3

**Table 4:** Decision Variables in **Base Model**

ID	Domain	Unit	Meaning
$K$	$\{\mathbb{R} \times \mathbb{R}\}^{ K }$	-	Set of substations
$Z_{ik}$	$\{0, 1\}$	-	1, if a substation $k \in K$ transfers electricity to a candidate location $i \in I$ ; 0, otherwise.
$\Pi_k^t$	$\mathbb{R}$	kW	Available power load (on average) of a transformer substation $k$ during period $t$
$c^h$	$\mathbb{R}$	Euro/kW	The average annual cost of expanding the capacity of a SS per kW.
$\mathbf{h}_k$	$\mathbb{Z}$	kW	Amount of capacity the DSO will expand at SS $k \in K$ .

**Table 5:** Notations, Parameters and Decision Variables introduced in **MPDP**

ID	Domain	Unit	Meaning
$\Omega$	$\mathbb{Z}$	-	Set of scenarios
$d_{ij}$	$\mathbb{R}$	hour	Walking distance between the candidate location $i \in I$ and another node $j \in I \cup J \cup K$
$\mathbf{h}_k$	$\mathbb{Z}$	kW	Amount of capacity the DSO will expand at SS $k \in K$ .
$\mathcal{Z}_{ik}(\omega)$	$\{0, 1\}$	-	1, if a substation $k \in K$ transfers electricity to a candidate location $i \in I$ under scenario $\omega \in \Omega$ ; 0, otherwise.
$c^\eta$	$\mathbb{R}$	Euro/kW	The expensive cost of using backstop technology.
$\phi^{II}$	$\mathbb{R}$	hour	Distance threshold for defining the neighborhood of CSs. Exclusively used in scenario generation as defined in Def. 3.9
$\tau_{i_1 i_2}$	$\mathbb{R}$	-	Distance decay factor between CSs $i_1 \in I$ and $i_2 \in I$ , $i_1 \neq i_2$ as defined in (3.57)
$\phi^{IK}$	$\mathbb{R}$	hour	Threshold for calculating the probability of connection between CSs and Substations. Exclusively used in scenario generation as defined in Def. 3.7
$\tau_{ik}$	$\mathbb{R}$	-	Distance decay factor between a CS $i \in I$ and a SS $k \in K$ as defined in (3.52)
$\eta_k^t(\omega)$	$\mathbb{R}$	kW	Scale of expensive backstop technology to be applied at $k \in K$ during period $t \in T$ under scenario $\omega \in \Omega$ .

**Table 6:** Notations, Parameters and Decision Variables introduced in **MPS**



# Contents

<b>1</b>	<b>Introduction</b>	<b>1</b>
<b>2</b>	<b>Literature Review</b>	<b>3</b>
2.1	Modeling Approach . . . . .	3
2.2	Impact of EV Charging on Electricity Grid . . . . .	5
2.3	EVCSAP under Uncertainty . . . . .	7
<b>3</b>	<b>Model Description</b>	<b>9</b>
3.1	Multi-Period MILP Base Model without Grid Network . . . . .	9
3.1.1	Charging Demand of Electric Vehicles . . . . .	10
3.1.2	Supply Capability of CSs . . . . .	14
3.1.3	Base Model . . . . .	16
3.2	MPDP with Grid Network Constraints . . . . .	20
3.2.1	Grid Congestion . . . . .	20
3.2.2	MPDP . . . . .	21
3.3	MPSP with Grid Network Constraints . . . . .	21
3.3.1	Grid Congestion under Uncertainty . . . . .	22
3.3.2	MPSP . . . . .	23
3.3.3	Scenario Generation . . . . .	23
<b>4</b>	<b>Computational Experiments and Case Study</b>	<b>29</b>
4.1	Case Description: Schutterwald . . . . .	29
4.2	Implementation . . . . .	34
4.3	Results . . . . .	34
4.3.1	Sensitivity Analysis . . . . .	35
4.3.2	Model Performance . . . . .	39
<b>5</b>	<b>Conclusions and Outlook on Future Research</b>	<b>43</b>
<b>A</b>	<b>A brief introduction to Facility Location under Uncertainty</b>	<b>45</b>
<b>B</b>	<b>Examples and Derivation of Definitions</b>	<b>49</b>
<b>C</b>	<b>EVCSAP Models in Compact Form</b>	<b>55</b>

<b>D Model Implementation</b>	<b>57</b>
<b>List of Figures</b>	<b>69</b>
<b>List of Tables</b>	<b>71</b>
<b>List of Algorithms</b>	<b>71</b>
<b>Index</b>	<b>73</b>
<b>Bibliography</b>	<b>77</b>

# Chapter 1

## Introduction

**Motivation and Problem Description.** The electrification of individual passenger transport is a promising solution to address the current challenges of oil import dependency, air pollution, and climate change. Ranked second place after the power sector, the transport sector alone accounts for 17 percent of GreenHouse Gas (GHG) emissions worldwide and is responsible for one-quarter of that in European countries [Dep22]. Achieving climate neutrality by 2050 will need a 90% decline in emissions in the transport sector [Age20]. Besides, the war in Eastern Europe has brought the need to reduce oil demand to the front, as stable supply chains and national security cannot merely depend on importing limited fossil energy sources. However, the transport sector with significant GHG has the highest reliance on fossil fuels of any sector: 95% of energy consumption in transport burns oil-derived fuels [Con21] and accounted for 37% of CO2 emissions from enduse sectors in 2021 [Bib+22]. Increasing the Electric Vehicle (EV) adoption rate is one of the ten measures proposed by the International Energy Agency to tackle the above problems.

Convenient access to charging points plays a critical role in the significant uptake of EVs. Most drivers living in apartments and parking on streets hesitate to switch to EVs due to the lack of accessible and affordable charging: In 2021, 42 percent of European urban EV owners had no access to home charging points [ACE22]. Therefore, numerous new *public* chargers are needed. Despite an estimated number of 375,000 Charging Stations (CSs) now sited in Europe, a recent analysis by McKinsey [Con+22] suggested that in even the most conservative scenario, the EU-27 will need more than 3.4 million operational public charging points by 2030, which on average equals 6,000 public charging point installations per week in the EU from 2021 to 2030.

The location of CSs strongly impacts how often and easily drivers use them and consequently influences the revenue of Charging Station Operators (CSOs). A stable energy supply of charging hubs relies on sufficient power resources from the grid. Upgrades of distribution grids, such as low- and medium-voltage transformer substations and lines, will be needed to manage significant additional loads and grid congestions [Bib+22]. Approx. seventy billion euros will be cumulatively invested in supporting public *EV CSs Allocation Planning* (EVCSAP) and the corresponding *grid upgrades* [Con+22]. To make full use of this investment, optimal EVCSAP has a strategic impact

on promoting EV adoption. The CSs roll-out must sustain the bullish EV markets to satisfy the Charging Demand (CD) while avoiding grid congestions. [Ber+21].

**Contributions.** This thesis proposes a new two-stage multi-period stochastic programming framework (**MPSP**) to help decision-makers determine the optimal allocation of public CSs in precise locations of urban areas. And the objective is to achieve maximum profit while avoiding grid congestion costs. The major contributions are as follows:

1. A new approach to estimate the charging (energy) Capacity of CSs (CC), which considers the impact of arrival frequency, parking time, and active charging duration of EVs on the actual CC.
2. A **MPSP** to solve the optimal EVCSAP while managing grid congestion under incomplete grid data.
3. A simple scenario generation algorithm to sample complex grid connection scenarios of CSs and SSs.

The first stage of this stochastic profit maximization framework is used to decide the locations of CSs and the expansion of Secondary Substations (SSs) in a node-based graph network. After the first-stage decisions are executed and the energy supply to CSs is found insufficient during intensive charging sessions, Backup or Backstop power Technologies (BT) need to be applied to reduce grid congestion. After observing overload during specific periods, the second stage determines how much BT power storage to use at each location to manage grid congestion. The optimization framework is implemented with the Python-based open-source optimization modeling language Pyomo [HWW11] [Byn+21]. The construction of the stochastic programming part utilizes the state-of-art stochastic programming software [Knu+20] MPI-SPPy. And the model is solved by the commercial solver CPLEX. A case study is executed in the German town Schutterwald (SW) with a network of 158 CD centers, 12 candidate locations for CSs, and 17 candidate locations for power expansion.

**Layout.** This thesis is structured as follows. In Chapter 2, the main contributions are explained in parallel with a literature review. In Chapter 3, we formally describe the proposed problem and the corresponding optimization model and present the scenario generation algorithm. Then, Chapter 4 illustrates the implementation of the proposed optimization frameworks and the results of the case study SW. Finally, Chapter 5 concludes this work with a discussion on future research opportunities.

# Chapter 2

## Literature Review

Recent years have witnessed significant growth in research interest in EVCSAP. This chapter presents an overview of some recent research trends; for fully comprehensive reviews, [Ahm+22], [Met+22] and [Deb+18] are recommended. The literature overview starts with a description of the popular modeling approaches for EVCSAP in section 2.1. In section 2.2, a short overview of studies considering grid impact of EVCSAP is presented. Finally, section 2.3 discusses the recent works of stochastic programming for EVCSAP.

### 2.1 Modeling Approach

EVCSAP, an alternative-fuel filling stations location problem, is an extension of the facility location problems (FLPs), which consists of determining the optimal location for one or several facilities under a bunch of constraints to serve demands in a set of points while considering some optimality criteria. Charging events usually take significantly longer than traditional gas refueling, and an EV can occupy a CP as a parking lot without recharging activity. These distinguish EVCSAP from the location problems of traditional-fuel refueling stations and bring new challenges to an accurate estimation of actual charging energy demand. Various models have been developed to deal with this. Among them, node-based and flow-based approaches are the most popular.

**Node-based (optimization) approaches** often formulate the problem as a vertex covering problem, such as p-median [KH79], p-center [Hak64], and maximal covering [CR74]. It selects the optimal locations from several nodes of candidate locations to meet or cover the demand at nodes. The methodology sounds simple, but its corresponding optimization problems belong to the NP-hard class [LNS19] since the vertex cover problem is NP-hard. Recent node-based models for EVCSAP are presented in [MN13], [CHG15], [Don+19], [Kab+20] and so on. As an initial step and to reduce the complexity of the optimization model, such approaches often aggregate CD through geographic information systems (GIS) software and then solve the model with modern solvers or (and) heuristic algorithms. Other popular non-optimization node-based approaches are

also worth mentioning. They use GIS to generate CD heat maps and select optimal locations with the help of statistical analysis [D+16] [Mor+22].

Node-based approaches are considered more appropriate for deploying CI location decisions in an urban or suburban setting. Because during a long-haul journey, several charging sessions can happen at any resting point. Such flow-based nature makes it inaccurate to approximate its corresponding CD by node-based approaches. Moreover, node-based approaches cannot achieve objectives such as maximizing the driving range of vehicles by locating fuel refilling stations.

**Flow-based approach** is a popular research stream in the recent decade to represent flow-based CD. Contrary to classical FLP models dealing with demands at nodes of a network, the method introduced by [Hod90] relies on a flow-capturing location model (FCLM) aiming to maximize the EV flow captured on the shortest path between origin-destination (OD) pairs. This arc-cover model regards a path as covered if there is at least one operational charging station placed along the nodes it passes. Comparisons of FCLM and p-median model implemented by, for example, [HR92], and [UK10], show that the FCLM approach is especially suitable to tackle fast-chargers planning problems involving inter-city travel. FCLM was later developed for alternative-fuel refilling stations vehicles to address the limited traveling range of alternative-fuel vehicles [KL05]. Since then, FCLM has been applied by a large number of researchers to solve EVCSAP.

In spite of the popularity of FCLM in academic research, solving it in realistic instances is nevertheless more challenging than solving node-based models of the same problem size. Because the number of OD pairs will inevitably inflate as the problem size increases, an extensive CD aggregation is often accepted to reduce the problem size, sacrificing the precision of CD representation as a trade-off.

Noticing the pros and cons of both approaches, recent work by [AGJ20] proposed a multi-period hybrid model to effectively cover charging demands and increase EV adoption over given time horizons. They apply both node-based and flow-based approaches in a single model to deal with CD in different types of regions. In addition, a new demand dynamic is proposed to represent the impact of the CIs planned in the last period on the EV adoption rate in the next period. Solving the hybrid model by solvers alone is insufficient for large areas. Thus a rolling-horizon heuristic algorithm was applied there.

**A realistic assessment of CC** is as essential as representing CD of CSs for defining the size of CSs to place and the scale of the power grid to upgrade since CC bridges the actual energy demand requested by EVs to the distribution system. In particular, we spotted a research gap in the proper estimation of CC.

The majority of the previous approaches approximated CC by ambiguous sizes of CSs, such as simply by the number or/and power rating of CPs [Kab+20] [AGJ20]

[CKK13] [MN13] [WL13]. However, this ambiguity usually results in an overestimation of the actual charging capacity, as long-time parking of EVs without much-charging demand wastes a lot of charging service capability of CPs [Tru19b]. [MN13] noticed the importance of different points of interests (POIs) categories on CP usage behavior and proposed a POI Regression method to rank their impact on chargers usage. The classical work [CHG15] and a recent research work [Kob+22] correlate CD and CC with parking time. Nonetheless, integrating the CI network into the grid system with the above approaches will require further work, as they cannot give acceptable estimations of power or energy usage.

Recognizing this, the CD and CC representation methods proposed in this study address the impact of the POIs statistics, including the number of visitors with EV charging demand, the state of charging (SOC) of EV batteries upon arrival, and the visiting duration of each EV arrival. Such statistics can be easily estimated through industrial experts' experience and reports or be simulated from mobility models such as the state-of-the-art "Agent-based e-Mobility Model" (ABM-eMob) [Hus+21]. The proposed method of CD approximation is an advanced hybrid method of those in [Sha+15] and [CHG15]. The former represents the CD of each EV by considering parking time without an active charging process, while the latter calculates the number of EV arrivals under walking distance-decayed to recharge EVs. In addition, our CD representation approach evaluates the effect of charging prices on the EV drivers' willingness to recharge, which leads to different estimated scales of EV fleets toward different CSs. Based on the CD approximation method, the approach to estimate CC of CSs, called exogenous (charging) energy supply capability (EESC), is one of the major contributions of this thesis. It addresses the impact of inconsistent durations of dwell time, different EV recharging frequencies, and various SOCs of EVs on the actual capacity of CSs and the utilization rate of CPs.

## 2.2 Impact of EV Charging on Electricity Grid

The increasing penetration of new CPs within the next few decades will significantly stress the current non-adapted grid infrastructure [Bib+22]. Expensive grid reinforcement is inevitable. Though the entire electricity network consists of both transmission<sup>1</sup> and distribution systems<sup>2</sup>, integration of new CSs to grid system only expects significant impacts in primary and secondary substations and medium- and low-voltage lines [ACE22] (cf. **Figure 2.1**).

The current capacity of SSs is insufficient to meet the increasing charging demand and efficient upgrades of distribution networks must be invested to avoid grid congestions. The optimal power upgrade will rely on the collaboration and cooperation of stakeholders,

---

<sup>1</sup>carrying high-voltage electricity from a power plant to a substation

<sup>2</sup>carrying medium- and low-voltage electricity from substations to end consumers

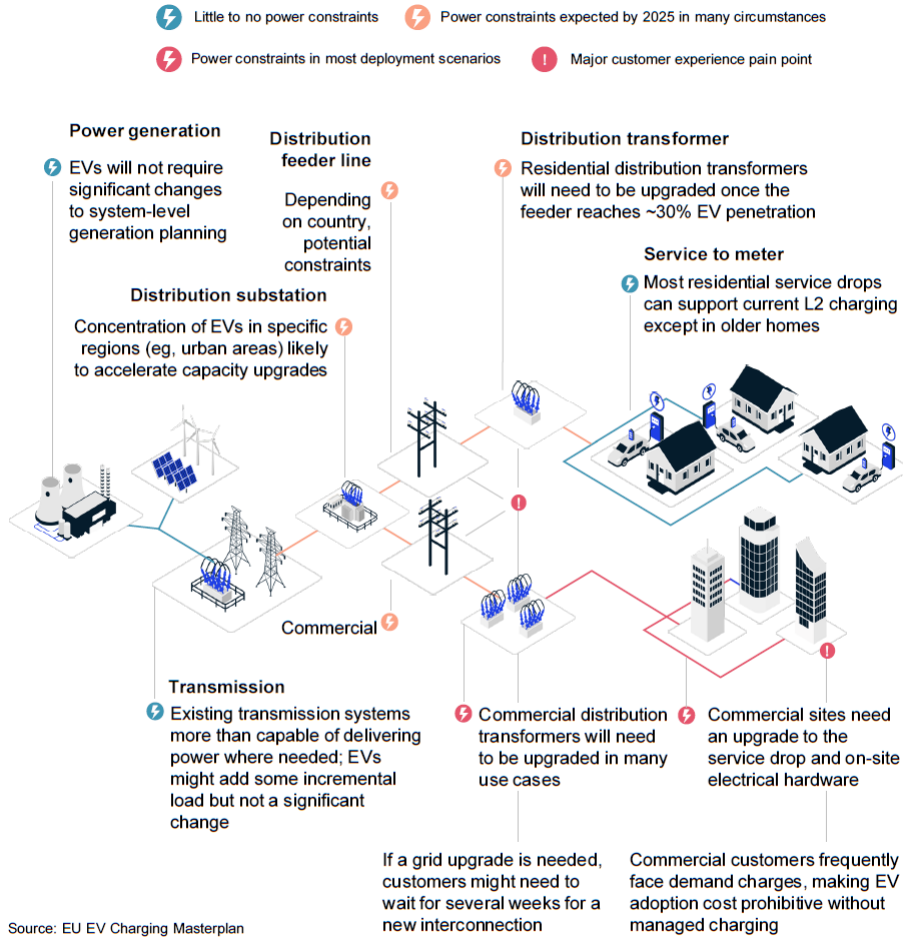


**Figure 2.1:** Illustration of the priority of grid upgrades [ACE22]

including utilities, regulators, distribution system operators (DSOs), and charging station operators (CSOs) [Ber+21]. For example, regarding the shared objectives of CSOs and DSOs to lower emissions, the two sectors' transformations are encouraged to coordinate much more broadly than now [QOB18] [Tru19a]. A recent research [Pow+22] pointed out that if CSOs can increase public charging accessibility by a great portion, many night-time (home) chargings will shift to daytime (public) chargings. This shift can significantly reduce the stress on the grid that the DSOs are facing. Such metrics of grid impact include the use of non-fossil fuel generation, storage requirements, emissions, etc. This insight is claimed to be robust across varying levels of EV adoption.

A preliminary literature review shows that the majority of past studies in EVCSAP

only focus on the transportation network, such as [MN13], [CHG15], [WL13]. There are research works accounting for grid problems, for instance, [MMA17] and [Luo+18]. [MMA17] proposed a multi-objective optimization framework to simultaneously reduce power losses and voltage fluctuations while managing EV charging and renewable energy sources. In [Luo+18], a mixed integer second-order cone programming utilizing POI statistics was proposed to optimally allocate multi-types of charging facilities while limiting the voltage magnitude and branch current. However, few of them considered or were able to deal with optimal planning of CI allocation and power expansion at the same time.

## 2.3 EVCSAP under Uncertainty

A reliable solution should be able to deal with unexpected events. Yet very limited studies consider system uncertainties, which frequently impact the charging decisions of EVs, the location decisions of CIs, and the upgrade decision of the distribution network. Referring to [LNS19] that studied facility location under uncertainty and stochastic location models with congestion, the uncertainties in EVCSAP are categorized as follows:

- Charging Demand Centers (POIs): EV market penetration rate in a specific planning scenario, an uncertain number of visitors to POIs at different time periods, unsure parking duration of different visits, various battery capacity and battery SOC of EVs upon arrival, etc.
- Charging Infrastructure: uncertain maximum power of recharging connections, unsure available power load from the grid, probability of equipment failure, etc.
- Secondary Substations: unexpected energy demand from other consumers such as household customers and commercial sides in the same grid area, volatile renewable energy generation, imperfect information of the grid connection of charging stations (i.e., the uncertainty of to which substation a certain location would be connected), etc.

There is still a number of researchers who studied EVCSAP under uncertainties. Most of the approaches focus on the stochastic charging demand of EVs. For example, [WS17] proposed a stochastic FCLM solved by L-shaped sample-average approximation (SAA) with a branch-and-cut method to capture uncertain EV flows. In comparison, [Kab+20] treated the power demand as a stochastic element. The authors presented a two-stage stochastic optimization approach solved by SAA and heuristics algorithms to determine the optimal planning of power grid expansion and charging station allocation. The first stage decides the optimal electricity grid expansion, and the decision for charging station placement is made in the second stage. However, their approach aggregated power demand and charging demand at a large scale and provided decisions in 0.5 mile<sup>2</sup> grid rather than exact locations.

The uncertainty of the grid connection points between CSs and SSs has not been covered by any literature so far. But industrial experts considered it as highly relevant<sup>3</sup>, as it is usually absent in the real planning stage. With limited information on grid connection, it is almost impossible to actively consider the corresponding grid reinforcement early in the project before delivering, installing, and connecting expensive CIs to the grid system that can not be withdrawn afterwards. Moreover, mitigating the uncertainties of the charging demand of EVs or the available power load of SSs can be achieved by rough approximation from statistics summarized from reports, questionnaires, or experienced experts. But this will not be easy in the case of uncertainty of grid connection as even the DSOs operating the SSs themselves do not always have the perfect grid connection information [G+16].

To address these concerns, this study is motivated to solve the EVCSAP under the uncertainty of grid connection. The objective is to maximize the revenue gained by satisfying the charging demand served by the optimally allocated public chargers while minimizing the cost of potential grid congestion at specific locations. The **MPSP** is consequently developed to achieve this goal. Charging demand in **MPSP** is represented through a node-based approach without spatial aggregation. Meanwhile, **MPSP** is formulated as a multi-period model to reduce the temporal aggregation of CD. In addition, SAA is applied to solve this stochastic program, and a corresponding sampling algorithm for generating grid connection scenarios is presented. The following chapter presents a formal description of this model.

---

<sup>3</sup>This challenge and its relevance were identified by Siemens research engineers in multiple projects dealing with the allocation of CI.

# Chapter 3

## Model Description

In this chapter, we propose a new approach to allocate electric vehicle charging infrastructure in urban areas. The impact of (long) parking duration on efficient charging demand and utilization rate of charging points was addressed in this new approach. Furthermore, the rapidly increasing EV charging market imposes new challenges on the stability of the current grid system. Placing charging infrastructures while minimizing grid congestion costs is another core problem of this work. We developed a Two-Stage Multi-Period Stochastic Mixed-Integer Linear Program to tackle this challenging EVCSAP with uncertain grid information.

This chapter will start with a **Base Model** without distribution network in section 3.1 for illustrating charging demand at points of interest and the recharging service supply capability of charging points. On top of the **Base Model**, constraints of the grid network will be added in section 3.2, and we name the **Base Model** with grid constraints **MPDP** (**M**ulti-**P**eriod **D**eterministic **M**ixed-**I**nteger **L**inear **P**rogramming Model). In section 3.3, the final model called **MPSP** (**M**ulti-**P**eriod **S**tochastic **M**ixed-**I**nteger **L**inear **P**rogramming), will be introduced to tackle the uncertainty of power availability.

### 3.1 Multi-Period MILP Base Model without Grid Network

As with other research on the EVCSAP, representing the CD of EVs is usually the first challenging part. We also start the description of **Base Model** from the representation of CD in section 3.1.1, which consists of estimating the number of EV arrivals and CD of each EV arrival. In addition, we suggest a new point of view on the approximation of (recharging) energy supply capability of CSs in section 3.1.2. In the last part, a multi-period MILP base model will be presented.

It is important to clarify notations before exploring the model. Locations of supermarkets, schools, museums, and so on are called Points of Interest (POI). We denote set  $J$  for those POIs as the charging demand centers and set  $I = I_0 \cup I_1$  as the set of candidate locations (parking areas in this study) for opening or updating CSs and allocating CPs.  $I_0$  denotes the set of candidate locations with existing CSs to be updated, and  $I_1$  is the set of candidate locations to open new CSs. Variables  $\mathbf{x}_i \in \{0, 1\}$ ,  $i \in I$  decide whether

to build a new CS ( $\mathbf{x}_i = 1, i \in I_1$ ) by investing  $c_i^x, i \in I_1$  Euro in each CS annually, or whether to update an existing CS  $\mathbf{x}_i = 1, i \in I_0$  at an annuity fee of  $c_i^x, i \in I_0$  Euro per CS, or not ( $\mathbf{x}_i = 0, i \in I$ ). The walking distance between a CS at  $i \in I$  and another node  $j \in I \cup J$  is represented by  $d_{ij}$ <sup>1</sup>. Regardless of the locations of existing CSs, the location of a new CS to build is required to be at least at a walking distance of  $\rho$  hour away from another new or existing CS. A CS can have several CPs. We denote  $n_i$  as the number of CPs already sited at a location  $i \in I$ , where  $n_i > 0 \forall i \in I_0; n_i = 0 \forall i \in I_1$ .  $m_i$  was denoted as the maximum number of extra CPs that can be sited at a candidate location  $i \in I$ . Accordingly, variables  $\mathbf{y}_i \in \mathbb{Z}, i \in I$  are denoted to decide the number of CPs to allocate at each opened or updated CS with the same annuity fee at  $c^y$  [Euro] per CP since only single type CP with power rating denoted as  $\pi$  [kW] is considered in this work. As pointed out in [War+13], different electricity prices result in modified charging patterns which lead to different charging demands. The recharging fees denoted as  $u_i, i \in I$  [Euro/kWh] at different CSs are thereby modeled inconstantly to address this issue. CI allocation decisions are limited by resources budgets  $N^x$  and  $N^y$ . The former declares the maximum number of existing CSs to update or new CSs to build. In contrast, the latter sets an upper bound number of extra CPs to install in all candidate locations in total. And in the context where it does not cause misunderstanding, we use the following expressions for simplicity:

- *CS  $i \in I$  (POI  $j \in J$ )* to refer the *CS located at  $i \in I$  (POI located at  $j \in J$ )*
- *EV arrivals at a POI  $j$*  as the short expression for *the EVs with charging demand, whose drivers visit POI  $j$*
- *EVs recharging at CS  $i$  from POI  $j$*  as the short expression for *the EVs, whose drivers visit POI  $j \in J$  and park their EVs at the CS  $i \in I$  for recharging*

### 3.1.1 Charging Demand of Electric Vehicles

This thesis proposed a node-based CD approximation method that addressed the problem of estimating the CD of EVs while considering the long parking time of EVs and the walking distance between CSs and POIs. We denote  $T$  as the set of periods of a day and  $\Delta t, t \in T$  [hour] as the period length since the CD of EVs is estimated based on the daily pattern in our model. And the necessity of multi-period comes from the fact that the number of visits at a particular POI during a day usually fluctuates widely. For instance, supermarkets are expected to have most of the visits during the day, while at night, rare people are found there after the close time. In the **Base Model** for

---

<sup>1</sup>In this thesis, distance is presented by *walking distance in hour* for the convenience of modeling. The default walking speed is assumed to be 5 km/hour. E.g., a 0.1 hour walking distance stands for 500 meters.

### 3.1 Multi-Period MILP Base Model without Grid Network

example, we set  $T := \{day, night\}^2$ , where  $\Delta t = 12$ ,  $\forall t \in T$ . In this model, all EVs are assumed to have the same battery with capacity  $B_{cap}$  [kWh]. We denote  $\mathcal{A}_j^t$  as the average number of EV arrivals with charging demand at POI  $j \in J$  during period  $t \in T$ . We assume that the flow of EV arrivals at any POI  $j \in J$  during any period  $t \in T$  follow the Poisson distribution and  $\mathcal{A}_j^t \in \mathbb{Z}_{\geq 0}$ . Although each EV can have a different State Of Charge (SOC) upon arrival and a different parking time, we treat the EVs visiting the same POI as the same. That is, for any arrival at a POI  $j \in J$  during period  $t \in T$ , its average visit duration [hour] and SOC upon arrival are denoted by  $\mathcal{T}_j^t \in \mathbb{R}_{\geq 0}$  and  $\delta_j^t \in [0, 1]$ , respectively.  $\mathcal{A}_j^t$ ,  $\mathcal{T}_j^t$  and  $\delta_j^t$  are called *POI Statistics* for POI  $j \in J$  at period  $t \in T$  in this thesis. By the assumption, for drivers visiting the same POI  $j^* \in J$  during a period  $t \in T$ , no matter at which CS  $i^* \in I$  to recharge their EVs, the SOC of EVs upon arrival at any  $i^* \in I$  will be regarded the same as  $\delta_{j^*}^t$ .

In addition, EVs are assumed to recharge immediately upon arrival, and their owners will not come back to unplug the vehicles until their activities are ended, as assumed in [FK13].

#### Price-Scaled-Distance-Decayed EV Arrivals

Furthermore, EV drivers are assumed to prefer **a.)** walking less and **b.)** recharging at cheaper CSs. Whereas from the perspective of CSs, such preference or willingness can be regarded as the attractiveness of CSs to EV drivers, which is represented by the following definition:

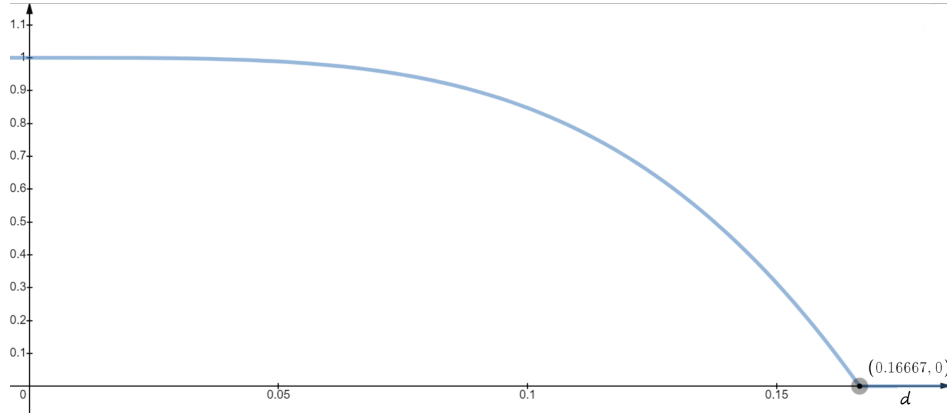


**Figure 3.1:** An Example of Function  $\tau(d, \phi)$  in Def.3.1 with  $\phi = \frac{1}{6}[\text{hour}]$  of walking distance

<sup>2</sup>Day: [8:00 to 20:00]; Night: [20:00 to 08:00]. The periods are different in **MPDP** and **MPS**

**Definition 3.1 (Distance Decay Function)**

Based on the work in [CHG15], we define a **distance decay function** by:

$$\tau(d, \phi) = \begin{cases} \frac{(-d^4 + \phi^4)}{\phi^4 \cdot \exp((\frac{d}{2\phi})^3)} & , \text{ if } d \leq \phi \\ 0 & , \text{ if } d > \phi \end{cases} \quad (3.1)$$

to present the charging preference **a**). Where  $d$  represents the distance between two places, and  $\phi$  is called the distance threshold. As shown in Fig.3.1,  $\tau(d, \phi)$  takes near to one if the two places are very close, and it will decrease as distance increases, becoming zero if  $d \geq \phi$ .  $\square$

Definition 3.2 is proposed to model the price-sensitivity of charging perference **b**):

**Definition 3.2 (Price-Scaled Distance)**

We denote  $\hat{d}_{ij}$  as the **price-scaled distance** between a CS  $i \in I$  and a POI  $j \in J$ :

$$\hat{d}_{ij} = \frac{u_i}{\bar{u}} \cdot d_{ij}, \quad i \in I, j \in J \quad (3.2)$$

where:

$$\bar{u} = \frac{\sum_{i \in I} u_i}{|I|}, \quad I \neq \emptyset$$

is the average charging price of all candidate locations. It means that the walking distance  $d_{ij}$  between a CS  $i \in I$  and a POI  $j \in J$  for EV drivers to recharge is scaled up or down to  $\hat{d}_{ij}$  by the charging price  $u_i$  at that CS  $i$  in comparison with the average charging price.  $\square$

For simplicity, we denote:

$$\tau_{ij} := \tau(\hat{d}_{ij}, \phi^{IJ}), \quad i \in I, j \in J \quad (3.3)$$

as the *charging attractiveness factor* of a CS located at  $i \in I$  to a POI  $j \in J$ , where  $\phi^{IJ}$  is the walking distance threshold for recharging EVs. For example,  $\tau_{ij} = 0$  shows that CS  $i$  is not attractive at all for EV arrivals at  $j$  to recharge. With this notation, we define:

$$\mathcal{A}_{ij}^t := \tau_{ij} \mathcal{A}_j^t, \quad i \in I, j \in J \quad (3.4)$$

as the *number of price-scaled-distance-decayed EV arrivals* at a POI  $j \in J$  during period  $t \in T$ , which are interested in recharging at a CS  $i \in I$ . Taking picture 3.1 for example, if  $\phi^{IJ} = 1/6$  hour, it means that if the price-scaled distance ( $\hat{d}_{ij}$ ) is more than ten minutes (1/6 hour) between a CS  $i \in I$  and all POIs  $J$ . Then that CS  $i$  will not attract or cover the CD of any EV arrival at any POI  $j \in J$  ( $\tau_{ij} = 0$ ,  $\mathcal{A}_{ij}^t = 0 \forall j \in J$ ). Because drivers will find it too far away to walk there to recharge at that CS considering the expensive recharging fee there.

In addition, those candidate locations for CSs which attract no EVs from POIs to recharge are called  $\phi$ -*u-isolated*, and formally defined as:

**Definition 3.3 ( $\phi$ -u-isolated)**

Given a set of POIs  $J$ , a CS  $i \in I$  is called  $\phi$ -u-isolated if:

$$\sum_{j \in J} \tau_{ij} = 0 \quad (3.5)$$

where  $\tau_{ij}$  as defined in (3.3). This means a  $\phi$ -u-isolated CS is too expensive or too far away and shows no attractiveness for EV drivers visiting any POI to recharge. Based on it, we define:

$$\bar{I} := \{i \mid \sum_{j \in J} \tau_{ij} = 0, i \in I\} \quad (3.6)$$

as the set of  $\phi$ -u-isolated candidate locations.  $\square$

**Charging Demand of each EV arrival**

Now we propose in definition 3.4 an approximation approach of the charging demand (CD) of each EV recharging process involving parking time and arrival SOC:

**Definition 3.4 (Charging Demand of each EV Arrival)**

During a period  $t \in T$ , given a walking distance threshold for recharging EVs  $\phi^{IJ}$ , we denote  $\mathcal{D}_{ij}^t$  as the Charging (energy) Demand of each EV visit to a POI  $j \in J$  recharging at a CS  $i \in I$ , and define it as:

$$\mathcal{D}_{ij}^t = \begin{cases} \min\{\pi \cdot \mathcal{T}_{ij}^t, (1 - \delta_j^t) \cdot B_{cap}\} & , \text{ if } \hat{d}_{ij} \leq \phi^{IJ} \\ 0 & , \text{ else.} \end{cases} \quad (3.7)$$

where

$$\mathcal{T}_{ij}^t := \mathcal{T}_j^t + 2d_{ij} \quad (3.8)$$

represents the parking time of the EV arrival at  $j$  recharging at the CS  $i$ .  $\square$

Definition 3.4 declares that there will be no charging demand  $\mathcal{D}_{ij}^t$  if the price-scaled distance between a CS and a POI is further than the walking distance threshold for recharging EVs ( $\mathcal{D}_{ij}^t = 0$ , if  $\hat{d}_{ij} > \phi^{IJ}$ ). It also shows that the CD of an EV arrival is influenced by the parking time and arrival SOC of that EV. That is, the CD is determined by the minimum of the energy served to the EV during the parking time and the energy that the battery needs until being fully recharged. For the first case, CPs actively supply energy for the whole parking period, and for the latter case, CP stops working when the battery is full. For a better understanding of this, please refer to Example B.1.

Furthermore, EVs at the same POI might choose different CSs to charge. Definition 3.4 implies that the estimated CD of each EV arrival can depend on which CS it parks at to recharge because different walking distances to different CSs result in different

lengths of parking time, which will lead to different CD estimated. For example, given a POI  $j_0 \in J$  and we define:

$$\hat{I} = \{i \mid \hat{d}_{ij_0} \leq \phi^{IJ}, i \in I\} \quad (3.9)$$

as the *set of CSs near  $j_0$  within the walking distance threshold  $\phi^{IJ}$* . If  $|\hat{I}| \geq 2$  and  $\exists i_0, i_1 \in \hat{I}$  such that:

$$d_{i_0 j_0} \neq d_{i_1 j_0} \quad \wedge \quad \pi \cdot (\mathcal{T}_{j_0}^t + 2d_{i_0 j_0}) \leq (1 - \delta_{j_0}^t) \cdot B_{cap}, \forall i \in \{i_0, i_1\}$$

Then it implies:

$$\mathcal{D}_{i_0 j_0}^t \neq \mathcal{D}_{i_1 j_0}^t$$

Due to this characteristic, we also name the CD of each EV arrival given in definition 3.4 the *Dynamic CD of each EV arrival*. If it is not explicitly mentioned, all CD referred in the following part of this thesis implies the *Dynamic CD*.

### 3.1.2 Supply Capability of CSs

Just as a warehouse has limited capacity, a CS has limited charging energy capacity or charging Energy Supply Capability (**ESC**) due to the limited number of CPs that can be installed. The most common approximation approach of **ESC** of a CP is to define it by taking the product of the power rating of a CP and the period length. We call this approach of the **ESC** of a CP the Theoretical Energy Supply Capability (**TESC**) and denote it as:

$$w(t) := \pi \cdot \Delta t \quad (3.10)$$

This common approach **TESC**, however, can sometimes produce a misleading estimation of the real **ESC**, especially when fast chargers are occupied by some EVs with high-level SOC parking for a long time. Because few fully-charged EVs can be unplugged and forced to leave immediately [Tru19b]. Example B.2 was given to show a typical overestimation of energy supply capacity by **TESC**.

Moreover, a CS usually serves EVs from various POIs with different POI statistics. These statistics can have a significant impact on the utilization rate of CPs installed at the CS. For example, an EV arrival with higher SOC often recharges less energy from a CS than an EV with lower arrival SOC. A CS located at the city center is often expected to satisfy more CD than the ones in rural areas due to more frequent arrivals. If that CS happens to be found near many grocery shops with shorter-time parking, its utilization will usually be higher than that of a CS located at a train station, where EV drivers can park their cars for the whole day and block the CPs without recharging. **TESC** again fails to tackle these impacts on the utilization rate of CPs brought by POI statistics. Under such circumstances, it urges a much more precise approximation method to address such exogenous impact by POI statistics on the ESC of CPs.

Regarding temporal issues, we first of all introduce the (*charging*) *Time Service Capability (TSC)* of CSs in definition 3.5:

**Definition 3.5 (TSC)**

During a period  $t \in T$ , the (charging) Time Service Capability of a CS  $i \in I$  is denoted as:

$$\mathcal{T}_i^t := (n_i + \mathbf{y}_i)\Delta t \quad (3.11)$$

□

Then, a more accurate approximation approach, the **Exogenous Energy Supply Capability (EESC)** was proposed by definition 3.6, to address the exogenous impact brought by diverse arrival SOC and Parking time of different frequency of EV arrivals from various POIs:

**Definition 3.6 (EESC)**

The Exogenous (Charging) Energy Supply Capability of non- $\phi$ -u-isolated CSs is defined as

$$\mathbf{w}_i^t = \begin{cases} (\mathbf{y}_i + n_i) \cdot \sum_{j \in J} \frac{\mathcal{A}_{ij}^t}{\sum_{j \in J} \mathcal{A}_{ij}^t \mathcal{T}_{ij}^t} \mathcal{D}_{ij}^t \cdot \Delta t & , i \in I \setminus \bar{I} \\ 0 & , i \in \bar{I} \end{cases} \quad (3.12)$$

By denoting:

$$\mathbf{w}_{ij}^t = \begin{cases} (\mathbf{y}_i + n_i) \cdot \frac{\mathcal{A}_{ij}^t}{\sum_{j \in J} \mathcal{A}_{ij}^t \mathcal{T}_{ij}^t} \mathcal{D}_{ij}^t \cdot \Delta t & , i \in I \setminus \bar{I}, j \in J \\ 0 & , i \in \bar{I}, j \in J \end{cases} \quad (3.13)$$

$\mathbf{w}_i^t$  can be simplified as:

$$\mathbf{w}_i^t = \sum_{j \in J} \mathbf{w}_{ij}^t$$

□

Definition 3.6 proposes that during a specific period, the charging energy a CS is able to supply depends not only on the number of installed charging points but also on exogenous statistics of EV arrivals from POIs. And for those  $\phi$ -u-isolated candidate locations, since there is no CD for them to cover, the ESC is regarded as zero. The derivation of EESC in appendix section B is recommended for a better understanding of it.

Furthermore, variables  $\mathbf{z}_{ij}^t$  are introduced to represent how much percentage of CD at a POI  $j \in J$  is satisfied by an opening CS  $i \in I$  during period  $t \in T$ . And for simplicity, for an opening CS  $i \in I$ ,  $\psi_i^t$  is denoted as *the amount of CD from its nearby POIs the CS i covers during period t*:

$$\psi_i^t := \sum_{j \in J} \mathcal{D}_{ij}^t \mathcal{A}_{ij}^t \mathbf{z}_{ij}^t, \quad \forall i \in I, t \in T \quad (3.14)$$

As a consequence, the *utilization rate (UR)*  $\gamma_i^t$  of a CS  $i \in I$  during period  $t \in T$  is defined as a ratio of the total amount of CD it covers ( $\psi_i^t$ ) to its **TESC** (3.10):

$$\gamma_i^t := \frac{\psi_i^t}{(\mathbf{y}_i + n_i)w(t)} = \frac{\psi_i^t}{(\mathbf{y}_i + n_i)\pi\Delta t} \quad (3.15)$$

For example, during a day of 24 hours, the TESC of a level-2<sup>3</sup> CP is 528kWh = 22kW · 24hour. A 50% UR of this CP in a day means that it covers or serves 264kWh = 528 · 50% CD. Alternatively, the CP's load this day is 264kWh.

### 3.1.3 Base Model

The Multi-Period MILP Base model is proposed in this section to determine the optimal allocation of EV CSs using the CD and ESC estimation presented in previous sections. We first summarize the notations introduced in **Base Model** in **Table 2**, **Table 3**, and **Table 4**.

With all the elements provided above, we can now propose **Base Model** as follows:

---

<sup>3</sup>A level-2 CP has a power rating of 22 kW

$$\max_{\mathbf{x}, \mathbf{y}, \mathbf{z}} \sum_{t \in T} \sum_{i \in I} \sum_{j \in J} u_i \mathcal{D}_{ij}^t \mathcal{A}_{ij}^t \mathbf{z}_{ij}^t \cdot 365 - \left( \sum_{i \in I} c_i^x \mathbf{x}_i + c^y \mathbf{y}_i \right) \quad (3.16)$$

$$\text{s.t.:} \quad \sum_{i \in I_0} \mathbf{x}_i \leq N_0 \quad (3.17)$$

$$\sum_{i \in I_1} \mathbf{x}_i \leq N_1 \quad (3.18)$$

$$\sum_{i \in I} \mathbf{x}_i \leq N^{\mathbf{x}} \quad (3.19)$$

$$\sum_{i \in I} \mathbf{y}_i \leq N^{\mathbf{y}} \quad (3.20)$$

$$\mathbf{x}_i \leq \mathbf{y}_i, \quad i \in I \quad (3.21)$$

$$\mathbf{y}_i \leq m_i \mathbf{x}_i, \quad i \in I \quad (3.22)$$

$$\mathbf{x}_i \mathbf{x}_j (\rho - d_{ij}) \leq 0, \quad i, j \in I, i \neq j \quad (3.23)$$

$$\sum_{j \in J} \mathcal{D}_{ij}^t \mathcal{A}_{ij}^t \mathbf{z}_{ij}^t \leq \mathbf{w}_i^t, \quad i \in I, t \in T \quad (3.24)$$

$$\sum_{j \in J} \mathcal{T}_{ij}^t \mathcal{A}_{ij}^t \mathbf{z}_{ij}^t \leq \mathcal{T}_i^t, \quad i \in I, t \in T \quad (3.25)$$

$$\sum_{i \in I} \mathcal{D}_{ij}^t \mathcal{A}_j^t \mathbf{z}_{ij}^t \geq \min \{ \mathcal{D}_j^t \mathcal{A}_j^t, \sum_{i \in I} \mathbf{w}_{ij}^t \}, \quad j \in J, t \in T \quad (3.26)$$

$$\sum_{i \in I} \mathbf{z}_{ij}^t \leq 1, \quad j \in J, t \in T \quad (3.27)$$

$$\mathbf{x}_i \in \{0, 1\} \quad i \in I \quad (3.28)$$

$$\mathbf{y}_i \in \mathbb{Z}, \quad i \in I \quad (3.29)$$

$$\mathbf{z}_{ij}^t \geq 0 \quad i \in I, j \in J, t \in T \quad (3.30)$$

The objective of **Base Model** (3.16) is to maximize the investment profit considering the placement annuity cost of CSs and of CPs. Where the first term represents the annual profit of satisfying covered CD, and the second summation term is the total annuity of locating CSs and installing chargers. Constraints (3.18) – (3.19) limit the scale of investment on CIs. Constraints (3.21) and (3.22) set a lower bound and an upper bound of the number of CPs to be sited after a CS is built or updated. It is required by constraints (3.23) that the location of a CS to build or to update is not too close (less than a walking distance of  $\rho$  hour) to another new or existing CS. One can see these constraints are active in the case that both  $\mathbf{x}_i = 0$  and  $\mathbf{x}_j = 0$  are one. Constraints (3.27) and (3.25) play two roles: (1) they ensure that the EESC (TSC) of a CS is not exceeded; and (2) they prevent CD of EV arrivals from being covered by non-open CSs. If opened CSs are found near a POI, EV arrivals at that POI are

expected to benefit at least a certain portion of charging service supplied by those CSs nearby. Thus we introduce a lower bound on CD coverage variables  $\mathbf{z}_{ij}^t$  by constraints (3.26), which propose that either all of the CD at a POI will be satisfied by the CSs nearby, when there are sufficient charging service supply nearby ( $\mathcal{D}_j^t \mathcal{A}_j^t$ ); Or at least an amount of the sum of estimated energy supply to a specific POI ( $\sum_{i \in I} \mathbf{w}_{ij}^t$ ) by CSs nearby should be offered to that POI.<sup>4</sup> Finally, constraints (3.27) – (3.30) claim the domain of decision variables. It is guaranteed by (3.27) that the total satisfied fraction of CD of EV arrivals at POI  $j \in J$  by all CSs during period  $t \in T$  will not exceed 100%, while constraints (3.30) allow the possibility that during some periods, the CD of EV arrivals at some POIs can be totally uncovered, i.e.,  $\sum_{i \in I} \mathbf{z}_{ij}^t = 0, \exists j \in J, t \in T$ . We interpret this as the case of lost CD that usually due to the insufficient supply capability of CSs.

Notice that constraints (3.23) are quadratic, and (3.26) are non-convex piecewise-linear constraints. These two groups of non-linear constraints will make the model hard to solve. Fortunately, with the help of linearization formulation techniques available in pieces of literature such as [Wil13] and [SA13], we can linearize MPDP as follows:

### Linearization of Quadratic Constraints

Since the positions of existing CSs are already known, we firstly reformulate constraints (3.23):

$$\mathbf{x}_i \mathbf{x}_j (\rho - d_{ij}) \leq 0, \quad i, j \in I, i \neq j$$

to (3.31) and (3.32):

$$\mathbf{x}_j (\rho - d_{ij}) \leq 0, \quad i \in I_0, j \in I_1 \quad (3.31)$$

$$\mathbf{x}_i \mathbf{x}_j (\rho - d_{ij}) \leq 0, \quad i, j \in I_1, i \neq j \quad (3.32)$$

On top of this, an additional binary variable  $\mathbf{x}_{ij}$  is introduced to replace the product of binary variables  $\mathbf{x}_i \mathbf{x}_j$  in (3.32) by:

$$\mathbf{x}_{ij} (\rho - d_{ij}) \leq 0, \quad \forall i, j \in I_1, i \neq j \quad (3.33)$$

where:

$$\begin{aligned} \mathbf{x}_{ij} &\leq \mathbf{x}_i, \quad i, j \in I_1, i \neq j \\ \mathbf{x}_{ij} &\leq \mathbf{x}_j, \quad i, j \in I_1, i \neq j \\ \mathbf{x}_i + \mathbf{x}_j - 1 &\leq \mathbf{x}_{ij}, \quad i, j \in I_1, i \neq j \\ \mathbf{x}_{ij} &\in \{0, 1\}, \quad i, j \in I_1, i \neq j \end{aligned} \quad (3.34)$$

The linearization is finished by substituting (3.23) with (3.31), (3.33) and (3.34).  $\square$

---

<sup>4</sup>Refer to appendix B for further details on this lower bound constraints.

### Linearization of Non-Convex piecewise-linear Constraints

Two additional auxiliary variables  $\chi_j^t$  and  $\mathcal{E}_j^t$ , and the *Big-M* parameters  $\mathcal{M}^t$  are introduced to linearize the non-convex piecewise-linear constraints (3.26):

$$\mathcal{D}_{ij}^t \mathcal{A}_j^t \mathbf{z}_{ij}^t = \min\{\mathcal{D}_j^t \mathcal{A}_j^t, \sum_{i \in I} \mathbf{w}_{ij}^t\}, \quad j \in J, t \in T$$

by replacing it with the following constraints:

$$\begin{aligned} \chi_j^t &\leq \mathcal{D}_j^t \mathcal{A}_j^t, \quad j \in J, t \in T \\ \chi_j^t &\leq \sum_{i \in I} \mathbf{w}_{ij}^t, \quad j \in J, t \in T \end{aligned} \tag{3.35}$$

$$\begin{aligned} \chi_j^t &\geq \mathcal{D}_j^t \mathcal{A}_j^t - \mathcal{M}^t (1 - \mathcal{E}_j^t), \quad j \in J, t \in T \\ \chi_j^t &\geq \sum_{i \in I} \mathbf{w}_{ij}^t - \mathcal{M}^t \mathcal{E}_j^t, \quad j \in J, t \in T \end{aligned} \tag{3.36}$$

$$\sum_{i \in I} \mathcal{D}_{ij}^t \mathcal{A}_j^t \mathbf{z}_{ij}^t \geq \chi_j^t, \quad j \in J, t \in T \tag{3.37}$$

$$\chi_j^t \in \mathbb{R}, \quad j \in J, t \in T \tag{3.38}$$

$$\mathcal{E}_j^t \in \{0, 1\}, \quad j \in J, t \in T \tag{3.39}$$

The first group of linear constraints (3.35) implies that:

$$\chi_j^t \leq \min\{\mathcal{D}_j^t \mathcal{A}_j^t, \sum_{i \in I} \mathbf{w}_{ij}^t\}, \quad j \in J, t \in T$$

and combined with the second group of linear constraints (3.36) and large enough proper<sup>5</sup>  $\mathcal{M}^t$ , they ensure that:

$$\chi_j^t = \min\{\mathcal{D}_j^t \mathcal{A}_j^t, \sum_{i \in I} \mathbf{w}_{ij}^t\}, \quad j \in J, t \in T$$

Together with other constraints (3.37), (3.38) and (3.39), they are equivalent to the original non-convex constraints (3.26).  $\square$

Altogether, by applying these linearization techniques to the original **Base Model** proposed before, we get the complete form of *linearized Base Model* in C.

---

<sup>5</sup>Discussion on the proper choice of  $\mathcal{M}^t$  is given in appendix B.

## 3.2 MPDP with Grid Network Constraints

As discussed in sec:intro-LR, the grid reinforcement will be essential to support the rollout of EVCI while avoiding grid congestion. Being aware of this problem, a new modeling approach, *stochastic programming*, and additional constraints are introduced on top of the **Base Model** in **MPSP** in section 3.3, to address the grid congestion caused by connecting chargers to the electricity network. But before diving into the world of uncertainty, it is worth taking a first look at the deterministic model **MPDP** to get well-prepared.

### 3.2.1 Grid Congestion

Rather than at centralized, high-voltage transmission systems, latest reports [ACE22] and [Con+22] demonstrate that integration of CSs to grid systems will primarily require power expansion at medium- and low-voltage distribution systems carrying electricity from SSs to end users. Since the low- and medium-voltage grids are where peak power issues are usually found and the largest congestion is expected (cf. Figure 2.1).

According to this, we denote  $K$  as the set of SSs with available power load capacity  $\Pi_k^t$  at each substation  $k \in K$  during period  $t \in T$ . Variables  $\mathbf{h}_k \in \mathbb{Z}$ ,  $k \in K$  [kW] decide the scale of power expansion at the substation  $k \in K$ . The annuity fee of expanding power capacity is treated consistently for any substation and denoted as  $c^h$  [Euro/kW]. The grid upgrade cannot solely exclude all risks of grid congestion since the expansion size can be inadequate. As a proper response to insufficient grid expansion, an alternative technology—*Backstop Technology* (BT) [BL11]—should be applied to generate extra power for a non-congested grid. Variables  $\eta_k^t$ ,  $k \in K, t \in T$  decide the scale of backstop technology to apply at substation  $k \in K$  during overloaded period  $t \in T$  at a consistent cost of  $c^\eta$  [Euro/kWh]. The cost of back-stop technology is usually expensive. Since we are optimizing from the perspective of CSOs, the costs  $c^h$  and  $\eta_k$  are considered as a portion of fees the CSOs need to take with DSOs for the SSs upgrades and BT applications due to the integration of their CIs. Parameter  $Z_{ik} \in [0, 1]$  is denoted as the *indicator of grid connection status* between a candidate location  $i \in I$  and a substation  $k \in K$ :

$$Z_{ik} = \begin{cases} 1, & \text{if } i \text{ is connected to } k \\ 0, & \text{else.} \end{cases} \quad \wedge \quad \sum_{k \in K} Z_{ik} \leq 1, \quad i \in I \quad (3.40)$$

where the inequalities in (3.40) guarantee that each candidate location for CSs can connect to at most one substation. In **MPDP**, we assumed the grid connection information to be perfect. Parameters and variables introduced in **MPDP** are summarized in Table 5.

### 3.2.2 MPDP

Now we propose the **MPDP** including grid expansion decisions and costs under the assumption that the connections between CSs and SSs are known:

$$\max_{\mathbf{x}, \mathbf{y}, \mathbf{z}, \mathbf{h}, \eta} \sum_{t \in T} \sum_{i \in I} \sum_{j \in J} u_i \mathcal{D}_{ij}^t \mathcal{A}_{ij}^t \mathbf{z}_{ij}^t \cdot 365 - (\sum_{i \in I} c_i^x \mathbf{x}_i + c^y \mathbf{y}_i + \sum_{k \in K} 50 \cdot c^h \mathbf{h}_k + \sum_{t \in T} \sum_{k \in K} 50 \cdot c^\eta \eta_k^t \cdot 365) \quad (3.41)$$

s.t.:

$$(3.17) - (3.30)$$

$$\mathbf{x}_i \leq \sum_{k \in K} Z_{ik}, \quad i \in I \quad (3.42)$$

$$\sum_{i \in I} Z_{ik} \psi_i^t \leq (\Pi_k^t + 50 \cdot \mathbf{h}_k + 50 \cdot \eta_k^t) \Delta t, \quad k \in K, t \in T \quad (3.43)$$

$$\mathbf{h}_k \in \mathbb{Z}, \quad k \in K \quad (3.44)$$

$$\eta_k^t \in \mathbb{Z}, \quad k \in K, t \in T \quad (3.45)$$

The new terms involving  $\mathbf{h}_k$  and  $\eta_k^t$  in objective (3.41) of **MPDP** correspond to the grid upgrade and Back-stop technology cost. Since it is rare to upgrade only several kilowatts of power load at SSs, the model requires the grid upgrades to be in the unit of [50 kW]. Similar regulations are also applied to the usage of backstop technology (in the unit of [50 kW]). Constraints (3.42) ensure that if no SS is connecting to CS  $i \in I$ , then no CS will be built at  $i$ . Grid congestion is managed by constraints (3.43), which force grid expansion to make sure, that for each substation  $k \in K$ , the total CD covered by its connected CSs can not exceed the grid load capacity at  $k$ . The final constraints (3.44) claim the range of new variables  $\mathbf{h}_k$ .

Similar as **Base Model**, **MPDP** can be linearized according to section 3.1.3 and section 3.1.3. The compact form of linearized **MPDP** is given in C

## 3.3 MPSP with Grid Network Constraints

In real cases, grid information is usually imperfect for CSOs. This can include, for instance, the number, locations, and sizes of SSs as well as the connection topology of SSs to CSs. To better support the decision-making processes of EVCSAP, it is important to embed such uncertainty of grid information in optimization models to obtain solutions that can anticipate it and manage grid congestions. Fortunately, such problems can often be cast within a *stochastic programming* modeling framework as introduced briefly in appendix A. In the following parts, we propose the **MPSP**, to address grid congestion caused by integrating EV CSs in the uncertain distribution network.

### 3.3.1 Grid Congestion under Uncertainty

The number and positions of SSs can be partly collected through Opensource Maps such as [OpenStreetMap](#) and so on. The uncertain available power capacity of SSs during different periods can be approximated by data from recent research works [Ber+21] [Powell2022] [G+16]; In **MPSP**, we assume perfect information of the number and positions as well as the available power loads of SSs during each period  $t \in T$ . Therefore, **MPSP** inherited all notations, parameters and decision variables from **Base Model** and **MPSP**, except for *indicator of grid connection status* in (3.40).

Particularly, we denote a set of scenarios  $\Omega$  for all possible realization of grid connections between SSs and candidate locations for CSs in the distribution network. Since the number of CSs and SSs are finite, we will have a finite number of grid connection scenarios. In **MPSP**, the only stochastic parameters are *indicators of stochastic grid connection status*  $\mathcal{Z}_{ik} := \mathcal{Z}_{ik}(\omega)$ ,  $i \in I, k \in K, \omega \in \Omega$ , and we suppose a full knowledge of the joint probability distribution of them. For convenience, we use  $\mathcal{Z}_{ik}(w)$  as random variables, while  $\mathcal{Z}_{ik}$  stands for a specific realization of the random variable. Given any realized scenario  $\omega \in \Omega$ ,  $\mathcal{Z}_{ik}$  satisfies (3.46):

$$\sum_{k \in K} \mathcal{Z}_{ik} = 1, \forall i \in I \quad \wedge \quad \mathcal{Z}_{ik} \in \{0, 1\}, \forall i \in I, k \in K \quad (3.46)$$

And we denote:

$$\mathcal{Z}(\omega) := ((\mathcal{Z}_{ik}(w))_{\{i \in I, k \in K\}}), \omega \in \Omega; \quad \mathcal{Z} := ((\mathcal{Z}_{ik})_{\{i \in I, k \in K\}})$$

for simplicity.

**MPSP** also involves a *two-stage optimization model* as illustrated in A. We denote  $X := (\mathbf{x}, \mathbf{y}, \mathbf{z}, \mathbf{h})$  as the set of first-stage decision variables. Notice that decision variables  $\mathbf{z}$  representing EVs CD coverage also belong to first-stage decisions since whether EVs from POIs recharge at some CSs is almost surely independent of the underlying connection between CSs and SSs. After the first-stage decisions regarding CI allocation, SSs expansion, and EVs CD coverage are settled, overload can be observed owing to the underlying actual grid connections. For example, due to the imperfect grid connection information, an SS connecting to many CSs is unfortunately not selected for an upgrade (or it is upgraded, but the expansion size is too small) in the first-stage decision. Under such circumstances, reactions need to be taken to mitigate grid congestion. Similar to **MPDP**, back-stop technology should be applied to generate extra load. We denote the second-stage decision variables,  $\eta_k^t(\omega)$ ,  $k \in K, t \in T, \omega \in \Omega$ , deciding the scale of *backstop technology* to apply at substation  $k \in K$  during overloaded period  $t \in T$  under scenario  $w \in W$  at a consistent cost of  $c^\eta$  [Euro/kWh].

### 3.3.2 MPSP

With **Table 6** summarizing the additional notations introduced in **MPSP**, we can now propose the two-stage stochastic programming model **MPSP**:

$$\max_{\mathbf{x}} \sum_{t \in T} \sum_{i \in I} \sum_{j \in J} u_i \mathcal{D}_{ij}^t \mathcal{A}_{ij}^t \mathbf{z}_{ij}^t \cdot 365 - \left( \sum_{i \in I} c_i^x \mathbf{x}_i + c^y \mathbf{y}_i + \sum_{k \in K} 50 \cdot c^h \mathbf{h}_k + \mathbb{E}_{\mathcal{Z}}[Q(X, \mathcal{Z}(\omega))] \right) \quad (3.47)$$

s.t.:

$$(3.17) - (3.30), \text{ and } (3.44)$$

where:

$$Q(X, \mathcal{Z}(\omega)) := \min_{\eta} \sum_{t \in T} \sum_{k \in K} 50 \cdot c^{\eta} \eta_k^t(\omega) \cdot 365 \quad (3.48)$$

$$\text{s.t.: } \mathbf{x}_i \leq \sum_{k \in K} \mathcal{Z}_{ik}(\omega), \quad i \in I, \quad (3.49)$$

$$\sum_{i \in I} \mathcal{Z}_{ik}(\omega) \psi_i^t \leq (\Pi_k^t + 50 \cdot \mathbf{h}_k + 50 \cdot \eta_k^t(\omega)) \Delta t, \quad k \in K, t \in T, \quad (3.50)$$

$$\eta_k^t(\omega) \in \mathbb{Z}, \quad k \in K, t \in T, \quad (3.51)$$

In addition to the objective (3.41) of **MPDP**, the objective (3.47) of **MPSP** involves a new expectation term  $\mathbb{E}_{\mathcal{Z}}[Q(X, \mathcal{Z}(\omega))]$  — the *recourse function* [BL11] — taken over all realizations of scenario  $\omega \in \Omega$  and first-stage decisions. Thus, this second-stage model (3.48)–(3.51) is the more difficult one, as for each scenario  $\omega \in \Omega$ , the value  $\mathcal{Z}(\omega)$  is the solution of a linear program. In other words, linear programs are defined to solve for every realization of grid connections  $\mathcal{Z}(\omega)$  and implemented decisions of CI planning and power upgrades. Accordingly, second-stage decisions  $\eta$  on the usage of backstop technology are possible to change in reaction to different observations of the random variables. Because of this, they are referred to as *recourse decisions* [LNS19]. Constraints (3.49) tightly guarantee that if there exists any connection scenario, where a candidate location is not connected to the grid, then it will not be chosen for CI construction or update. Constraints (3.50) guard grid stability by two options: 1) Given concrete first-stage decisions, to purchase expansive supplementary power as recourse; 2) To encourage the optimizer to consider alternative first-stage decisions, either more power expansion to increase energy supply or, a smaller scale of CSs planning. Finally, The last group of constraints defines the domain of recourse decisions.

### 3.3.3 Scenario Generation

In stochastic programming, defining or generating scenarios is itself a relevant problem. As it is either important to instantiate large model involving realizations of all scenarios,

or practical to restrict the set of scenarios in a sampling scheme used within solution procedures such as Monte Carlo methods [LNS19].

Another major contribution of this thesis is the efficient scenario generation algorithm — **2D-C-S-NET** (Distance Decayed CS-SS Connection Scenario Generation under Neighborhood Effect) — for defining the possible topologies of grid connection between SSs and CSs. It is an algorithm principally based on the following grid knowledge from industry experts:

- i.) The closer the distance between a CS and a SS is, the higher the possibility of a connection between them will be. Furthermore, within a certain small distance threshold, this possibility of connection will almost not increase. Whereas if they are far away from each other than a distance threshold, it will be impossible for them to be connected [G+16].
- ii.) Given two CSs  $i_1, i_2 \in I, i_1 \neq i_2$  in a neighborhood, and two SSs  $k_1, k_2 \in K, k_1 \neq k_2$  with  $d_{i_2 k_1} = d_{i_2 k_2}$ . Based on i.),  $i_2$  is evenly possible to connect to  $k_1$  or  $k_2$ . But if  $i_1$  is found to be connected to  $k_2$ , its neighbor CS  $i_2$  is then more likely to connect to SS  $k_2$  than SS  $k_1$  (an additional possibility of connection is rewarded to  $k_2$  due to the neighborhood connection of  $i_1$  to  $k_2$ ). And the closer  $i_1$  is to  $i_2$ , the higher the additional grid connection possibility of  $i_2$  will be rewarded to  $k_2$ . For convenience, we name this statement as *neighborhood effect*.

The above two statements can be well represented by utilizing the distance-decay function introduced in definition 3.1. We denote  $\phi^{IK}$  the *distance threshold of grid connection* and  $\phi^{II}$  the *threshold of neighborhood radius*. On top of these, we define:

**Definition 3.7 (Weights of Grid Connection)**

$$\tau_{ik} := \tau(d_{ik}, \phi^{IK}), \quad i \in I, k \in K \quad (3.52)$$

as the grid connection weights. And for convenience, we denote:

$$\tau_i := (\tau_{ik_1}, \tau_{ik_2}, \dots, \tau_{ik_{|K|}}), \quad i \in I \quad (3.53)$$

as the vector of grid connection weights of a CS  $i \in I$  □

And grid connection probability distribution of CSs is defined as follows:

**Definition 3.8 (Probability Distribution of CS-SS Grid Connection )**

Given  $I := \{i_1, i_2, \dots, i_{|I|}\}$  the set of CSs and  $K := \{k_1, k_2, \dots, k_{|K|}\}$  the set of SSs, we denote  $\mathcal{Z}_i := (\mathcal{Z}_{ik_1}, \mathcal{Z}_{ik_2}, \dots, \mathcal{Z}_{ik_{|K|}})^T$ ,  $i \in I$  as the vectors containing the grid connection information of CSs, where  $\mathcal{Z}_{ik}$ ,  $i \in I, k \in K$  as defined in (3.46). Then the grid connection probability distribution of  $\mathcal{Z}_i$ ,  $i \in I$  is given by:

$$\mathbb{P}[\mathcal{Z}_i = (\mathcal{Z}_{ik_1}, \mathcal{Z}_{ik_2}, \dots, \mathcal{Z}_{ik_{|K|}})^T] = \prod_{k \in K} p_{ik}^{\mathcal{Z}_{ik}} \quad i \in I \quad (3.54)$$

where  $p_{ik}, i \in I, k \in K$  are defined as:

$$p_{ik} := \mathbb{P}[\mathcal{Z}_{ik} = 1] := \begin{cases} \frac{\tau_{ik}}{\sum_{\bar{k} \in K} \tau_{i\bar{k}}} & \text{if } \sum_{\bar{k} \in K} \tau_{i\bar{k}} > 0 \\ 0 & \text{else.} \end{cases}, \quad i \in I, k \in K \quad (3.55)$$

$$\mathbb{P}[\mathcal{Z}_{ik} = 0] := 1 - \mathbb{P}[\mathcal{Z}_{ik} = 1], \quad i \in I, k \in K \quad (3.56)$$

with  $\tau_{ik}, i \in I, k \in K$  the weights of grid connection as defined in (3.52). To prove that (3.55) and (3.56) define valid probability distribution for  $\mathcal{Z}_{ij}, i \in I, j \in J$  is trivial. And notice that (3.54) defines a special case of the multinomial distribution.  $\square$

Based on the above definition, a grid connection example expressing the grid knowledge i.) is given in **Figure 3.2**, where in that case,  $\mathbb{P}[\mathcal{Z}_1 = (1, 0)] = 1$ ;  $\mathbb{P}[\mathcal{Z}_1 = (0, 1)] = 0$ .

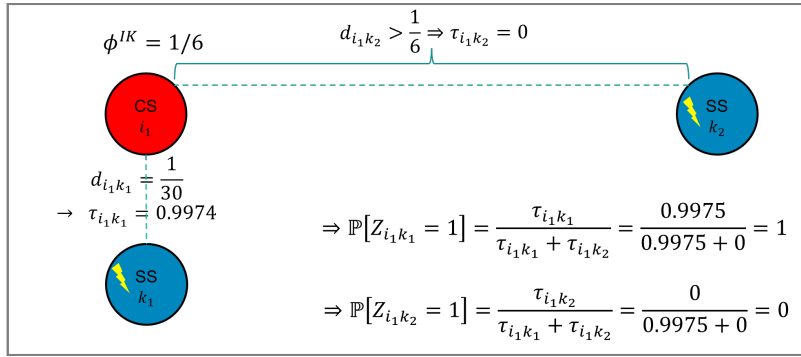


**Figure 3.2:** Grid Connection Probability defined by Grid Connection Weights.

To translate the statement ii.) of neighborhood effect, we define:

**Definition 3.9 (Factors of Neighborhood Effect)**

$$\tau_{i_1 i_2} := \tau(d_{i_1 i_2}, \phi^{II}), \quad i_1, i_2 \in I, i_1 \neq i_2 \quad (3.57)$$

as neighborhood effect factors, which will be added on grid connection weights before applying (3.55) for calculating the probability of grid connection.  $\square$

It is critical to notice that the neighborhood effect depends on the order of observations. For the instance in **Figure 3.3**, after neighborhood effect is applied,  $\mathbb{P}[\mathcal{Z}_2 = (0, 1)] = \frac{2}{3}$ ;  $\mathbb{P}[\mathcal{Z}_2 = (1, 0)] = \frac{1}{3}$ . Whereas if  $\mathcal{Z}_{i_1 k_2}$  was unknown and we spotted  $i_2$  connecting to  $k_1$  at first, then a scenario where  $i_1$  connecting  $k_1$  will be more likely to be generated.

Finally, we propose the **2D-C-S-NET** in **Algorithm 1**. This algorithm generate a list  $\Omega = \{\mathcal{Z}(\omega = 1), \mathcal{Z}(\omega = 2), \dots, \mathcal{Z}(\omega = |\Omega|)\}$  of  $|\Omega|$  samples of scenario realizations. Notice that in the algorithm,  $\omega \notin \Omega$ , because  $\omega$  is the index of a scenario, while  $\mathcal{Z}(\omega)$  is the one containing observed grid connection information from the scenario  $\omega$ . And duplicates

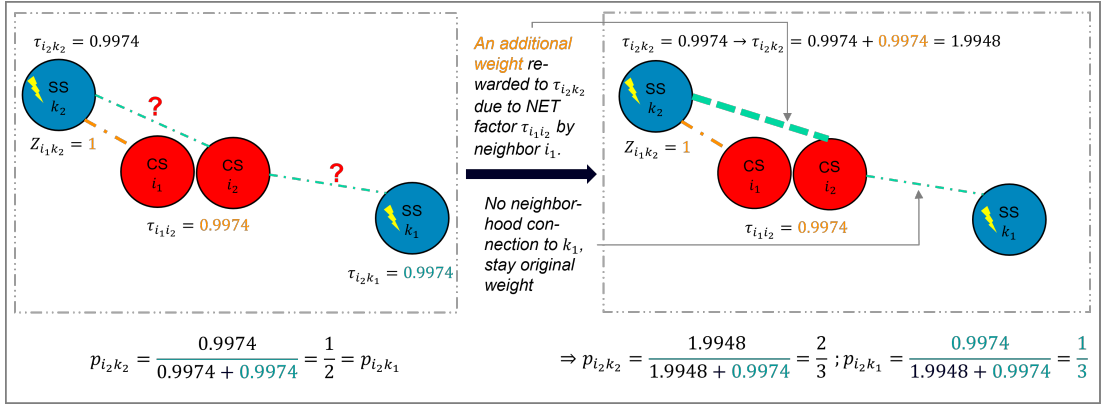


**Figure 3.3:** Grid Connection Probability defined by Grid Connection Weights under Neighborhood Effect.

are allowed in  $\Omega$ , because what this algorithm offered is a *sampling method*. Though seldom, it does exist such a possibility that several samples of scenario realizations represent the same scenario. Line 5 shuffled the set of CSs to generate a random order of observations of the CS-SS grid connection. Line 6 defined a set of observed CSs that are used for calculating neighborhood effects on other CSs. Line 11–line 13 calculate the neighborhood effect vector  $R_i \in \mathbb{R}^K$  and re-define the weight vector  $\tau_i \in \mathbb{R}^K$  of grid connection. For example, in **Figure 3.4**, the original grid connection weights of  $i_2$  is

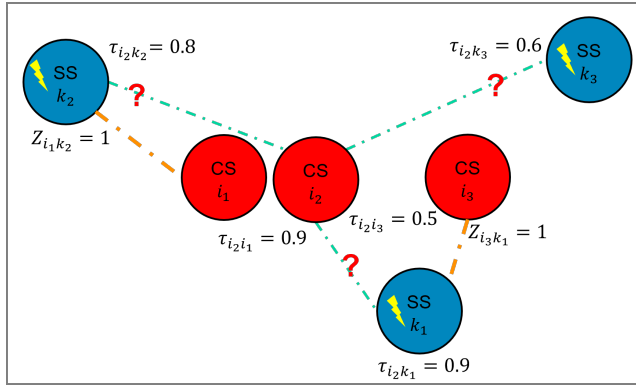


**Figure 3.4:** Illustration on Vector Calculation of Grid Connection Weights under Neighborhood Effect.

$\tau_{i2} = (0.9, 0.8, 0.6)$ . But grid connections information of CSs  $i_1$  and  $i_3$  are observed before CS  $i_2$ , thus  $\tau_{i2}$ —the weights of grid connection of CS  $i_2$ —will be affected by both

---

**Algorithm 1:** Distance Decayed CS-SS Connection Scenario Generation under Neighborhood Effect

---

```

input :  $|\Omega| \in \mathbb{Z}; \tau_{i_1 i_2}, i_1, i_2 \in I, i_1 \neq i_2; \tau_{ij}, i \in I, j \in K$ 
output :  $\Omega$  /* list of Generated Scenarios */

1  $\omega \leftarrow 1$  /* index of a scenario */
2  $\Omega \leftarrow \emptyset$ 
3 while  $\omega \leq |\Omega|$  do generate a cs-ss connection scenario  $\omega$  for all CSs
4    $\mathcal{Z}(\omega) \leftarrow \mathbf{0}$  /* defalt  $\mathbf{0}$ : all CSs disconnected */
5    $I^*(\omega) \leftarrow \text{Shuffled } I$ 
6    $\bar{I} \leftarrow \emptyset$  /* Set of CSs with observed CS-SS connection */
7   for  $i \in I^*(\omega)$  do sample connection status for a CS  $i$ 
8     if  $\sum_{k \in K} \tau_{ik} \leq 0$  then no SSs near  $i$  to connect
9       skip to the next iteration and continue to sample the connection status of
          other CS  $i$ .
10    end
11     $R_i \leftarrow \sum_{i^* \in \bar{I}} \tau_{ii^*} \mathcal{Z}_{i^*}$  /* rewards based on cs-cs dist.-decay. */
12     $\tau_i \leftarrow \tau_i + R_i$  /* add rewards to original weights */
13     $p_{ik} \leftarrow \frac{\tau_{ik}}{\sum_{k \in K} \tau_{ik}}, \forall k \in K$  /* calculate connection prob. */
14    sample  $\mathcal{Z}_i(\omega)$  according to probability distribution defined in definition 3.8
15     $\mathcal{Z}_i := \mathcal{Z}_i(\omega)$  append  $i$  to  $\bar{I}$  /* add  $i$  to set of connected CSs */
16  end
17  append  $\mathcal{Z}(\omega)$  to  $\Omega$ 
18   $\omega \leftarrow \omega + 1$ 
19 end

```

---

of these two observed CSs with:

$$R_{i_2} = \tau_{i_2 i_1} \mathcal{Z}_{i_1} + \tau_{i_2 i_3} \mathcal{Z}_{i_3} = 0.9 * (0, 1, 0) + 0.5 * (1, 0, 0) = (0.5, 0.9, 0)$$

$$\tau_{i_2} = \tau_{i_2} + R_{i_2} = (0.9, 0.8, 0.6) + (0.5, 0.9, 0) = (1.4, 1.7, 0.6)$$

Finally, the algorithm terminates after generating  $|\Omega|$  i.i.d. samples. Consequently, with the  $|\Omega|$  i.i.d. samples generated from **2-D-C-S-NET**, the **MPSP** can be written as *Extensive Form* (EF) with Sample Average Approximation by following the similar approaches in appendix A:

### EF of MPSP

$$\max_{\mathbf{x}, \mathbf{y}, \mathbf{z}, \mathbf{h}, \eta} \sum_{t \in T} \sum_{i \in I} \sum_{j \in J} u_i D_{ij}^t \mathcal{A}_{ij}^t \mathbf{z}_{ij}^t \cdot 365 - \left( \sum_{i \in I} c_i^x \mathbf{x}_i + c^y \mathbf{y}_i + \sum_{k \in K} 50 \cdot c^h \mathbf{h}_k + \frac{1}{|\Omega|} \sum_{w=1}^{|\Omega|} Q(X, \mathcal{Z}(\omega)) \right) \quad (3.58)$$

s.t.:

$$(3.17) - (3.30)$$

$$\mathbf{x}_i \leq \sum_{k \in K} \mathcal{Z}_{ik}(\omega), \quad i \in I, \omega \in \{1, 2, \dots, |\Omega|\} \quad (3.59)$$

$$\sum_{i \in I} \mathcal{Z}_{ik}(\omega) \psi_i^t \leq (\Pi_k^t + 50 \cdot \mathbf{h}_k + 50 \cdot \eta_k^t(\omega)) \Delta t, \quad k \in K, t \in T, \omega \in \{1, 2, \dots, |\Omega|\} \quad (3.60)$$

$$\mathbf{h}_k \in \mathbb{Z}, \quad k \in K \quad (3.61)$$

$$\eta_k^t(\omega) \in \mathbb{Z}, \quad k \in K, t \in T, \omega \in \{1, 2, \dots, |\Omega|\} \quad (3.62)$$

with  $Q(X, \mathcal{Z}(\omega))$  defined as in (3.48).

# Chapter 4

## Computational Experiments and Case Study

**Abstract** This chapter presents the computational performance of the proposed **MPSP** in the German town Schutterwald (SW). In addition, the model **MPDP** is provided as a comparison baseline for **MPSP** to show the significance of the impact of grid connection uncertainty on the decisions and profit of EVCSAP. The chapter starts with a description of the case SW, in section 4.1, including data collection and data processing. The implementation method is briefly mentioned in section D, followed by the computational results in section 4.3<sup>1</sup>. The results consist of a sensitivity analysis and model performances. Notice that the graph network and set of parameters described in section 4.1 were solely created to test models' computational performance, and there must be a discrepancy with the actual situation. Yet it should be emphasized that the models are flexible enough for applying precise and representational data.

### 4.1 Case Description: Schutterwald

The German town Schutterwald in the district of Ortenau in Baden-Württemberg, Germany, is chosen for the case study. This choice is due to the good geographical grid knowledge in this region from our previous study's synthetic data. Nevertheless, the grid connection between SSs and candidate locations for CSs is unknown. For this study, only the consolidated area of the town and the main neighboring areas with concentrated populations are covered. Types of POIs including *charging\_station*, *parking*, *leisure*, *sport*, *shop*, *amenity*, *historic*, *substations* are considered and their locations and sizes are retrieved from [OpenStreetMap \(OSM\) API](#) [empty citation]. Parking areas are selected as candidate locations for building new CSs. The number of parking lots restricts the maximum number of CPs can be installed at different candidate locations. In fact, no existing charging stations are registered in OSM, neither in [Open Charge Map](#)<sup>2</sup>Open Charge Map. The information of the only one existing charging station in the case SW is extracted from the [charging stations card](#)

---

<sup>1</sup>Due to the restriction on the number of pages of the thesis, the large amount of relevant data of figures presented in this chapter will be attached as digital files instead of as text in the thesis appendix.

<sup>2</sup>Source: <https://openchargemap.org/site>

by German Bundesnetzagentur<sup>3</sup>. The case of SW has 158 POIs, 1 existing charging station, 11 candidate locations for building new CSs and 15 candidate substations for power expansion ( $|I_0| = 1, |I_1| = 11, |J| = 158, |K| = 15$ ) is provided in **Figure 4.1**. Its corresponding graph network are presented in **Figure 4.2**. In total, 100 CPs can be installed among these candidate locations with opening CSs. The default budgets for both **MPDP** and **MPSP** are, maximally, eight new CSs to build, one existing CS to update, but the sum of the number of new CSs and updated exisiting CSs should not exceed eight, and 80 CPs to allocate. ( $N_0 = 8, N_1 = 1, N^x = 8, N^y = 80$ )

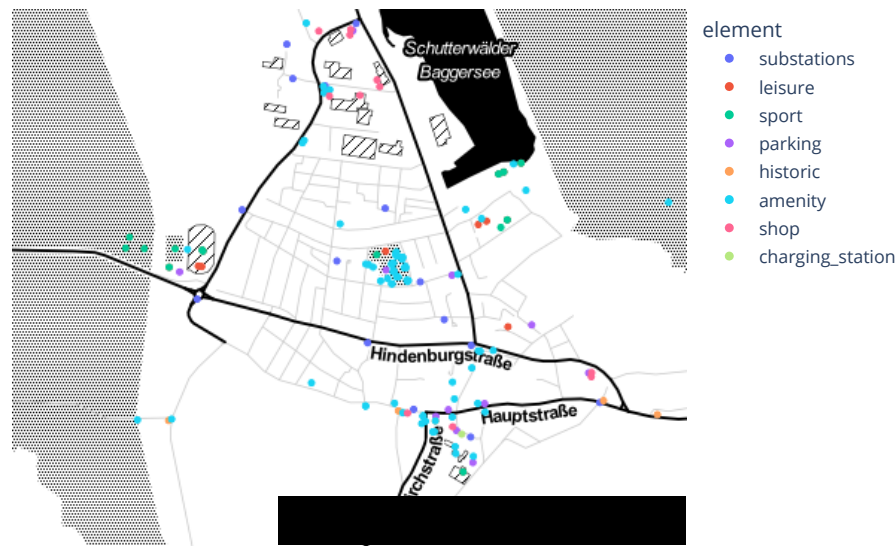


**Figure 4.1:** Map of Schutterwald with POIs, SSs and Candidate Locations for CSs

A typical day is divided into three Periods ( $|T| = 3$ ) according to the grid load periods [Ber+21]. They are **day\_normal** (08:00–17:30 and 19:30–20:00), **day\_peak** (17:30–19:30) and **night** (20:00–08:00). POIs statistics are simulated through Python by sampling from the Beta Distribution for arrival SOCs, the Normal Distribution for visiting duration of EV drivers, and the Poisson Distribution for the number of EV arrivals (cf. **Figure 4.3**). Parameters of different distributions at different types of

---

<sup>3</sup>Source: <https://www.bundesnetzagentur.de/DE/Fachthemen/ElektrizitaetundGas/E-Mobilitaet/Ladesaeulenkarthe/start.html>

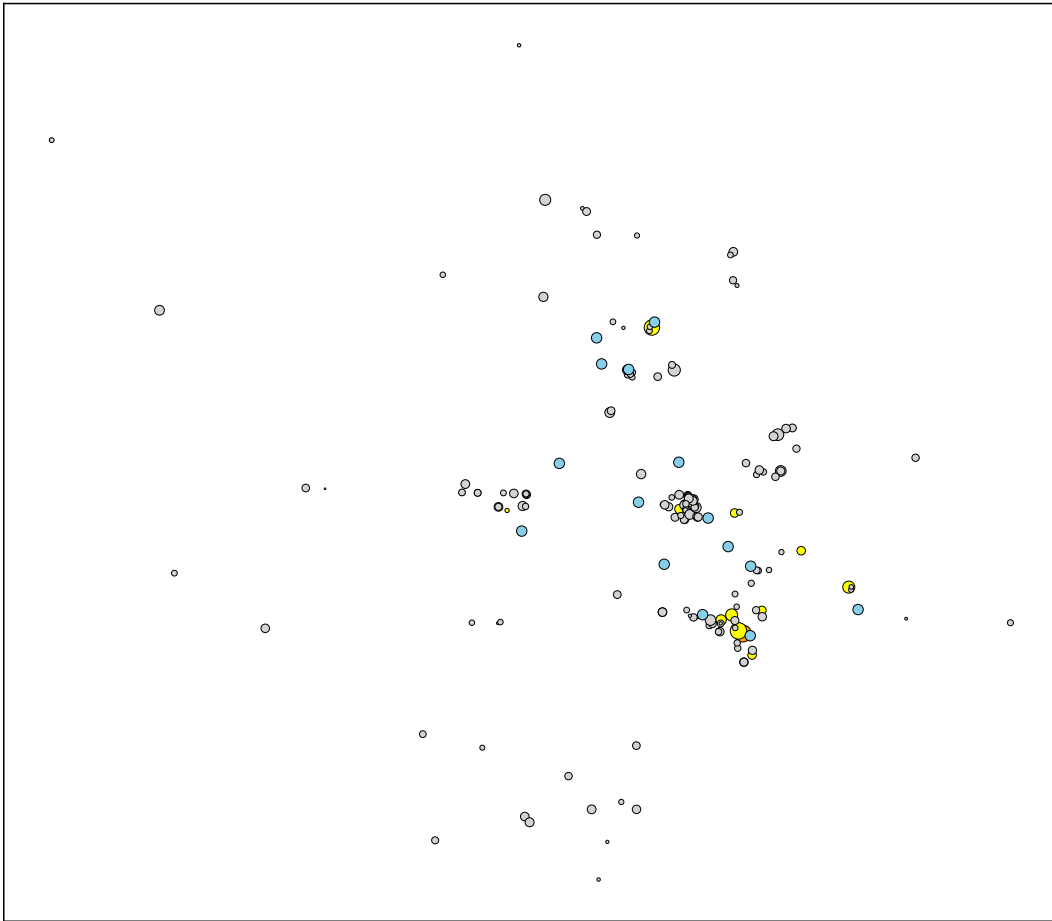


**Figure 4.2:** Graph Network of Schutterwald with POIs, Candidate Locations for CSs and Substations. *skyblue nodes: SSs; Gray nodes: POIs (Size represents the number of EV arrivals); yellow nodes: Candidate locations for building new CSs (size represents the maximum number of CPs can be installed); orange nodes: The candidate location for updating the only existing CS in SW (in the cluster below largely covered by a yellow node and a blue node.)*

POIs are calculated based on population and vehicle density statistics in SW with a high EV penetration rate assumed to be 55%.

Take the number of EV arrivals at the POI type *shop* (supermarkets), for example. According to [Deu22], on average, per 1000 inhabitants own 613 passenger cars in 2021 in Baden-Württemberg. Regarding a population of ca. 7200 in SW<sup>4</sup>, this equals

<sup>4</sup>Source: <https://www.schutterwald.de/de/gemeinde-schutterwald/informationen/>

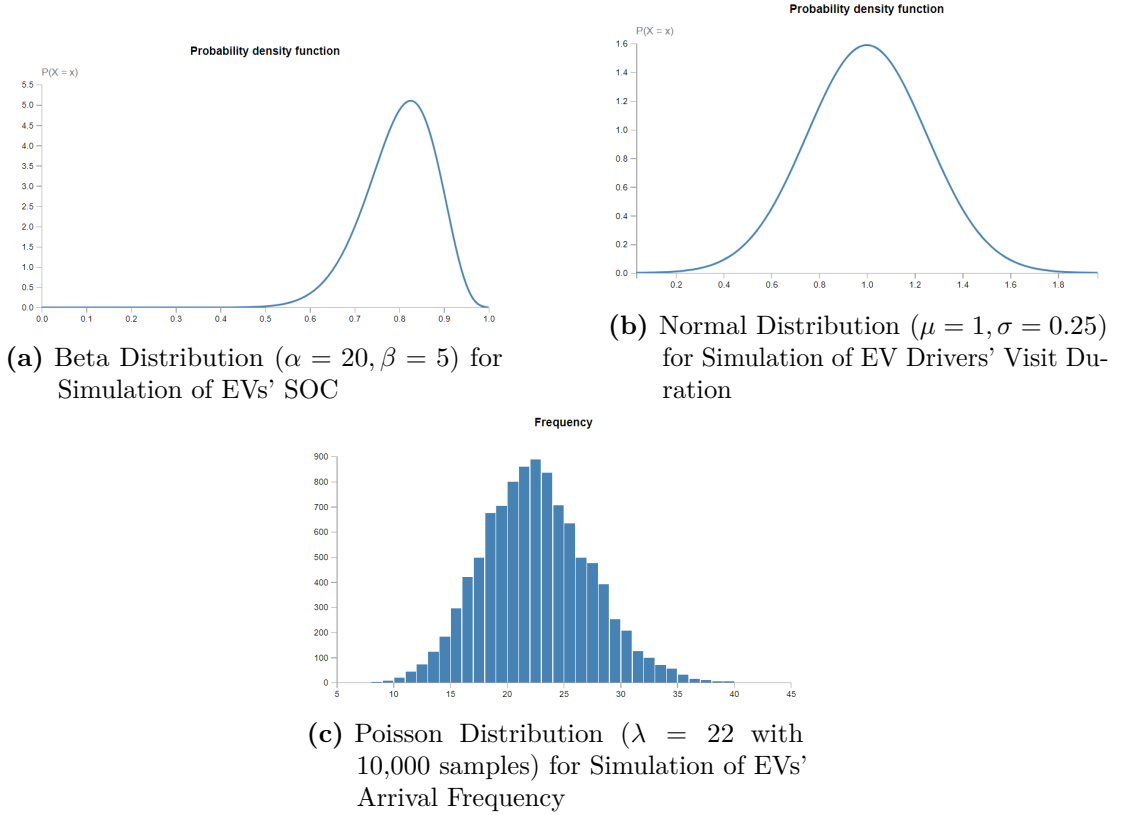


**Figure 4.3:** Probability Distributions for Simulation of POIs Statistics

to a number of  $7200/1000 \cdot 613 \cdot 0.55 = 2427.48$  EVs in this region. Based on the observation of five supermarkets in SW from Google Maps, and under the assumption that each driver buys groceries every third day, each supermarket will share a number of  $(2427.48/3)/5 = 161.83$  buyers arriving by EVs. For a 12-hour daytime, the hourly number of EV arrivals will be  $161.83/12 = 13.48$ . During the 12-hour night period, even some POIs such as museums are closed, if drivers found available CSs near these POIs, they might choose to park and charge their EVs there. Due to this, a very small number ( $> 0$ ) of EV arrivals to some POIs is assumed. On the other hand, the 12-hour daytime is divided into peak grid load and normal grid load periods. The peak load daytime overlaps with one of the grocery shopping peaks, and more EV arrivals per hour will thus be assumed for the `day_peak` period. Finally, the rates (means) of the Poisson Distributions for simulating number of EV arrivals are defined as: `{day_normal: 130, day_peak: 30, night: 5}`. Similar approaches can be applied for other types of POIs.

---

zahlen-daten-fakten

Parameters of probability distributions of visiting duration and SOCs are based on simulations from the eMobility model ABM\_eMob [Hus+21] and web results. The mean value of arrival SOCs falls at around 80%. And the duration of stays at different POIs can range from 15 minutes to hours depending on specific types, while at night, the durations of stays are assumed to be around six hours.

By assuming the life span of a new or updated CS and a new CP to be ten years, the annuity fee of updating an existing CS is imposed to be 2500 Euro  $c_i^x = 2500$ ,  $i \in I_0$ , and the annuity fee of building a new CS to be 3000 Euro  $c_i^x = 3000$ ,  $i \in I_1$ . Whereas installing a new CP costs 2250 Euro annually  $c^y = 2250$  [AGJ20] [Tru19a] [ACE22]. The power rating of all CPs is assumed to be 22 kW ( $\pi = 22$ ). The charging price is set consistently as 0.51 Euro/kWh [Com22] ( $u_i = 0.51$ ,  $i \in I$ ). All new CSs must be at least a two-minute walking distance away from each other and from existing CSs  $\rho = 2/60$  hour.

All EVs are assumed as battery electric vehicles, and the average battery capacity of all EVs is assumed to be 50 kWh ( $B_{cap} = 50$  [Com22]). The walking distances between two locations are calculated based on the approximated road distance between them and the walking speed to recharge EVs (assumed as 5 km/hour). Road distances are approximated by the Euclidean distance between two locations<sup>5</sup> with an upscale factor of  $\frac{4}{3}$  [HUG17]. Since the Euclidean distance of two locations is a straight-line distance and underestimates the real length of roads. In consequence, an Euclidean distance of 300 meters represents a road distance of  $300 \cdot \frac{4}{3} = 400$  meters and a walking distance of  $400/5000 = 0.08$  hour. Despite the validation tests, the default walking distance threshold to recharge EVs is five minutes ( $\phi^{IJ} = 5/60$  hour).

By applying a power factor of 1, The full power load capacity of all SSs is assumed to be 400 kW. The available percentages of power load for EV charging at different periods are assumed to be 20% (80 kW) in day\_normal, 12% (48 kW) in day\_peak, and 30% (120 kW) at night, respectively [G+16]. CSOs are expected to pay a cost of 500 Euro/kW for power expansion at each SS ( $c^h = 500$ ). The price of applying backstop technology to reduce grid congestion is assumed to be five Euro/kWh each time<sup>6</sup> ( $c^\eta = 5$ ). Regarding the generation of grid connections scenarios, the maximum distance of possible connection is  $\frac{1}{10}$  hour (walking distance) ( $\phi^{IK} = \frac{1}{10}$ ), which is equivalent to an approximated road distance of 500 meters. And the neighborhood effect on grid connection is restricted to a radius of  $\frac{1}{15}$  hour (walking distance) ( $\phi^{II} = \frac{1}{15}$ ).

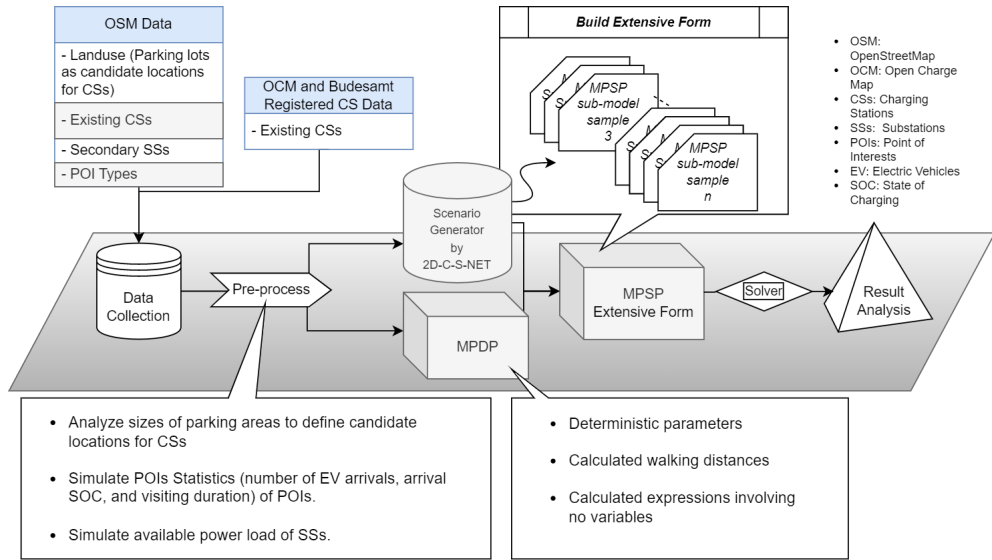


Figure 4.4: Work Flow of MPSP Implementation

## 4.2 Implementation

The above case in SW is solved by implementing the linearized formulation of **MPSP** in (C) in the Python-based open-source optimization modeling language **Pyomo** [HWW11] [Byn+21] with its modeling extension **MPI-SPPy** [Knu+20] for stochastic programming (SP). Each instance of the problem is executed on a laptop computer with an Intel Core i7-6600U CPU and 8.00 GB RAM. The CPLEX 22.1.0 with its standard solving method is used as the optimization solver. Figure 4.4 presents an overview of the implementation work flow. For the consistency of the thesis, a comprehensive illustration of implementation methods will be postponed in Appendix D.

## 4.3 Results

This section starts with the results of the sensitivity analysis. Subsequently, computational performances of **MPSP** are presented. In parallel, results of **MPDP** are provided for comparison.

<sup>5</sup>Calculated based on GPS-coordinates between two locations by haversine formula [https://en.wikipedia.org/wiki/Haversine\\_formula](https://en.wikipedia.org/wiki/Haversine_formula)

<sup>6</sup>Notice that this is expensive. Since paying a fee of 5 Euro/kWh during one of a day periods means paying  $5 \cdot 365 = 1825$  Euro/kWh annually according to the second-stage cost (3.48) of **MPSP**

### 4.3.1 Sensitivity Analysis

A proper generation of possible grid connection scenarios is crucial for this thesis. In scenario-based stochastic programming, the choice of number of scenarios is another essential problem [Sha03] [BL11]. A sensitivity analysis is performed to test the convergence of **MPSP** in the SW case in respect of the number of samples used. In addition, budgets of the maximum number of CPs to install critically determine the amount of CD the CSOs can serve and make a profit from. Therefore, the following sections analyze the sensitivity from these three perspectives.

## CSs Neighborhood Effect on CS-SS Connection scenarios generation

The reliable performance of **2D-C-S-NET** depends on the proper choice of two distance threshold factors. The maximum distance of grid connection between a SS and a CS ( $\phi^{IK}$ ) is the first one. It can be properly defined due to the limit length of cables [G+16]. Whereas no statistics is available for a proper choice of the second factor, the neighborhood effect factor ( $\phi^{II}$ ). Accordingly, a range from 0 to  $\frac{1}{10}$  hour walking distance with an interval of 1/60hour is assumed for the sensitivity analysis. Solely in this section, different values of  $\phi^{II}$  are presented in the unit of meter as approximated road distances, which corresponds to a range between 0 and 500 meters. One of the connection scenario and the IDs of CSs and SSs can be seen on **Figure 4.5**.

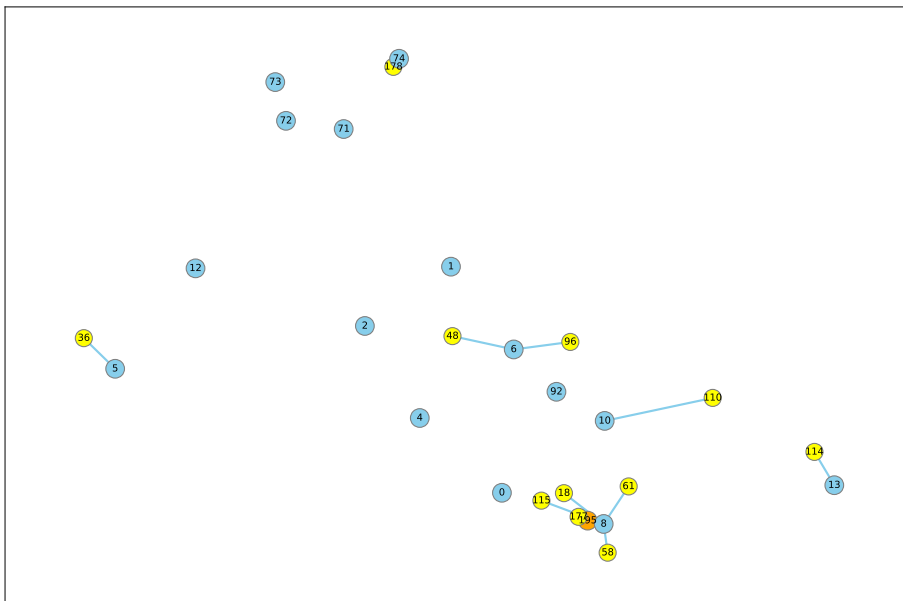


**Figure 4.5:** An Example of Grid Connection between CSs and SSs. (This scenario is used for MPDP)

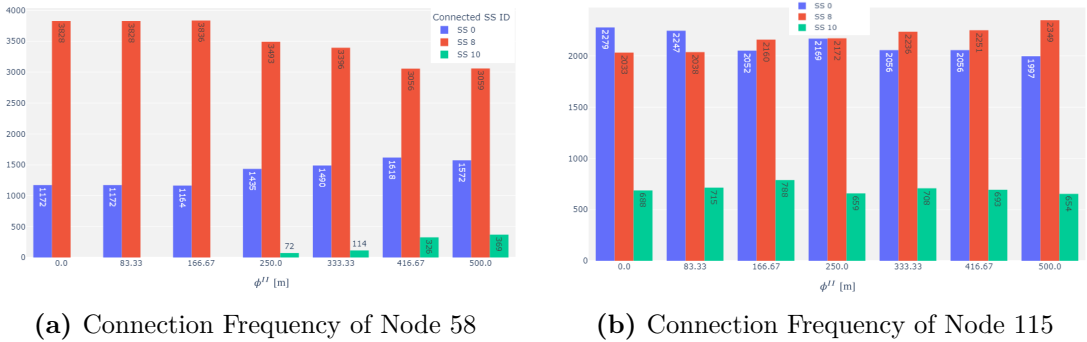


**Figure 4.6:** Connection Frequency of CSs to SSs among 5000 Samplings under different Neighborhood Effect Factors

Preliminary experiments show that sampling 5000 grid connection scenarios from **2D-C-S-NET** for each test value of  $\phi^{II}$  is sufficient. Looking at the candidate location 58 (yellow) for building a new CS, **Figure 4.6a** shows that when  $\phi^{II}$  is less than 167 meters, Node 58 is only possible to connect to SS 8 or SS 0. However, as  $\phi^{II}$  becomes greater than 250 meters, the connection status of node 58's neighbors, node 18 and node 61, shows impact on its grid connection possibilities. The possible connections of node 18 or node 61 to SS 10 (refer to **Figure 4.5**) bring SS 10 as its *new* grid connection candidate. The larger  $\phi^{II}$  is, the deeper this impact is. It is worth mentioning that for each value of  $\phi^{II}$  among 5000 samplings, the red bars are always higher than purple bars, which corresponds to the fact that the distance between Node 58 and SS 8 is nearer than that of node 58 between SS 0. This can be regarded as a subsidiary validation of the distance decay impact on the grid connection weights. The other **Figure 4.6b** shows that the neighborhood effect can let the popular candidate (SS 0) become less popular. When no neighborhood impact is applied ( $\phi^{II} = 0$ ), node 115 connects to SS 0 the most frequently: in 2279 samples among all 5000 samples; whereas large  $\phi^{II}$  decreases this frequency to be less than that of connections between node 115 and SS 8.

According to this sensitivity analysis and experts' knowledge from industry, the value of  $\phi^{II} = 1/15[\text{hour}]$  (an equivalence of 333.33 meters approximated road distance) is chosen for the case study in SW.

### Convergence of MPSP

The proposed **MPSP** is solved by *exterior sampling* [Ahm11] approaches that decouple the sampling and optimization procedures. A Monte Carlo Method is applied by sampling  $M$  i.i.d. grid connection scenarios from **2D-C-S-NET**, then the expectation objective (3.48) in the problem is replaced by a sample average. According to [AS02], the number of samples  $M$  required to get a fairly accurate solution with high probability is usually not too large.  $M$  grows at most linearly with respect to the dimensions of

the problem and logarithmically with the total number of possible scenarios  $Q$ . This analysis tests the performance of **MPSP** against  $M$  ranging from one to 500<sup>7</sup> **Figure 4.7** illustrates the trends of profit and costs w.r.t. the number of samples from one to 500. Overall, especially the objective of **MPSP** (expected profit of EVCSAP) converges as  $M$  greater than 200, whereas the grid expansion cost fluctuates until more than 300 samples are included for tests. On the contrary, figures **4.8b** and **4.8a** show that the

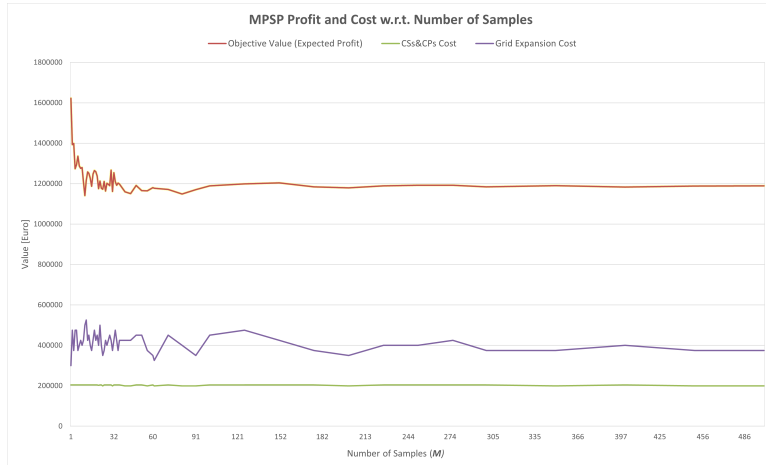


**Figure 4.7:** Number of Samples vs. Objective and Costs

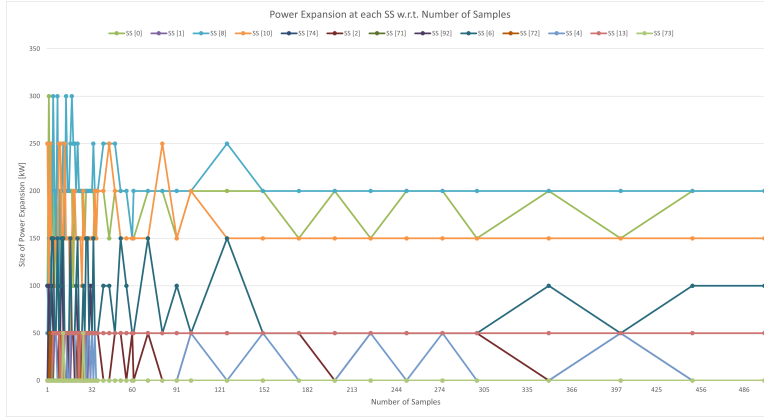
converged solutions to CS allocation and power expansion planning require at least 300 samples.

### Budget of CPs and Profit

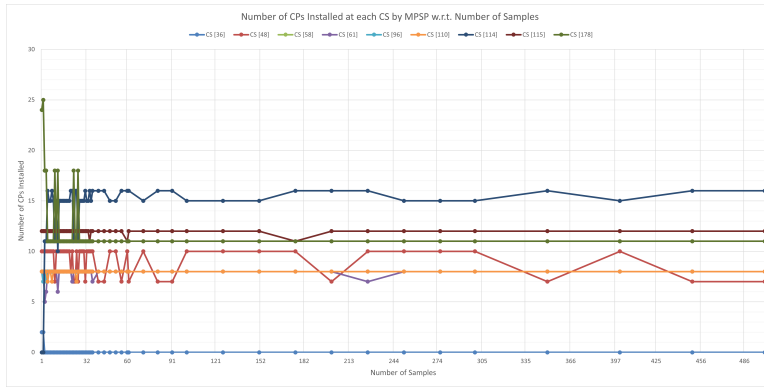
With the above observations and regarding the computational resources at hand, an **MPSP** with 300 samples of grid connection scenarios is tested for ten different budgets of the number of CPs ranging from 10 to 100. In comparison, ten tests for corresponding budgets on **MPDP** with grid connection scenario<sup>8</sup> shown in **Figure 4.5** are implemented. The impact of CPs budgets on the objectives and costs are presented in line Graph **4.9**. As displayed, the annual profit (objective value) of **MPDP** with perfect grid information is obviously higher than that of **MPSP** without grid connection information. This trend differs more significantly as more CPs are installed. In the extreme case where

<sup>7</sup>Due to restriction of computational resources, the test did not cover all 500 cases, the tested number of samples  $M$  is presented in figures **4.8b** and **4.8a** by dots (e.g., only  $M \in \{400, 450, 500\}$  are tested from range 400 to 500).

<sup>8</sup>This is defined by taking the most frequent grid connection of each candidate location running through all 20,000 generated samples with parameter  $\phi^{II} = 1/15$  [hour] (333.33 meters). E.g., according to **4.6b**, node 115 should connect to SS 8.



(a) Number of Samples vs. Power Expansion Decisions



(b) Number of Samples vs. CPs Allocation Decisions

Figure 4.8: Convergence test of MPSP in SW Case

100 CPs are available for allocation, **MPSP** turns out to be conservative because of the lack of grid information and install only the same number of CPs as in the budget case of 90 CPs (CSs placement costs stay the same among these two cases) to reduce the risk of grid congestion. And in such case, CI planning under uncertainty in **MPSP** is 33% less profitable than its counterpart **MPDP** due to the conservative planning and expensive extra fee payed to backstop-technologies. This result encourages CSOs to collaborate with DSOs at the early stage before their CI planning.

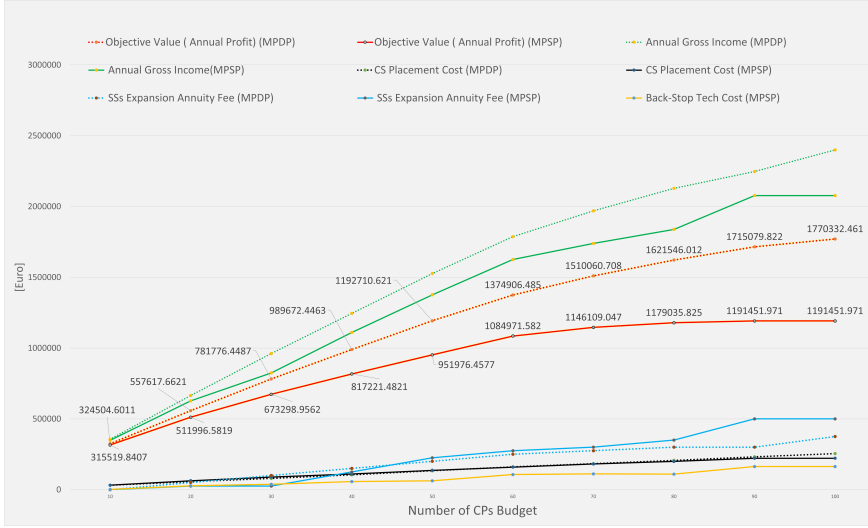


Figure 4.9: Budget of CPs vs. Profit and Costs

### 4.3.2 Model Performance

#### Network Graph Results

The network graph 4.10 is provided to demonstrate the EVCSAP decisions and the functionality of lower bound constraints (3.26) on CD coverage variables  $\mathbf{z}_{ij}^t$ . This graph presents the CD coverage results of the **MPDP** with settings described in section 4.1 and grid connection scenario defined as 4.5. As a convenience of showing the deterministic case, power expansion (darkblue nodes) is straightforward by comparing this EVCSAP planning graph with grid connection scenario 4.5.

Overall, all opening CSs serve the CD from all its nearby POIs rather than just from several of them. This feature is enforced by the lower bound constraints. For example, the small new CS (the smallest red node on the left) is "connected" to POIs nearby with very thin edges, satisfying at least a portion of CD from each POI; whereas the CD from POIs in the bottom cluster with four charging stations nearby are covered well (with thick edges).

#### Utilization Rate of CPs

The UR defined in 3.15 is another important criterion of EVCSAP. Figure 4.11 provides the UR of CPs at opening CSs in the **MPDP** and an **MPSP** built upon 500 sampled grid connection scenarios. Notice that the decisions on CSAP alter slightly in two cases. CS 36 is open in **MPDP**, whereas it is replaced by CS 114 in **MPSP**. Overall, installed CPs in the case of **MPSP** generally perform worse than their opponents in

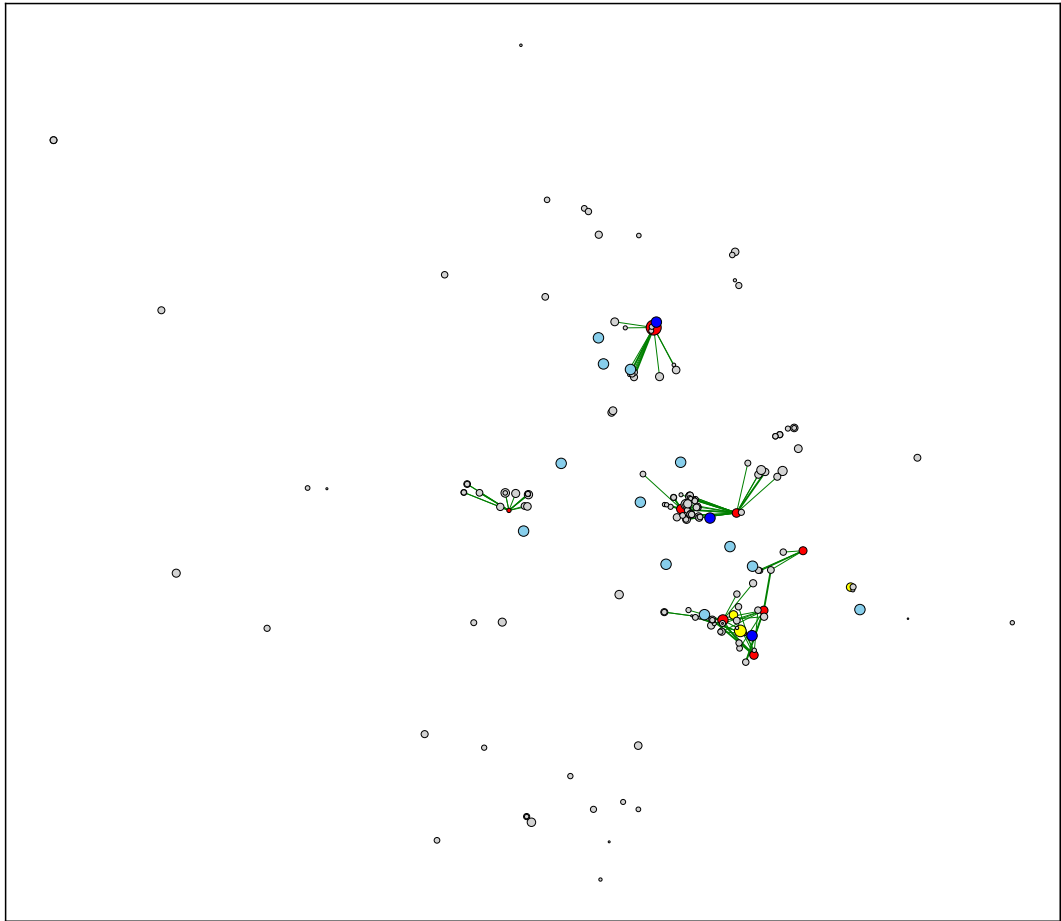


**Figure 4.10:** An Example of CD Coverage during day\_normal period in **MPDP**.

Darkblue nodes: Expanded SSs;

Red nodes: New CSs (node size represents installed number of CPs);

Grean edges: CS-POI CD coverage pairs, edge width represents percentage of CD covered by corresponding CSs.

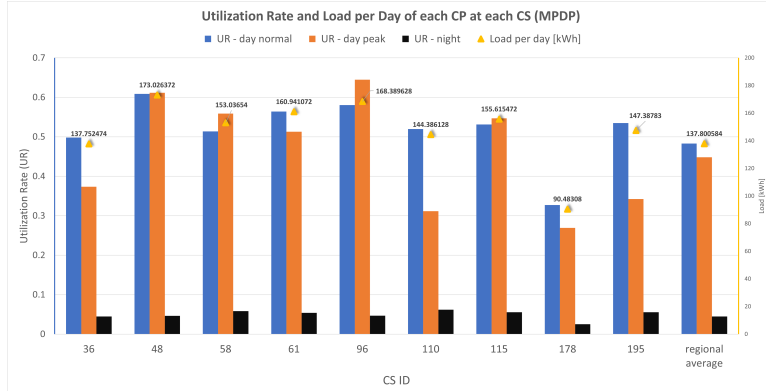
**MPDP.** UR at night is reasonably low due to the over-night parking<sup>9</sup>. Though UR during daytime is higher than at night, most of the CPs only show a UR at around 50%. The last group of bars shows an average UR of planned CPs within the whole SW region. The load per CP per day in **MPSP** corresponds to a UR of 23.4%, whereas this figure in **MPDP** is 26%. The quality of these model statistics can be validated

---

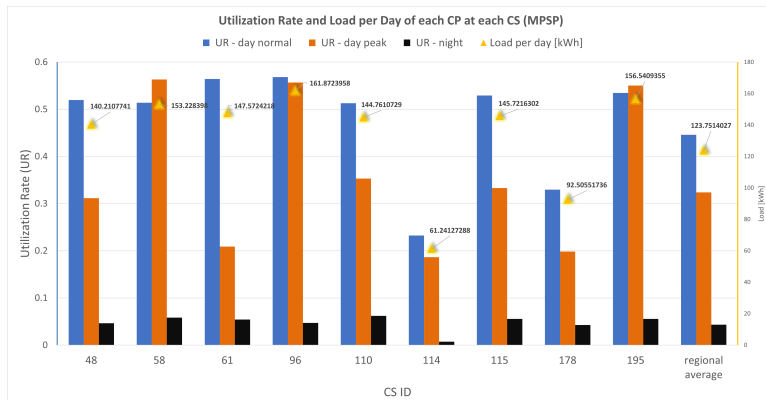
<sup>9</sup>By the assumption that the power rating of CPs is 22 kW and all BEVs have 50kWh batteries, it takes a CP less than 90 minutes to fully recharge an EV.

### 4.3 Results

indirectly through a comparison with the real-time data of an operational 22kW CP in Basel, whose load per day is around 105 kWh.



(a) MPDP



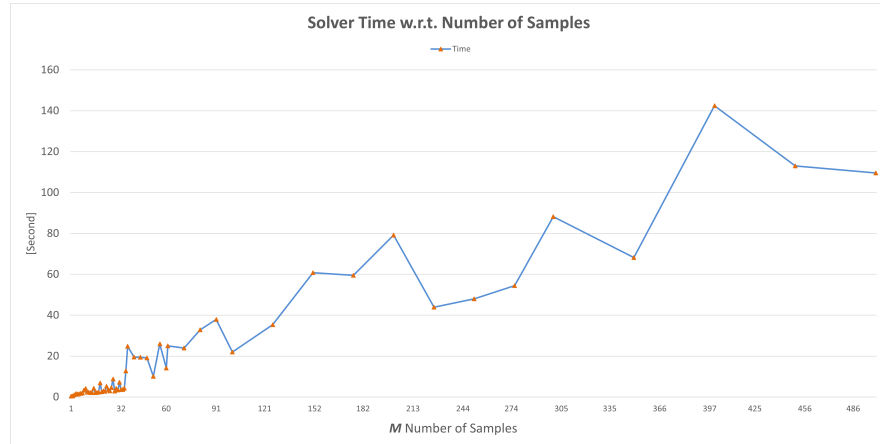
(b) MPSP

Figure 4.11: Utilization Rate and Daily Load of CPs

### Computational Performance

Preliminary experiments excluded non-linear models as it takes CPLEX a very long time to even solve the deterministic models of case SW. And the non-linearized stochastic programmings are non-solvable for CPLEX. Figure 4.12 compares the solver time used for different sample sizes. According to the graph, even for the MPSP with  $M = 500$  sampled scenarios which has 5,133,705 constraints and 3,420,501 variables, it took the solver less than two minutes to find the optimal solution with the percentage of optimality gap less than 0.1%. However, this does not include the model construction

time and time to pass the large model to the solver. When setting up a small model with  $M \leq 200$  samples, it normally takes  $3 \cdot M$  seconds on average to build, pass the model to the solver and solve it. However, because of the limited memory of the device used, setting up larger samples take a much longer time. For a model with more than 300 samples, it is normal to take hours on this device to build and solve it. Moreover, **Figure 4.12** does not show a line with a linear trend, probably due to the unstable performance of the device.



**Figure 4.12:** Solver time w.r.t. Number of Samples

# Chapter 5

## Conclusions and Outlook on Future Research

**Conclusions.** This thesis develops a novel two-stage multi-period stochastic optimization framework for EVCSAP under incomplete grid information. The optimization framework deals with urban CI and grid networks involving uncertain grid connections between charging stations and secondary substations. It aims at maximizing profit gained by serving charging demand while minimizing the cost of grid congestion. Accordingly, a scenario generation algorithm for grid connection is developed considering the effect of distance decay and neighborhood connection on the probabilities of grid connections between CSs and SSs. Since only public-accessible data is required for the first deterministic stage and the second-stage model data can be provided by the scenario generation algorithm **2D-C-S-NET**, this framework enjoys the flexibility of being applied to various urban regions. However, the initial computational experiments in this study solely support the optimality of this framework in networks with hundreds of nodes. Case studies in larger areas need to be accomplished for further validation.

To our best knowledge, this proposed optimization model is the first to deal with EVCSAP with pending grid connections. Such uniqueness assists the CSOs in designing congestion-free CI planning with imperfect grid information while satisfying the rocketing EV charging demand and maximizing profits.

Last but not least, an innovative approach is derived to approximate the actual recharging energy supply capability of CSs and to estimate the realistic utilization rate of CPs. It addresses the impact of different EV charging patterns from various types of POIs on the charging energy capacity of CSs. This estimation approach offers insights for CSOs into the profitability of CPs and CD density at different CPs, which help to decide the size of CI placement and predict the risk of grid congestion. In addition, the results comparing CSAP performances in deterministic and stochastic cases in 4.3 encourage CSOs to engage with local DSOs at an early stage to access better grid information for more profitable and grid-friendly EVCSAP planning. After all, such collaboration is mutually beneficial. Because in order to anticipate and manage electricity demand for better grid operations such as smart charging, DSOs need visibility into charging behaviors. Such communication between CSs and the electricity distribution system

can help load management by shifting unurgent EV CD in peak load periods to periods where general energy demand is low [Con+22].

**Outlook on future research.** A number of future research opportunities are motivated by this work. Due to the three stakeholders involved, namely the CSOs, DSOs, and EV drivers, multi-objective optimization or the game-theory-based multi-stage optimization approaches can be applied to address different incentives of participants.

Furthermore, voltage stability of power grids is also required during EV charging. Adding further constraints on **MPSP** can effortlessly address this concern. Yet, in many power problems, the focus is usually on the reliability of systems or the systems' ability to meet demand. This reliability can be interpreted as requiring a lower bound on the probability of satisfying demand while using no backstop technologies [SDR09]. Accordingly, chance-constrained or probabilistic-constrained optimization models will be more appropriate. For example, by replacing the second-stage expectation model with the following constraints:

$$\mathbb{P}\left[\sum_{i \in I} Z_{ik}(w) \psi_i^t \leq \Psi_k + h_k\right] \geq \theta, \quad \forall k \in K, t \in T$$

where  $\theta \in [0, 1]$  denotes such probability. Moreover, this model can adopt general uncertainties from charging behaviors, availability of power load capacity, etc.

More realistic assumptions need to be considered for future works as well. For instance, this model should be upgraded to integrate multiple types of CPs. Since a combined design of slow chargers and fast chargers within an EVCSAP is not seldom in real life. Furthermore, researchers can improve the distance measure used in the model significantly by retrieving actual road distances from GIS software. A better distance measure will enhance the performance of **MPSP** and **2D-C-S-NET** in complex geographical regions, for example, in mountainous areas. In addition, a better solution for managing grid congestion usually requires more precise time intervals. However, dividing the periods into tiny intervals will result in error-prone estimations of CD and EESC. For example, if the CD of an EV parking for 3 hours and recharging at a CS is simulated as the data for a 2-hour peak-load period, the model will fail to approximate this CD precisely. Fortunately, such CDs have been modeled as transferable demands and addressed by [CHG15].

Finally, this thesis only studies the case of a small town, and the sensitivity analysis of the impacts of charging price on CD and the effects of the expansion fee on decisions at different stages is not implemented due to time restrictions. Future work should execute large-scale case studies in regions such as Basel with achievable real-world charging data to validate the model performance further. Alternatively, evaluating **MPSP**'s solutions performance in simulation environments such as the ABM\_eMob developed by [Hus+21] is as well a genuine approach for model validation.

## Appendix A

# A brief introduction to Facility Location under Uncertainty

EVCSAP belongs to Facility Location Problems (FLP). As an example, this appendix chapter briefly introduces the stochastic programming for facility location problems under uncertainty based on the uncapacitated facility location problem (UFLP).[\[LNS19\]](#). Notice that the notations used in this chapter are independent of notes in the other chapters of this thesis.

### The deterministic uncapacitated facility location problem

We start with the classical one-stage deterministic UFLP. The set  $I$  is denoted as the candidate locations for locating operational facilities to satisfy the clients with demands  $d_j$ ,  $j \in J$  from a set  $J$  of demand centers. Each client at demand center  $j \in J$  can be supplied from an open facility where the commodity is made available. The problem is choosing the number and locations of facilities to open to maximize profit (or minimizing costs), without considering the facility sizes. Let  $\mathbf{x}_i$  be a binary variable to decide whether to open and operate a facility at  $i \in I$  ( $\mathbf{x}_i = 1$ ) at a fixed cost of  $c_i$ , or not to ( $\mathbf{x}_i = 0$ ). Denote  $\mathbf{z}_{ij}$  as the fraction of the demand of client  $j \in J$  served from opening facility  $i \in I$ . Let  $q_{ij}$  be the unit of integer profit earned by serve commodity from  $i$  to  $j$ . When  $q_{ij} \leq 0$ , it can be interpreted as costs. The classical problem UFLP reads as follows:

$$\max_{x,z} - \sum_{i \in I} c_i \mathbf{x}_i + \sum_{i \in I} \sum_{j \in J} q_{ij} \mathbf{z}_{ij} \quad (\text{A.1})$$

s.t.

$$\sum_{i \in I} \mathbf{z}_{ij} \leq 1, \quad j \in J \quad (\text{A.2})$$

$$0 \leq \mathbf{z}_{ij} \leq \mathbf{x}_i, \quad i \in I, j \in J \quad (\text{A.3})$$

$$\mathbf{x}_i \in \{0, 1\}, \quad i \in I \quad (\text{A.4})$$

where the constraints (A.2) ensure that commodities more than a client  $j$ 's demand will not be served. Constraints (A.3) ensure that only operational facilities can offer commodities to clients.

In EVCSAP the demand centers can be POIs or service areas along the highway, etc. And the candidate locations for facilities are that for CSs, which can be parking lots and so on. Demand commodity is interpreted as the charging energy. However, the difference is that the CSs will not serve the charging energy to drivers, their clients. Instead, CSs "attract" their clients to recharge (buy commodities) at the facilities.

### **Two-stage Stochastic Programming for UFLP with integer recourse**

Many facility location problems involve unpredictable outcomes. Congestions can occur due to unexpected surged demand or shortage of supply and disruptions might be spotted owing to abrupt failure in the network, and so forth. Decisions of the costly facility location are, however, hard to reverse. And their impact often spans a long time horizon. Researchers have been developing essential tools for many decades to model and tackle FLP under uncertainties. Stochastic programming is one of the promising approaches.

Stochastic Programming involves multi-stage models. Here only the two-stage models will be presented. To observe a realization  $\omega$  of a set of uncertainties  $\Omega$ , can be interpreted as checking a specific outcome from random experiments. In terms of stochastic programming,  $\omega$  is called a scenario (a certain state of an event), and  $\Omega$  is denoted as the set of all possible scenarios. Additionally,  $\xi$  is denoted as the random variable containing the problem data (information) of a scenario  $\omega \in \Omega$ . As a result, in two-stage models, the set of decisions is divided into two groups:

1. **First-stage** decisions (denote as  $\mathbf{x}$ ):

Decisions must be made before the random information ( $\omega$ ) is revealed. For example, they can be the decisions to open a facility or not or to allocate charging infrastructures.

2. **Second-stage** decisions (denote as  $\mathbf{z}(\omega, \mathbf{x})$ ):

Decisions to implement after uncertain information ( $\xi(\omega)$ ) is disclosed, or reactions to the observed values of random information. For example, in the UFLP example above, the uncertainties can be the profits of serving clients from operational facilities due to the unstable costs of raw materials, transportation and distribution of goods, etc. Then the second-stage decisions will be where to and how many commodities to distribute after observing the costs or profits under a specific scenario.

The sequence of events and decisions is summarized as:

$$\mathbf{x} \rightarrow \xi(\omega) \rightarrow \mathbf{y}(\omega, \mathbf{x})$$

I.e., fix first-stage decisions  $\rightarrow$  observe random information  $\rightarrow$  make the second-stage decisions regarding the fixed first-stage decisions and observed random information [BL11].

---

We now assume the profits of serving commodities in the above UFLP as the only uncertain information, i.e.,  $\xi(\omega) = ((q_{ij}(\omega))_{i \in I, j \in J})$ . The distribution decisions is assumed to be dependent of scenario  $\omega$  and denoted as  $\mathbf{z}_{ij}(\omega)$ . The standard form for a two-stage stochastic UFLP with integer recourse is as follows:

$$\max_x - \sum_{i \in I} c_i \mathbf{x}_i + \mathbb{E}_\xi [Q(x, \xi(\omega))] \quad (\text{A.5})$$

s.t.

$$\mathbf{x}_i \in \{0, 1\}, \quad i \in I \quad (\text{A.6})$$

where:

$$Q(x, \xi(\omega)) := \min_{\mathbf{z}} \sum_{i \in I} \sum_{j \in J} q_{ij}(\omega) \mathbf{z}_{ij}(\omega) \quad (\text{A.7})$$

s.t.

$$\sum_{i \in I} \mathbf{z}_{ij}(\omega) \leq 1, \quad j \in J, \quad (\text{A.8})$$

$$0 \leq \mathbf{z}_{ij}(\omega) \leq \mathbf{x}_i, \quad i \in I, j \in J, \quad (\text{A.9})$$

constraints (A.8) and (A.9) under a specific scenario set the similar restrictions as (A.2) and (A.9), respectively. And the deterministic distribution profit in (A.1) is replaced here by an expected value (profit) function depending on all scenarios. Notice that according to [Ahm11],  $\mathbb{E}_\xi [Q(x, \xi(\omega))]$  has none of the desirable properties for optimization. It is non-convex and even discontinuous (only semicontinuous)

### Extensive Form

If the underlying probabilistic distribution of  $\xi$  is assumed to be known, and we denote its cumulative distribution as:  $\mathbf{F}_\xi(x) := \mathbb{P}[\{\omega | \xi \leq x\}]$ , where  $\mathbb{P}$  is a probability measure. Then (A.5)–(A.9) can be written as the following *Extensive Form* (EF):

$$\max_{x,z} - \sum_{i \in I} c_i \mathbf{x}_i + \sum_{\omega \in \Omega} \mathbb{P}[\xi = \xi(\omega)] \sum_{i \in I} \sum_{j \in J} q_{ij}(\omega) \mathbf{z}_{ij}(\omega) \quad (\text{A.10})$$

s.t.

$$\mathbf{x}_i \in \{0, 1\}, \quad i \in I \quad (\text{A.11})$$

$$\sum_{i \in I} \mathbf{z}_{ij}(\omega) \leq 1, \quad j \in J, \omega \in \Omega \quad (\text{A.12})$$

$$0 \leq \mathbf{z}_{ij}(\omega) \leq \mathbf{x}_i, \quad i \in I, j \in J, \omega \in \Omega \quad (\text{A.13})$$

### Sample Average Approximation

In real-world problems, evaluating expected function w.r.t. the underlying distribution of random variables is itself a challenging problem. The first challenge is that the information is usually imperfect and the distribution of random variables will be unavailable. In addition, the number of possible realizations can be extremely large. For example, in this study of EVCSAP under imperfect grid connection information, the distribution of grid connections is first unknown. Moreover, the number of possible grid connections can be a large combinatorial number as the size of the corresponding network grows.

Under such circumstances, the statistical estimation of the expected value function via Monte Carlo sampling is preferred [Sha03]. This estimation is often achieved as follows: Generate a sample  $\{\xi_1, \xi_2, \dots, \xi_M\}$  of  $M$  realizations of the random variable  $\xi$ , and consequently approximate the expected value function  $\mathbb{E}_\xi[Q(x, \xi(\omega))]$  by the sample average function  $\frac{1}{M} \sum_{m=1}^M Q(x, \xi_m)$ . Then the obtained sample average approximation of the extensive form will be:

$$\max_{x,z} - \sum_{i \in I} c_i \mathbf{x}_i + \frac{1}{M} \sum_{m=1}^M Q(x, \xi_m) \quad (\text{A.14})$$

s.t.

$$\mathbf{x}_i \in \{0, 1\}, \quad i \in I \quad (\text{A.15})$$

$$\sum_{i \in I} \mathbf{z}_{ij}(\omega) \leq 1, \quad j \in J, m \in \{1, 2, \dots, M\} \quad (\text{A.16})$$

$$0 \leq \mathbf{z}_{ij}(\omega) \leq \mathbf{x}_i, \quad i \in I, j \in J, m \in \{1, 2, \dots, M\} \quad (\text{A.17})$$

The convergence analysis and the corresponding resolution approaches of the formulations above can be found in, e.g., [AS02].

## Appendix B

# Examples and Derivation of Definitions

### Example B.1 (CD Approximation)

Imagine on a sunny weekend day  $t$  ( $\Delta t = 24\text{hours}$ ), an EV driver visiting the art museum Alte Pinakothek at location  $j$  for  $\mathcal{T}_j^t := 2.8\text{ hours}$  in total. The EV driver must charge the EV nearby to make sure to get home after the visit since the 44-kWh-battery EV ( $B_{cap} := 44 \text{ kWh}$ ) is at only 50% state of charging (SOC) ( $\delta_j^t = 0.5$ ) upon arrival. There is a CS near the Pinakothek at location  $i$  with available level-2 CPs<sup>1</sup>. Besides, the walking distance between  $i$  and  $j$  is  $d_{ij} = 0.1 \text{ hour}$ . Then the total parking time of the EV at the CS  $i$  to be:

$$\mathcal{T}_{ij}^t = \mathcal{T}_j^t + 2d_{ij} = 3 \text{ hours}$$

which is the summation of the time its owner spends in the Museum and the total walking time of going to and coming back from there. Naturally, the charging process either lasted until the EV was fully charged or until the EV driver finishes the visit and unplugs the charger without the battery being fully charged. Written in a formula, the CD or the energy served by this charging process raised by the EV driver's visit to museum  $j$  is given by:

$$\mathcal{D}_{ij}^t = \min\{\pi \cdot \mathcal{T}_{ij}^t, (1 - \delta_j^t) \cdot B_{cap}\} = \min\{22 \times 3, (1 - 0.5) \times 44\} = 22 \text{ kWh}$$

This visiter can then drive a fully charged EV on his way home.

In another case, imagine another EV driver buying groceries at a supermarket  $j^*$  for  $\mathcal{T}_{j^*} = 0.25 \text{ hour}$  and recharging at the same CS  $i$  which is at a 3-min walking distance to the supermarket ( $d_{ij^*} = 0.05 \text{ hour}$ ) with available level-2 CPs. Assume that the arrival SOC at the supermarket  $j^*$  to be  $\delta_{j^*} = 0.75$  and  $B_{cap} = 44$ . Then the CD or the energy served by this charging process raised by the visit to supermarket  $j^*$  is given by:

$$\mathcal{D}_{ij^*} = \min\{\pi \cdot (\mathcal{T}_{ij^*}^t), (1 - \delta_{j^*}) \cdot B_{cap}\} = \min\{22 \times 0.35, (1 - 0.75) \times 44\} = 7.7 \text{ kWh}$$

And the SOC of this EV after recharge will be  $(44 * 0.75 + 7.7)/44 = 0.925$ . That is, the EV leaves the supermarket without being fully charged.  $\square$

---

<sup>1</sup>Each L-2 CP has a power rating of  $\pi = 22 \text{ kW}$

**Example B.2 (Overestimation Problem with TESC)**

With the same notations in example B.1, it takes  $\Delta\hat{t} := \mathcal{D}_{ij}^t/\pi = 1 \text{ hour}$  to fully recharge that EV. This means the EV will park and occupy the CP for

$$\mathcal{T}_j^t + 2d_{ij} - \Delta\hat{t} = 2 \text{ hours}$$

without being recharged until its owner leaves the arena and drives it away. This will waste the **TESC** by an amount of

$$\pi \cdot (\mathcal{T}_{j^*}^t + 2d_{ij^*} - \Delta\hat{t}) = 44 \text{ kWh}$$

, which is twice the amount of the actual CD energy ( $\mathcal{D}_{ij}^t = 22 \text{ kWh}$ ) this CP will serve during these three hours. In another word, TESC overestimates the ESC of each CP at  $i$  by two times for this case.  $\square$

## Derivation of EESC

Given a CS  $i \in I$  which is not  $\phi$ - $u$ -isolated, and a set of POIs  $J$  near CS  $i$ . We derive this approximation method by first looking at the simplest case where the CS  $i$  serves CD of EV arrivals from only one single POI  $j \in J$ . If all CPs sited  $i$  only serve CD of EV arrivals from a POI  $j$ , then during period  $t$  with length  $\Delta T \text{ hours}$ , the whole service time of that CS  $i$  is occupied by EVs from  $j$ . And one single CP at  $i$  can in consequence satisfy maximally:

$$N_{ij}^t := \frac{\Delta t}{\mathcal{T}_{ij}^t}$$

of EV arrivals parking for  $\mathcal{T}_{ij}^t$  hours from  $j$ . The corresponding maximal recharging energy this CS  $i$  with  $n_i$  CPs can supply is:

$$n_i \cdot N_{ij}^t \mathcal{D}_{ij}^t \text{ kWh}$$

As mentioned above, the exogenous impact on ESC of CS  $i$  by its nearby different POIs needs to be addressed. In this case, the service time CS  $i$  can offer to recharge will be shared by those POIs. On top of the following two model assumptions:

- i. Given the same arrival SOC and parking length, the more frequently the EVs visiting a POI  $j \in J$  arrive at  $i$  for charging, the more energy supply capability those EVs occupy.
- ii. Given the same arrival frequency of EVs at CS  $i$  from POI  $j$ , the longer time the EVs park, the more energy supply capability those EVs occupy.

We further denote:

$$\Delta T_{ij}^t := \mathcal{A}_{ij}^t \mathcal{T}_{ij}^t \quad (\text{B.1})$$

as the total service time requested by all *price-scaled-distance-decayed EV arrivals* ( $\mathcal{A}_{ij}^t$ ) from a POI  $j \in J$  at a CS  $i \in I$ . And:

$$\Delta T_i^t := \sum_{j \in J} \mathcal{A}_{ij}^t \mathcal{T}_{ij}^t \quad (\text{B.2})$$

the whole service time requested by entire *price-scaled-distance-decayed EV arrivals* ( $\sum_{j \in J} \mathcal{A}_{ij}^t$ ) from all POIs  $J$  near a CS  $i \in I$ . Then for each CP sited at CS  $i$ , the shared service time by decayed EV arrivals from POI  $j \in J$  is denoted as  $\Delta \mathcal{T}_{ij}^t$  and estimated by:

$$\Delta \mathcal{T}_{ij}^t := \frac{\Delta T_{ij}^t}{\Delta T_i^t} \cdot \Delta t \quad (\text{B.3})$$

In consequence, for EV arrivals from  $j \in J$  sharing the service time of CS  $i$  with other POIs  $J \setminus j$ , one single CP at CS  $i$  is estimated to satisfy the CD of:

$$N_{ij}^t := \frac{\Delta \mathcal{T}_{ij}^t}{\mathcal{T}_{ij}^t} \quad (\text{B.4})$$

EV arrivals from  $j$ .

If the existing CS  $i$  with  $n_i$  CPs was selected to be updated by installing  $y_i$  new CPs, the corresponding ESC of this CS  $i$  for EV arrivals from a POI  $j$  of all POIs  $J$  after updated is then estimated as:

$$\mathbf{w}_{ij}^t := (\mathbf{y}_i + n_i) \cdot N_{ij}^t \mathcal{D}_{ij}^t \quad \text{kWh} \quad (\text{B.5})$$

Regarding all nearby POIs  $J$ , the corresponding recharging ESC of the CS  $i$  to be updated is then estimated as:

$$\mathbf{w}_i^t := (\mathbf{y}_i + n_i) \cdot \sum_{j \in J} N_{ij}^t \mathcal{D}_{ij}^t = \sum_{j \in J} \mathbf{w}_{ij}^t \quad \text{kWh} \quad (\text{B.6})$$

Altogether, by plugging (B.1)-(B.4) in (B.5), we arrive at the definition 3.6

### Illustration on the Lower Bound of CD Coverage

As mentioned in section 3.2, constraints (3.26):

$$\sum_{i \in I} \mathcal{D}_{ij}^t \mathcal{A}_j^t \mathbf{z}_{ij}^t \geq \min\{\mathcal{D}_j^t \mathcal{A}_j^t, \sum_{i \in I} \mathbf{w}_{ij}^t\}, \quad j \in J, t \in T$$

imply that at least an amount of CD of EV arrivals at a POI  $j_0 \in J$  should be satisfied, if a set of CSs

$$\hat{I} = \{i \mid \hat{d}_{ij_0} \leq \phi^{IJ}, i \in I\} \quad (\text{B.7})$$

are found nearby that POI within the walking distance threshold  $\phi^{IJ}$ . Recall that  $\hat{d}_{ij_0}$  represents the price-scaled-distance as defined in definition 3.2

We suggest that this lower bound should

- a) either be the approximated amount of the whole CD of all EVs at  $j_0$ , or
- b) it should be the amount of the sum of estimated energy supply by CSs nearby to  $j_0$ .
- b) can be easily represented by  $\sum_{i \in \hat{I}} \mathbf{w}_{ij_0}^t$  thanks to (3.13) in definition 3.4 of EESC; While due to the *dynamic* characteristic (3.1.1) of EV CD defined in 3.4, the former one, a), can not be directly obtained by *the product of the number of EV arrivals and the CD of each EV arrival*. Since EV arrivals at the same POI might have different estimations of CD when they park and charge at different CSs. To tackle this, we use the visiting duration  $\mathcal{T}_j^t$  at a POI  $j \in J$  during  $t \in T$ , which does not include the walking distance to CSs for recharging, as a conservative substitute of the approximation of parking time. And we define the *static CD of each EV arrival* at POI  $j \in J$  during period  $t \in T$  as:

$$\mathcal{D}_j^t = \min\{\pi \cdot \mathcal{T}_j^t, (1 - \delta_j^t) \cdot B_{cap}\} \quad (\text{B.8})$$

Based on this, it is now possible to estimate the *whole static CD at a POI  $j \in J$  during period  $t \in T$*  as:

$$\mathcal{D}_j^t \mathcal{A}_j^t \quad (\text{B.9})$$

With the materials introduced above, we now validate the lower bound constraints (3.26).

**We first prove that if no CSs are found nearby  $j_0$ , then the lower bound is redundant:**

$$\hat{I} = \emptyset \Rightarrow \mathbf{z}_{ij_0}^t \geq 0, \forall i \in \hat{I}, t \in T \quad (\text{B.10})$$

**Proof:** (3.7) and (3.13) implies that:

$$\mathcal{D}_{ij_0}^t = 0 \wedge \mathbf{w}_{ij_0}^t = 0, \text{ if } i \in I \setminus \hat{I}$$

plugging it together with  $\hat{I} = \emptyset$  in (3.26), we get

$$\sum_{i \in I} 0 \mathcal{A}_{j_0}^t \mathbf{z}_{ij_0}^t \geq \min\{\mathcal{D}_{j_0}^t \mathcal{A}_{j_0}^t, \sum_{i \in I} 0\} \Rightarrow 0 \geq 0$$

which shows the redundancy of (3.13) in this case.  $\square$

---

**Now we validate the case when  $\hat{I} \neq \emptyset$ :** By (3.13),  $\hat{I} \neq \emptyset$  implies that  $\mathbf{w}_{ij_0}^t > 0, \forall i \in \hat{I}$ .

If  $\min\{\mathcal{D}_{j_0}^t \mathcal{A}_{j_0}^t, \sum_{i \in I} \mathbf{w}_{ij_0}^t\} = \sum_{i \in I} \mathbf{w}_{ij_0}^t$ , the recharging service supply capability of CSs nearby is insufficient. If  $\mathcal{A}_{j_0}^t = 0$ , (3.26) is again redundant. Else for  $\mathcal{A}_{j_0}^t > 0$ , (3.26) of  $j_0$  is equal to:

$$\sum_{i \in I} \mathcal{D}_{ij_0}^t \mathcal{A}_{j_0}^t \mathbf{z}_{ij_0}^t \geq \sum_{i \in I} \mathbf{w}_{ij_0}^t > 0, \quad t \in T$$

Since  $\mathbf{z}_{ij}^t \geq 0, \forall i \in I$ , it holds that  $\exists i^* \in \hat{I}$ , s.t.  $\mathbf{z}_{i^*j_0}^t > 0$ , which means  $\mathbf{z}_{i^*j_0}$  is bounded from below by a non-zero value.

**Else,** if  $\min\{\mathcal{D}_{j_0}^t \mathcal{A}_{j_0}^t, \sum_{i \in I} \mathbf{w}_{ij_0}^t\} = \mathcal{D}_{j_0}^t \mathcal{A}_{j_0}^t$ , the recharging service supply capability of CSs nearby is sufficient to satisfy the whole static CD at POI  $j_0$ . And (3.26) of  $j_0$  turns to:

$$\sum_{i \in I} \mathcal{D}_{ij_0}^t \mathcal{A}_{j_0}^t \mathbf{z}_{ij_0}^t \geq \mathcal{D}_{j_0}^t \mathcal{A}_{j_0}^t \geq \sum_{i \in I} \mathbf{w}_{ij}^t > 0, \quad t \in T \quad (\text{B.11})$$

It implies that  $\mathcal{A}_{j_0}^t > 0$  and  $\mathcal{D}_{j_0}^t > 0$ , thus constraints (3.26) are equal to:

$$\sum_{i \in I} \mathcal{D}_{ij_0}^t \mathbf{z}_{ij_0}^t \geq \mathcal{D}_{j_0}^t, \quad t \in T \quad (\text{B.12})$$

As it holds that:

$$\mathcal{D}_{ij_0}^t \geq \mathcal{D}_{j_0}^t > 0, \quad \forall i \in I$$

and because of  $\mathbf{z}_{ij}^t \geq 0, \forall i \in I$ , it holds that  $\exists i^* \in \hat{I}$ , s.t.  $\mathbf{z}_{i^*j_0}^t > 0$ .  $\square$

### Choice of **Big-M**

To ensure that (3.35) and (3.36) imply:

$$\chi_j^t = \min\{\mathcal{D}_j^t \mathcal{A}_j^t, \sum_{i \in I} \mathbf{w}_{ij}^t\}, \quad j \in J, t \in T$$

$\mathcal{M}^t, t \in T$  should be large enough to satisfy:

$$\mathcal{M}^t \geq \max\{\mathcal{D}_j^t \mathcal{A}_j^t, \sum_{i \in I} \mathbf{w}_{ij}^t\}, \quad \forall j \in J, t \in T$$

While MILP is usually solved by branch-and-bound method, large  $\mathcal{M}^t, t \in T$  usually result in loose and bad bounds, thus make the problem hard to solve. Another issue is,  $\mathcal{M}^t, t \in T$  are part of the coefficient matrix. Mixing very large coefficients with much smaller coefficients can create numerical instability, leading the solver to spend more time computing linear program pivots and possibly leading to totally erroneous solutions [Rub18]<sup>2</sup>. Therefore, in order to avoid unsolvable cases, proper  $\mathcal{M}^t, t \in T$  should not be too large. According to our computational experiments experience, the CSs are

---

<sup>2</sup>Notice that this referred article is only a posted blog online rather than a published research work

always insufficient to satisfy the total CD of EV arrivals in a whole region, even if we open and update all candidate locations and install full-capacity CPs. Therefore, we recommend the value of  $\mathcal{M}^t :=, t \in T$  to be *the upper bound of total regional charging demand during period  $t \in T$* :

$$\mathcal{M}^t := \sum_{j \in J} \min\{\pi \cdot (\mathcal{T}_j^t + 2 * \phi^{IJ}), (1 - \delta_j^t) \cdot B_{cap}\} \mathcal{A}_j^t, \quad t \in T \quad (\text{B.13})$$

where the upper bound comes from:

$$\mathcal{A}_j^t \geq \mathcal{A}_{ij}^t, \quad \forall i \in I, j \in J, t \in T$$

and

$$\min\{\pi \cdot (\mathcal{T}_j^t + 2\phi^{IJ}), (1 - \delta_j^t) \cdot B_{cap}\} \geq \mathcal{D}_{ij}^t, \quad \forall i \in I^*, j \in J, t \in T,$$

Where:

$$I^* := \{i \mid u_i \geq \bar{u}, i \in \bar{I}\}$$

and  $u_i, \bar{u}, \bar{I}$  as defined in definition 3.2 and (3.6). Though (B.13) still gives a relatively loose upper bound, it provides much better computational results than blindly setting  $\mathcal{M}^t, t \in T$  as extraordinarily large.

Nevertheless, if necessary, one can also specialize *Big- $\mathcal{M}$ s* with respect to each POI as  $\mathcal{M}_j^t, j \in J, t \in T$  and use:

$$\mathcal{M}_j^t := \max\{B_{cap} \cdot \mathcal{A}_j^t, \sum_{i \in I} \tau_{ij} \cdot (m_i + n_i)\pi\}$$

as tighter values for *Big- $\mathcal{M}$ s*

## Appendix C

### EVCSAP Models in Compact Form

#### Linearized Base Model

$$\max_{\mathbf{x}, \mathbf{y}, \mathbf{z}} \sum_{t \in T} \sum_{i \in I} \sum_{j \in J} u_i \mathcal{D}_{ij}^t \mathcal{A}_{ij}^t \mathbf{z}_{ij}^t \cdot 365 - (\sum_{i \in I} c_i^x \mathbf{x}_i + c^y \mathbf{y}_i) \quad (C.1)$$

s.t.:

$$\sum_{i \in I_0} \mathbf{x}_i \leq N_0 \quad \sum_{i \in I_1} \mathbf{x}_i \leq N_1 \quad (C.2)$$

$$\sum_{i \in I} \mathbf{x}_i \leq N^{\mathbf{x}} \quad \sum_{i \in I} \mathbf{y}_i \leq N^{\mathbf{y}} \quad (C.3)$$

$$\mathbf{x}_i \leq \mathbf{y}_i, \quad i \in I \quad \mathbf{y}_i \leq m_i \mathbf{x}_i, \quad i \in I \quad (C.4)$$

$$\mathbf{x}_j (\rho - d_{ij}) \leq 0, \quad i \in I_0, j \in I_1 \quad \mathbf{x}_{ij} (\rho - d_{ij}) \leq 0, \quad \forall i, j \in I_1, i \neq j \quad (C.5)$$

$$\mathbf{x}_{ij} \leq \mathbf{x}_i, \quad i, j \in I_1, i \neq j \quad \mathbf{x}_{ij} \leq \mathbf{x}_j, \quad i, j \in I_1, i \neq j \quad (C.6)$$

$$\mathbf{x}_i + \mathbf{x}_j - 1 \leq \mathbf{x}_{ij}, \quad i, j \in I_1, i \neq j \quad \mathbf{x}_{ij} \in \{0, 1\}, \quad i, j \in I_1, i \neq j \quad (C.7)$$

$$\sum_{j \in J} \mathcal{D}_{ij}^t \mathcal{A}_{ij}^t \mathbf{z}_{ij}^t \leq \mathbf{w}_i^t, \quad i \in I, t \in T \quad \sum_{j \in J} \mathcal{T}_{ij}^t \mathcal{A}_{ij}^t \mathbf{z}_{ij}^t \leq \mathcal{T}_i^t, \quad i \in I, t \in T \quad (C.8)$$

$$\chi_j^t \leq \mathcal{D}_j^t \mathcal{A}_j^t, \quad j \in J, t \in T \quad \chi_j^t \leq \sum_{i \in I} \mathbf{w}_{ij}^t, \quad j \in J, t \in T \quad (C.9)$$

$$\chi_j^t \geq \mathcal{D}_j^t \mathcal{A}_j^t - \mathcal{M}^t (1 - \mathcal{E}_j^t), \quad j \in J, t \in T \quad \chi_j^t \geq \sum_{i \in I} \mathbf{w}_{ij}^t - \mathcal{M}^t \mathcal{E}_j^t, \quad j \in J, t \in T \quad (C.10)$$

$$\sum_{i \in I} \mathcal{D}_{ij}^t \mathcal{A}_{ij}^t \mathbf{z}_{ij}^t \geq \chi_j^t, \quad j \in J, t \in T \quad \chi_j^t \in \mathbb{R}, \quad j \in J, t \in T \quad (C.11)$$

$$\mathcal{E}_j^t \in \{0, 1\}, \quad j \in J, t \in T \quad \sum_{i \in I} \mathbf{z}_{ij}^t \leq 1, \quad j \in J, t \in T \quad (C.12)$$

$$\mathbf{x}_i \in \{0, 1\} \quad i \in I \quad \mathbf{y}_i \in \mathbb{Z}, \quad i \in I \quad (C.13)$$

$$\mathbf{z}_{ij}^t \geq 0 \quad i \in I, j \in J, t \in T \quad (C.14)$$

## Linearized MPDP

$$\begin{aligned} \max_{\mathbf{x}, \mathbf{y}, \mathbf{z}, \mathbf{h}, \eta} & \sum_{t \in T} \sum_{i \in I} \sum_{j \in J} u_i \mathcal{D}_{ij}^t \mathcal{A}_{ij}^t \mathbf{z}_{ij}^t \cdot 365 - (\sum_{i \in I} c_i^x \mathbf{x}_i + c^y \mathbf{y}_i + \sum_{k \in K} 50 \cdot c^h \mathbf{h}_k + \sum_{t \in T} \sum_{k \in K} 50 \cdot c^\eta \eta_k^t \cdot 365) \\ \text{s.t.:} & \quad (\text{C.2}) - (\text{C.14}) \end{aligned} \quad (\text{C.15})$$

$$\mathbf{x}_i \leq \sum_{k \in K} Z_{ik}, \quad i \in I \quad (\text{C.16})$$

$$\sum_{i \in I} Z_{ik} \psi_i^t \leq (\Pi_k^t + 50 \cdot \mathbf{h}_k + 50 \cdot \eta_k^t) \Delta t, \quad k \in K, t \in T \quad (\text{C.17})$$

$$\mathbf{h}_k \in \mathbb{Z}, \quad k \in K \quad (\text{C.18})$$

$$\eta_k^t \in \mathbb{Z}, \quad k \in K, t \in T \quad (\text{C.19})$$

## Linearized MPSP

$$\begin{aligned} \max_{\mathbf{x}} & \sum_{t \in T} \sum_{i \in I} \sum_{j \in J} u_i \mathcal{D}_{ij}^t \mathcal{A}_{ij}^t \mathbf{z}_{ij}^t \cdot 365 - (\sum_{i \in I} c_i^x \mathbf{x}_i + c^y \mathbf{y}_i + \sum_{k \in K} 50 \cdot c_k^h \mathbf{h}_k + \mathbb{E}_{\mathcal{Z}}[Q(X, \mathcal{Z}(\omega))]) \\ \text{s.t.:} & \quad (\text{C.2}) - (\text{C.14}), \text{ and } (\text{C.18}) \end{aligned} \quad (\text{C.20})$$

where:

$$Q(X, \mathcal{Z}(\omega)) := \min_{\eta} \sum_{t \in T} \sum_{k \in K} 50 \cdot c^\eta \eta_k^t(\omega) \cdot 365 \quad (\text{C.21})$$

$$\text{s.t.: } \mathbf{x}_i \leq \sum_{k \in K} \mathcal{Z}_{ik}(\omega), \quad i \in I, \quad (\text{C.22})$$

$$\sum_{i \in I} \mathcal{Z}_{ik}(\omega) \psi_i^t \leq (\Pi_k^t + 50 \cdot \mathbf{h}_k + 50 \cdot \eta_k^t(\omega)) \Delta t, \quad k \in K, t \in T, \quad (\text{C.23})$$

$$\eta_k^t(\omega) \in \mathbb{Z}, \quad k \in K, t \in T, \quad (\text{C.24})$$

# Appendix D

## Model Implementation

### Implementation

The MPI-SPPy is developed based on the idea that one starts with a deterministic Pyomo model and extends it to anticipate uncertainty. Thus the codes of **MPDP** will be used as implementation examples in section D, followed by the explanation of SP with MPI-SPPy for **MPSp** in section D

#### Deterministic Model by Pyomo

Pyomo is an object-oriented modeling language for optimization. A Pyomo *model* object consists of a collection of modeling *components* that define the optimization problem. These modeling components include sets (`Set`), parameters (`Param`), variables (`Var`), objective(s) (`Objective`), constraints (`Constraint`), expressions (`Expression`<sup>1</sup>), etc [Har+17].

A simple modeling process with Pyomo contains the following basic steps:

1. Create a model instance and declare its components
2. Pass this instance to a solver (e.g., CPLEX) to find a solution
3. Report and analyze results from the solver

Several lines of `Python` codes is provided in the following sections to illustrate these steps.

#### Step 1: Create a model instance and declare components

This section explains the mentioned Pyomo modeling components by a part of codes from the deterministic MILP model **MPDP**.

---

<sup>1</sup>The Expression component is useful for representing common sub-expressions, such as  $w_{ij}^t$  in (B.5). Reusing common sub-expressions in multiple contexts can help avoid the overhead of regenerating the same expression each time and improve memory efficiency.

**1.a** Build an empty (concrete) model frame:

```
import pyomo.environ as pyo
model = pyo.ConcreteModel(name = 'MPDP')
3
```

The Pyomo *concrete*<sup>2</sup> models immediately initialize each component during construction by Python data such as `list`, `dictionary`, `Pandas DataFrame`.

Using the command `model.display()` can access the model information:

```
[Input:] model.display()
[Output:]
    Model MPDP ; Variables: None ; Objectives: None ; Constraints: None
```

**1.b** Declare sets:

```
model.I_newBuild = pyo.Set(initialize = setup_data['I_newBuild'],
                           doc = 'Candidate locations for NEW CS.')
3   model.I_update = pyo.Set(initialize = setup_data['I_update'],
                           doc = 'Candidate locations with EXISITING CSs and CPs.')
   model.I = model.I_update | model.I_newBuild
6
```

The `Set` components represents a collection of data that can include numeric (e.g., integer), or symbolic (e.g., string) elements. As components of a concrete model, they are initialized immediately by the corresponding data `setup_data['I_newBuild']` and `setup_data['I_update']`. The last line defines a set `I` that is the union of the sets `I_newBuild` and `I_update`.

Similarly, the information of `Set` component can be accessed by the command `model.setname.display()`, e.g.:

```
[Input:] model.I.display()
[Output:]
    I_newBuild : Candidate locations for NEW CS.
    Size=1, Index=None, Ordered=Insertion
    Key : Dimen : Domain : Size : Members
    None :      1 : Any : 11 : {18, 36, 48, 58, 61, 96,
                           110, 114, 115, 177, 178}
```

which shows that the indices of candidate locations for building new CSs are  $\{18, 36, \dots\}$ .

---

<sup>2</sup>The other type of Pyomo model, the *abstract* model, first builds a model frame, then feeds the data from disparate (non-Python) sources (e.g., JSON File, CSV File, YAML File, etc.), to initialize all components [Har+17].

---

### 1.c Declare parameters:

```
model.N_totalCSs = pyo.Param(initialize = setup_data['N_totalCSs'],
    domain = pyo.NonNegativeIntegers,
    mutable = True,
    doc = 'Max number of CSs (existing or new) to update or open ↵
        in total.')
model.n = pyo.Param(model.I,
    initialize = setup_data['n'],
    mutable = True,
    domain = pyo.NonNegativeIntegers,
    doc = 'Number of CPs already sited in candidate locations i \in ↵
        I.')

```

These lines define a non-indexed parameter `N_totalCSs` and the indexed parameters  $n_i$ ,  $i \in I$  for MPDP. The index set is claimed by line 6 as `model.I`. Line 2 and line 9 declare the domain of parameters. Setting parameters as `mutable` in line 8 allows them to be modified for repeated solves and tests.

Similarly, `model.ParamName.display()` delivers information of parameters  $n_i$ ,  $i \in I$ :

```
[Input:] model.n.display()
[Output:]
n : Number of CPs already sited in an (existing) opened CS at
i \in I.
    Size=12, Index=I, Domain=NonNegativeIntegers,
    Default=None, Mutable=True
    Key : Value
    18 : 0.0; 36 : 0.0; ... ... 195 : 2.0
```

which shows that two CPs are sited at an existing CS at the location 195.

### 1.d Define (decision) variables:

```
model.x = pyo.Var(model.I,
    domain = pyo.Binary,
    initialize = 0,
    doc = '''1, either an existing CS at i \in I_update will be ↵
        updated, or a candidate location i \in I_newBuild will be chosen ↵
        for a new CS; 0, otherwise.''')
model.y = pyo.Var(model.I,
    domain = pyo.NonNegativeIntegers,
    initialize = 0,
    doc = 'Number of CPs to be installed at candidate location i \in ↵
        I.')
model.z = pyo.Var(model.I, model.J, model.T,
```

```

12     domain = pyo.UnitInterval,
13     initialize = 0,
14     doc = 'The fraction of EV arrivals (with CD) at CD center j \in I
15     \in J that recharges at CS i \in I during t \in T.')

```

Pyomo supports discrete and continuous variables. For instance, the domain of variables  $x_i$ ,  $i \in I$  is claimed as binary in line 2, and that of  $z_{ij}^t$ ,  $i \in I, j \in J, t \in T$  as the unit interval in line 12. Optionally, variables can be initialized for warm start and potential resolution acceleration, e.g., by line 11.

### 1.e Define expressions:

```

def p_scaled_walk_dist_expr(model, i, j):
    u_average = sum(model.u[i] for i in model.I)/len(model.u)
    price_scaled_dist = (model.u[i] / u_average) * (model.d[i,j])
    return price_scaled_dist
model.d_pScaled = pyo.Expression(model.I, model.J,
3       expr = p_scaled_walk_dist_expr,
6       doc = 'Price (u[i]) scaled walking distance (in hour) between a
        ↵ candidate location i \in I and a CD center j \in J.')

```

The lines above implement the expression price-scaled-walking-distance indexed by sets `model.I` and `model.J` as defined in (3.2). Rules of the expression are claimed in line 6 by a Python function. This expression involves no decision variables and can actually be defined before decision variables are declared.

However, the following expression of EESC as defined in definition 3.6 involving decision variables  $y_i$ ,  $i \in I$  must be declared after these decision variables are introduced:

```

def EESC_expr(model, i, t):
    eff_CC_i_t = sum(model.w_cs2poi[i,j,t] for j in model.J)
    return eff_CC_i_t
model.w = pyo.Expression(model.I, model.T,
3       expr = EESC_expr,
6       doc = 'exogenous charging energy supply capability at a CS i \n
        ↵ in I during t \in T')

```

and notice that the above expression utilizes another expression `model.w_cs2poi[i, j, t]` as defined in (3.13).

### 1.f Define objective:

```

model.obj_total_profit = pyo.Objective(
    rule = model.gross_revenue - (model.cs_placement_cost + \
3       model.grid_expansion_cost),
    sense = pyo.maximize)

```

---

The objective of **MPDP** as given in (3.41) is defined as above. The components regarding revenue and costs are predefined model expressions. A flag to indicate the sense (maximize or minimize) is declared in line 4.

Furthermore, Pyomo allows multiple objectives to exist in the same model. For instance, the following codes declare another objective that considers no grid expansion cost:

```
model.obj_profit_no_grid = pyo.Objective(
    rule = model.gross_revenue - model.cs_placement_cost,
    sense = pyo.maximize)
```

**Before** solving a model with many objectives, command `model.obj_name.deactivate()` **must** be called to deactivate the needless objective(s).

### 1.g Define constraints:

```
def CSchargeCap_rule(model, i, t):
    CD_at_i_during_t = sum(model.calD[i,j,t] * model.calA[j,t] * \
3     model.tau[i,j] * model.z[i,j,t] for j in model.J)
    return CD_at_i_during_t <= model.w[i,t] # boolean
model.cons_CSchargeCap = pyo.Constraint(model.I, model.T,
6     rule = CSchargeCap_rule,
     doc = "Total CD served at i \in I during period t \in T does ~
→ not exceed the EESC of CS i \in I")
#####
9 def CSserviceTimeCap_rule(model, i, t):
    total_park_time_at_i_during_t = sum(
        model.z[i,j,t] * model.tau[i,j] * model.calA[j,t] * \
12     (model.calT[j,t] + 2*model.d[i,j]) for j in model.J
    )
    TSC_at_i_during_t = model.DeltaT[t]*(model.y[i]+model.n[i])
15    return total_park_time_at_i_during_t <= TSC_at_i_during_t
model.cons_CS_service_time_Cap = pyo.Constraint(
    model.I, model.T,
18    rule = CSserviceTimeCap_rule,
    doc = "total length of parking time by covered CDs does not ~
→ exceed total service time of CPs at CS i."
)
```

21

Constraints define additional restrictions on the optimization variables. Equality (`==`) and general inequality (`<=` or `>=`) constraints are supported by Pyomo. The Constraint components contain expressions and the proper relational functions (operators), e.g., functions `CSchargeCap_rule` and `CSserviceTimeCap_rule`.

Similarly, commands `model.var_name.display()`, `model.obj_name.display()`, and `model.constr_name.display()` can be called separately to check specific components. Alternatively, command `model.display()` can be applied to check the information of

all components of variables, objective(s), and constraints<sup>3</sup>:

```
[Input:] model.display()
[Output:]
Model MPDP
Variables:
    x : 1, either an existing CS at i \in I_update will be
        updated, or a candidate location i \in I_newBuild will be
        chosen for a new CS; 0, otherwise.
    Size=12, Index=I
    Key : Lower : Value : Upper : Fixed : Stale : Domain
          18 :      0 :      0 :      1 : False : False : Binary
    .....
Objectives:
    obj_profit_no_grid : Size=1, Index=None, Active=False
    Key : Active : Value
    None : True : 0.0
    obj_total_profit : Size=1, Index=None, Active=True
    Key : Active : Value
    None : True : 0.0
Constraints:
    cons_CSchargeCap : Size=36
    Key : Lower : Body : Upper
    (18, 'day_normal') : None : 0.0 : 0.0
    .....
```

Up to this point, a short explanation of the mentioned Pyomo components has been provided by a part of **MPDP** model codes. For a comprehensive understanding of modeling with Pyomo, example 3.2 on implementation of a warehouse location problem in chapter 3 of [Har+17] is recommended.

The following small section illustrates how to pass the model to solvers to find an optimal solution.

### Step 2: Pass the instance to a solver

Pyomo supports a large variety of solvers such as CPLEX, Gurobi, GLPK. The following codes call the CPLEX solver to solve a **MPDP** model:

```
from pyomo.opt import SolverFactory
3   Solver = SolverFactory('cplex')
      solver_results = Solver.solve(MPDP)
```

And the solver message is accessible through:

---

<sup>3</sup>However, it is not recommended to use `model.display()` to print information of a large scale model as it is time-consuming due to generation of extraordinary long texts

---

```

[Input:] print(solver_results)
[Output:]
Problem:
- Name:
  Lower bound: 1599429.40246346
  Upper bound: 1599429.40246346
  Number of constraints: 3486
  Number of variables: 6842
  Number of nonzeros: 14704
  Sense: maximize
.....
Termination message: MIP - Integer optimal solution\x3a
  Objective = 1.5994294025e+06
.....

```

It shows that the linearized **MPDP** instance with 6842 variables and 3486 constraints is solved within a second of solver time to get the optimal EVCSAP decision.

It is worth mentioning that some solvers support a warm start based on the current values of variables. To use this feature, set the values of variables in the instance (either by the keyword argument `initialize`, or pre-define them directly index by index) and pass `warmstart=True` to the `Solver.solve()` method, e.g.:

```

model.x[18] = 1 # directly pre-define x[18]
model.y[18] = 4 # directly pre-define y[18]
3
Solver = SolverFactory("cplex")
results = Solver.solve(instance, warmstart=True)
6

```

### Step 3: Report and analyze results from the solver

After a model instance is solved, the updated values (status) of model components can be retrieved through `.display()` method. For example, from the solved model above, the following information can be accessed:

```

[Input:] model.y.display()
      # Number of CPs installed at candidate locations
[Output:]
y : Number of CPs to be installed at location i \in I.
Size=12, Index=I
Key : Lower: Value : Upper : Fixed : Stale : Domain
      36 : 0 : 2.0 : None : False : False : NonNegativeIntegers
.....
195 : 0 : 0.0 : None : False : False : NonNegativeIntegers

[Input:] model.w.display()
      # EESC of different candidate locations
      # Notice: The existing 195 already has two CPs

```

## Appendix D Model Implementation

---

```
[Output:]  
w : Size=36  
Key : Value  
(36, 'day_normal') : 219.11113485638174  
.....  
(195, 'night') : 29.389906597104506  
  
[Input:] model.cons_CSchargeCap.display()  
# Status of Constraints on Charging Energy Capacity of CSs  
[Output:]  
cons_CSchargeCap : Size=36  
Key : Lower : Body : Upper  
(36, 'day_normal') : None : -8.526512829121202e-14 : 0.0  
.....  
(195, 'night') : None : 7.105427357601002e-15 : 0.0
```

The commands above are useful for checking model information.

For data analysis, however, it is more advantageous to use commands `.get_values()` (for variables) and `.extract_values()` (for parameters and expressions) to directly extract Python dictionary from the model:

```
[Input:] model.y.get_values() # Decision variable y  
# Extract the dictionary of installed CPs  
[Output:]  
{195: 0.0, 18: 0.0, 36: 2.0, 48: 10.0, 58: 8.0, ...}  
  
[Input:] model.m.extract_values() # Parameter m  
# Extract the dictionary of the maximum number of CPs can be  
# installed at each candidate location  
[Output:]  
{195: 2.0, 18: 16.0, 36: 2.0, 48: 10.0, 58: 8.0, ...}  
  
[Input:] model.w.extract_values() # Expression w  
# Extract the dictionary of the EESC of each CS  
# Notice that this will output expressions instead of values  
[Output:]  
{(195, 'day_normal'):  
 <pyomo.core.expr.numeric_expr.SumExpression at 0x1fa827bcd0>,  
 .....,  
 }  
# Use 'pyo.value()' method to evaluate the values of expressions  
[Input:]  
w_expression_dict = model.w.extract_values()  
w_value_dict = { w_idx : pyo.value(w_expr) \  
 for (w_idx, w_expr) in w_expression_dict.items() }  
w_value_dict  
[Output:]  
{(195, 'day_normal'): 235.26993886952584,  
 .....
```

---

The introduction to the steps of the basic Pyomo modeling process finishes here. For advanced techniques, the [Pyomo Documentation](#) and [Byn+21] are recommended.

## Two-Stage Stochastic Programming with MPI-SPPy

SP in Pyomo is empowered by [MPI-SPPy](#), which supports for solving multi-stage stochastic programs based on a scenario discretization of the uncertainty. This section briefly introduces the work process of solving MPSP with [MPI-SPPy](#).

Any scenario-based method solving optimization problems under uncertainty is solving the extensive form (EF) as introduced in section 19. Some of the methods solve it by decomposition algorithms such as Progressive Hedging and Benders' Decomposition [BL11]. According to the experiment results of [MPSP](#), directly passing the EF of [MPSP](#) to [CPLEX](#) without applying decomposition algorithms can efficiently solve the proposed EVCSAP problem in our tested case in Schutterwald. Therefore, only the direct EF method is introduced in the following part.

A typical modeling process with [MPI-SPPy](#) contains the following basic steps:

1. Define the *scenario\_creator*
2. Create an EF instance and pass it to a solver (e.g., [CPLEX](#)) to find a solution.
3. Report and analyze results from the solver.

Several lines of codes of [MPSP](#) implemented in Python are provided in the following sections to illustrate these steps.

### Step 1: Define a *scenario\_creator*

[MPI-SPPy](#) applies the [Python function](#) named *scenario\_creator* to transform the deterministic model of a specific scenario into a stochastic model that the [MPI-SPPy](#) can manipulate. Each call of the *scenario\_creator* function builds a Pyomo model according to a given *scenario\_name*. The typical structure of a *scenario\_creator* for a two-stage SP is as follows:

```
import mpisppy.utils.sputils as sputils

3 def scenario_creator(scenario_name, data_all_scenarios):
    # 0. Build a Pyomo model with data of the given scenario:
    scenario_data = data_all_scenarios[scenario_name]
    scenario_model = build_model(scenario_data)
    # 1. Declare the first-stage objective and variables:
    sputils.attach_root_node(model = scenario_model,
        firstobj = scenario_model.first_stage_objective,
        varlist = scenario_model.first_stage_variables)
    # 2. Attach the probability of the given scenario to the
    #     scenario_model:
```

```
    scenario_model._mpisppy_probability = 1.0 / 3
    return model
```

As shown, apart from building a model of a given scenario, a scenario\_creator accomplishes two important tasks: 1.) Define which part of the objective and which set of variables belong to the first stage of the scenario\_model; 2.) Define the probability that the given scenario occurs. If this probability is not specified, MPI-SPPy will assume that all scenarios are equally likely.

The scenario\_creator for **MPSP** is provided below:

```
import mpisppy.utils.sputils as sputils

3  def csap_scenario_creator(scenario_name, mpdp_frame_data: dict,
                           all_sces_dict: dict, linearize_model: bool = True,
                           model_name: str = 'EVCSAP_MPSP') -> pyo.ConcreteModel:
6      # 0. Build a Pyomo model instance of MPSP:
6      connect_sce = all_sces_dict[scenario_name].stack().to_dict()
9      sce_model = _build_mpssp_csap_from_mpdp_frame(
9          mpdp_frame_data = mpdp_frame_data,
9          cs_ss_connect_sce = connect_sce,
9          m_name = model_name,
9          linearized = linearize_model )
12     # 1. Declare the first-stage objective and variables of MPSP:
12     sputils.attach_root_node(model=sce_model,
15         firstobj = sce_model.first_stage_profit,
15         varlist = [sce_model.x, sce_model.y, sce_model.z,
15                    # CSs, CPs planning and CD coverage variables
18                    sce_model.x_hat, sce_model.chi, sce_model.cale,
18                    # Auxiliary variables for linearization
18                    sce_model.h
18                    # SSs expansion variables
21                ])
21     # 2. Attach the probability of the given scenario:
24     model._mpisppy_probability = 1.0 / len(all_sces_dict)
24     return model
```

In line 1 the mpdp\_frame\_data provided the values of deterministic data, which are extracted from a built **MPDP**. In addition, grid connection scenarios of CSs and SSs are sampled beforehand by Algorithm 1 and stored in the all\_sces\_dict (a Python dictionary). First stage objective of **MPSP** defined in (3.47) and the corresponding decision variables are declared in line 15. In line 24, the probability of each sample generated from algorithm **2D-C-S-NET** is defined as even.

### Step 2: Create and solve an EF instance

An EF of **MPSP** model can be directly built through MPI-SPPy as follows:

```
from mpisppy.opt.ef import ExtensiveForm
# 0. Define solver options:
```

---

```

3     options = {"solver": "cplex"}
4     # 1. Build the EF instance according to defined solver scenarios
5     #      by the scenario_creator:
6     MPSP_ef = ExtensiveForm(options = solver_options,
7                               all_scenario_names = CS_SS_con_sces_names,
8                               scenario_creator = csap_scenario_creator,)
9     # 2. Pass EF to the solver to solve:
10    solver_results = MPSP_ef.solve_extensive_form()

```

Line 3 defines which solver to use. Additional options, including the number of device threads to use, whether to apply a warm start, etc. are applicable. Given  $m$  scenario names, the method `ExtensiveForm()` in line 6 will build an EF by calling the `scenario_creator`  $m$  times for building  $m$  scenario models to form the EF. The last line passes the EF to the predefined solver to solve.

### Step 3: Report and analyze results from the solver

Solver messages can be printed. Below we provided a test case with 50 scenarios restricted by 507255 constraints. CPLEX used less than 12 seconds to solve this SP:

```

[Input:]
    print(solver_results['Problem'], solver_results['Solver'])
[Output:]
Problem:
    Lower bound: 1175296.8087210667
    Upper bound: 1175408.9633
    .....
    Termination message: MIP - Integer optimal, Objective = 1.1752968087e+06
    Branch and bound:
        Number of bounded subproblems: 2696
        Number of created subproblems: 2696
    Error rc: 0
    Time: 11.484379768371582

```

Solutions to an EF are accessible through the `.get_root_solution()` command. As all scenarios share the same first-stage decisions, MPI-SPPy provides the solutions with a prefix that indicates the name of the first created scenario\_model (e.g., with the prefix '`'13947'` below):

```

[Input:] # retrieve variables values:
    solution = ef.get_root_solution()
    for (var_name, var_value) in solution.items():
        print(var_name, var_value)
[Output:]
    '13947'.x[48] 1.0
    .....
    '13947'.y[48] 7.0
    .....
    '13947'.z[48,54,day_normal] 0.01643714959555176
    .....

```

## *Appendix D Model Implementation*

---

```
'13947'.z[58,161,day_normal] 1.0
.....
'13947'.h[8] 5.0
.....
```

Accessing the second-stage decisions of a sub-model for a specific scenario is possible by using an Python `iterator` named `scenarios()`. It can yield scenario sub-models in an EF. By applying `.get_values()` method on a specific sub-model, second-stage decisions and costs can be retrieved. For the detailed usage of this `iterator`, please refer to [MPI-SPPy EF Directly](#).

# List of Figures

2.1	Illustration of the priority of grid upgrades [ACE22]	6
3.1	An Example of Function $\tau(d, \phi)$ in Def.3.1 with $\phi = \frac{1}{6}[\text{hour}]$ of walking distance	11
3.2	Grid Connection Probability defined by Grid Connection Weights.	25
3.3	Grid Connection Probability defined by Grid Connection Weights under Neighborhood Effect.	26
3.4	Illustration on Vector Calculation of Grid Connection Weights under Neighborhood Effect.	26
4.1	Map of Schutterwald with POIs, SSs and Candidate Locations for CSs	30
4.2	Graph Network of Schutterwald with POIs, Candidate Locations for CSs and Substations. <i>skyblue nodes: SSs; Gray nodes: POIs (Size represents the number of EV arrivals); yellow nodes: Candidate locations for building new CSs (size represents the maximum number of CPs can be installed); orange nodes: The candidate location for updating the only existing CS in SW (in the cluster below largely covered by a yellow node and a blue node.)</i>	31
4.3	Probability Distributions for POIs Statistics	32
4.4	Work Flow of <b>MPSP</b> Implementation	34
4.5	An Example of Grid Connection between CSs and SSs. (This scenario is used for <b>MPDP</b> )	35
4.6	CS-SS Connection	36
4.8	The average and standard deviation of critical parameters	38
4.10	An Example of CD Coverage during day_normal period in <b>MPDP</b> . Darkblue nodes: Expanded SSs; Red nodes: New CSs (node size represents installed number of CPs); Grean edges: CS-POI CD coverage pairs, edge width represents percentage of CD covered by corresponding CSs.	40
4.11	Utilization Rate and Daily Load of CPs	41
4.12	Solver time w.r.t. Number of Samples	42



# List of Tables

1	Table of Abbreviations . . . . .	ix
2	Notations in <b>Base Model</b> . . . . .	x
3	Parameters in <b>Base Model</b> . . . . .	xi
4	Decision Variables in <b>Base Model</b> . . . . .	xii
5	Notations, Parameters and Decision Variables introduced in <b>MPDP</b> . .	xii
6	Notations, Parameters and Decision Variables introduced in <b>MPSP</b> . .	xiii



## List of Algorithms

1	Distance Decayed CS-SS Connection Scenario Generation under Neighborhood Effect . . . . .	27
---	---	----



# Index

## Symbols

---

$\hat{d}_{ij}$ , 12  
 $\mathcal{D}_{ij}^t$ , 13  
 $B_{cap}$ , 11  
 $I$ , 9  
 $I_0$ , 9  
 $I_1$ , 9  
 $J$ , 9  
 $K$ , 20  
 $N^x$ , 10  
 $N^y$ , 10  
 $Z_{ik}$ , 20  
 $\Pi_k^t$ , 20  
 $\gamma_i^t$ , 16  
 $\psi_i^t$ , 15  
 $\mathbf{h}_k$ , 20  
 $\mathbf{x}_i$ , 9  
 $\mathbf{y}_i$ , 10  
 $\mathcal{A}_{ij}^t$ , 12  
 $\phi$ - $u$ -isolated, 13  
 $\pi$ , 10  
 $c^{\mathbf{h}}$ , 20  
 $c^y$ , 10  
 $c_i^x$ , 10  
 $d_{ij}$ , 10  
 $n_i$ , 10  
 $u_i$ , 10  
 $\Delta T_{ij}^t$ , 51  
 $\tau_{ij}$ , 12  
 $\tau_{ik}$ , 24  
 $\Omega$ , 22  
 $Z_{ik}$ , 22  
 $\rho$ , 10

## MPDP

---

**MPSP**, 9

Distance threshold  
 $\phi^{IJ}$ , 12

## C

---

Charging Demand

$\mathcal{T}_{ij}^t$ , 13  
 $\mathcal{A}_{ij}^t$ , 12  
 $\mathcal{D}_{ij}^t$ , 13  
 Dynamic CD, 14  
 Static CD, 52

## D

---

Distance Decay, 11  
 Distance threshold, 12

$\phi^{II}$ , 24  
 $\phi^{IK}$ , 24

## E

---

$\text{ESC}$ , 14  
 EESC, 15  
 TESC, 14

## G

---

Grid Congestion, 20  
 Backstop Technology, 20

## P

---

$\text{POI}$ , 9  
 POI Statistics, 11  
 $\mathcal{A}_j^t$ , 11  
 $\mathcal{T}_j^t$ , 11  
 $\delta_j^t$ , 11

*INDEX*

---

**S** \_\_\_\_\_  
SOC, 11

**U** \_\_\_\_\_  
utilization rate, 16

**T** \_\_\_\_\_  
TSC, 15

# Bibliography

- [ACE22] T. E. A. M. A. (ACEA). *European Electric Vehicle Charging Infrastructure Masterplan*. Mar. 2022. URL: <https://www.acea.auto/files/Research-Whitepaper-A-European-EV-Charging-Infrastructure-Masterplan.pdf>.
- [Age20] E. E. Agency. *Transport: increasing oil consumption and greenhouse gas emissions hamper EU towards environment and climate objectives*. European Environment Agency, 2020. URL: <https://www.eea.europa.eu/publications/transport-increasing-oil-consumption-and>.
- [Ahm+22] F. Ahmad, A. Iqbal, I. Ashraf, M. Marzband, and I. khan. “Optimal location of electric vehicle charging station and its impact on distribution network: A review”. In: *Energy Reports* 8 (2022), pp. 2314–2333. ISSN: 2352-4847. DOI: <https://doi.org/10.1016/j.egyr.2022.01.180>. URL: <https://www.sciencedirect.com/science/article/pii/S2352484722001809>.
- [Ahm11] S. Ahmed. “Two-Stage Stochastic Integer Programming: A Brief Introduction”. In: *Wiley Encyclopedia of Operations Research and Management Science*. John Wiley & Sons, Ltd, 2011. ISBN: 9780470400531. DOI: <https://doi.org/10.1002/9780470400531.eorms0092>. eprint: <https://onlinelibrary.wiley.com/doi/pdf/10.1002/9780470400531.eorms0092>. URL: <https://onlinelibrary.wiley.com/doi/abs/10.1002/9780470400531.eorms0092>.
- [AS02] S. Ahmed and A. Shapiro. “The Sample Average Approximation Method for Stochastic Programs with Integer Recourse”. In: 2002. URL: <https://www2.isye.gatech.edu/~sahmed/saasip.pdf>.
- [AGJ20] M. F. Anjos, B. Gendron, and M. Joyce-Moniz. “Increasing electric vehicle adoption through the optimal deployment of fast-charging stations for local and long-distance travel”. In: *European Journal of Operational Research* 285.1 (2020), pp. 263–278. ISSN: 0377-2217. DOI: <https://doi.org/10.1016/j.ejor.2020.01.055>. URL: <https://www.sciencedirect.com/science/article/pii/S0377221720300928>.

## Bibliography

---

- [Ber+21] C. Bermejo, T. Geissmann, T. Möller, F. Nägele, and R. Winter. *The impact of electromobility on the German electric grid*. June 2021. URL: <https://www.mckinsey.com/industries/electric-power-and-natural-gas/our-insights/the-impact-of-electromobility-on-the-german-electric-grid>.
- [Bib+22] E. M. Bibra, E. Connelly, S. Dhir, M. Drtil, P. Henriot, I. Hwang, J.-B. L. Marois, S. McBain, L. Paoli, and J. Teter. *Global Electric Vehicle Outlook 2022*. International Energy Agency (IEA), 2022. URL: <https://www.iea.org/reports/global-ev-outlook-2022>.
- [BL11] J. Birge and F. V. Louveaux. “Introduction to Stochastic programming (2nd edition), Springer verlag, New York”. In: 2011.
- [Byn+21] M. L. Bynum, G. A. Hackebeil, W. E. Hart, C. D. Laird, B. L. Nicholson, J. D. Siirola, J.-P. Watson, and D. L. Woodruff. *Pyomo—optimization modeling in python*. Third. Vol. 67. Springer Science & Business Media, 2021.
- [CHG15] J. Cavadas, G. Homem de Almeida Correia, and J. Gouveia. “A MIP model for locating slow-charging stations for electric vehicles in urban areas accounting for driver tours”. In: *Transportation Research Part E: Logistics and Transportation Review* 75 (2015), pp. 188–201. ISSN: 1366-5545. DOI: <https://doi.org/10.1016/j.tre.2014.11.005>. URL: <https://www.sciencedirect.com/science/article/pii/S136655451400194X>.
- [CKK13] T. D. Chen, K. Kockelman, and M. Khan. “The electric vehicle charging station location problem: A parking-based assignment method for Seattle”. In: *Transportation Research Board 92nd Annual Meeting* (Jan. 2013).
- [CR74] R. Church and C. ReVelle. “The maximal covering location problem”. In: *Papers of the Regional Science Association* 32.1 (Dec. 1974), pp. 101–118. URL: <https://link.springer.com/article/10.1007/BF01942293>.
- [Com22] E. Commission. *European Alternative Fuels Observatory*. 2022. URL: <https://alternative-fuels-observatory.ec.europa.eu/consumer-portal/available-electric-vehicle-models>.
- [Con21] U. N. S. T. Conference. “FACT SHEET CLIMATE CHANG”. In: (2021). URL: [https://www.un.org/sites/un2.un.org/files/media\\_gstc/FACT\\_SHEET\\_Climate\\_Change.pdf](https://www.un.org/sites/un2.un.org/files/media_gstc/FACT_SHEET_Climate_Change.pdf).
- [Con+22] J. Conzade, F. Nägele, S. Ramanathan, and P. Schaufuss. *Europe’s EV opportunity and the charging infrastructure needed to meet it*. Nov. 2022. URL: <https://www.mckinsey.com/industries/automotive-and-assembly/our-insights/europe-s-ev-opportunity-and-the-charging-infrastructure-needed-to-meet-it>.

- 
- [D+16] G. D, D. I, Z. A, Z. P, D. P, and T. C. *Optimal allocation of electric vehicle charging infrastructure in cities and regions*. Scientific analysis or review LD-NA-27894-EN-C (print),LD-NA-27894-EN-N (online),LD-NA-27894-EN-E (ePub). Luxembourg (Luxembourg): JRC, 2016. DOI: [10.2790/183468](https://doi.org/10.2790/183468)(print) ,[10.2790/353572](https://doi.org/10.2790/353572)(online) ,[10.2790/286542](https://doi.org/10.2790/286542)(ePub). URL: <https://publications.jrc.ec.europa.eu/repository/handle/JRC101040>.
- [Deb+18] S. Deb, Tammi, K., K. Kalita, and P. Mahanta. *Review of recent trends in charging infrastructure planning for electric vehicles*. WIREs Energy Environ, 2018. URL: <http://doi.wiley.com/10.1002/wene.306>.
- [Dep22] S. R. Department. “Transportation emissions worldwide - statistics & facts”. In: (2022). URL: <https://www.statista.com/topics/7476/transportation-emissions-worldwide/#dossierKeyfigures>.
- [Deu22] S. B. Deutschland. “Pkw-Dichte im Jahr 2021 auf Rekordhoch, Pressemitteilung Nr. N 058 vom 15. September 2022”. In: 2022. URL: <https://www.sciencedirect.com/science/article/pii/S0191261516304349>.
- [Don+19] G. Dong, J. Ma, R. Wei, and J. Haycox. “Electric vehicle charging point placement optimisation by exploiting spatial statistics and maximal coverage location models”. In: *Transportation Research Part D: Transport and Environment* 67 (2019), pp. 77–88. ISSN: 1361-9209. DOI: <https://doi.org/10.1016/j.trd.2018.11.005>. URL: <https://www.sciencedirect.com/science/article/pii/S1361920918303729>.
- [FK13] T. Franke and J. F. Krems. “Interacting with limited mobility resources: Psychological range levels in electric vehicle use”. In: *Transportation Research Part A: Policy and Practice* 48 (2013). Psychology of Sustainable Travel Behavior, pp. 109–122. ISSN: 0965-8564. DOI: <https://doi.org/10.1016/j.tra.2012.10.010>. URL: <https://www.sciencedirect.com/science/article/pii/S0965856412001498>.
- [G+16] P. G, G. F, M. AM, R. P. L. A, and F. G. *Distribution System Operators Observatory 2016*. LD-NA-27927-EN-C (print),LD-NA-27927-EN-N (online). Luxembourg (Luxembourg), 2016. URL: <https://publications.jrc.ec.europa.eu/repository/handle/JRC101680>.
- [Hak64] S. L. Hakimi. “Optimum Locations of Switching Centers and the Absolute Centers and Medians of a Graph”. In: *Operations Research* 12.3 (1964), pp. 450–459. ISSN: 0030364X, 15265463. URL: <http://www.jstor.org/stable/168125> (visited on 01/08/2023).

## Bibliography

---

- [HWW11] W. E. Hart, J.-P. Watson, and D. L. Woodruff. “Pyomo: modeling and solving mathematical programs in Python”. In: *Mathematical Programming Computation* 3.3 (2011), pp. 219–260.
- [Har+17] W. E. Hart, C. D. Laird, J.-P. Watson, D. L. Woodruff, G. A. Hackebeil, B. L. Nicholson, and J. D. Siirola. *Pyomo - optimization modeling in Python*. May 2017. URL: <https://link.springer.com/book/10.1007/978-3-319-58821-6>.
- [HR92] M. J. Hodgson and K. E. Rosing. “A network location-allocation model trading off flow capturing and p-median objectives”. In: *Annals of Operations Research* 40.1 (Dec. 1992), pp. 247–260.
- [Hod90] M. J. Hodgson. “A Flow-Capturing Location-Allocation Model”. In: *Geographical Analysis* 22.3 (1990), pp. 270–279. DOI: <https://doi.org/10.1111/j.1538-4632.1990.tb00210.x>. eprint: <https://onlinelibrary.wiley.com/doi/pdf/10.1111/j.1538-4632.1990.tb00210.x>. URL: <https://onlinelibrary.wiley.com/doi/abs/10.1111/j.1538-4632.1990.tb00210.x>.
- [HUG17] B. HUGHES. *Straight-Line Distance as an Estimate for Driving Routes*. 2017. URL: <https://blog.cdxtech.com/post/straight-line-distance-as-an-estimate-for-driving-routes>.
- [Hus+21] D. Husarek, V. Salapic, S. Paulus, M. Metzger, and S. Niessen. “Modeling the Impact of Electric Vehicle Charging Infrastructure on Regional Energy Systems: Fields of Action for an Improved e-Mobility Integration”. In: *Energies* 14 (Nov. 2021). DOI: [10.3390/en14237992](https://doi.org/10.3390/en14237992).
- [Kab+20] M. Kabli, M. A. Quddus, S. G. Nurre, M. Marufuzzaman, and J. M. Usher. “A stochastic programming approach for electric vehicle charging station expansion plans”. In: *International Journal of Production Economics* 220 (2020), p. 107461. ISSN: 0925-5273. DOI: <https://doi.org/10.1016/j.ijpe.2019.07.034>. URL: <https://www.sciencedirect.com/science/article/pii/S0925527319302713>.
- [KH79] O. Kariv and S. L. Hakimi. “An Algorithmic Approach to Network Location Problems. I: The p-Centers”. In: *SIAM Journal on Applied Mathematics* 37.3 (1979), pp. 513–538. ISSN: 00361399. URL: <http://www.jstor.org/stable/2100910> (visited on 01/08/2023).
- [Knu+20] B. Knueven, D. Mildebrath, C. Muir, J. D. Siirola, J.-P. Watson, and D. L. Woodruff. *A Parallel Hub-and-Spoke System for Large-Scale Scenario-Based Optimization Under Uncertainty*. 2020.

- 
- [Kob+22] S. Kober, M. Schiffer, S. Sorgatz, and S. Weltge. *Driver-aware charging infrastructure design*. 2022. DOI: [10.48550/ARXIV.2212.05084](https://doi.org/10.48550/ARXIV.2212.05084). URL: <https://arxiv.org/abs/2212.05084>.
- [KL05] M. Kuby and S. Lim. “The flow-refueling location problem for alternative-fuel vehicles”. In: *Socio-Economic Planning Sciences* 39.2 (2005), pp. 125–145. ISSN: 0038-0121. DOI: <https://doi.org/10.1016/j.seps.2004.03.001>. URL: <https://www.sciencedirect.com/science/article/pii/S0038012104000175>.
- [LNS19] G. Laporte, S. Nickel, and F. Saldanha da Gama, eds. *Location Science*. 2nd ed. Springer Nature, 2019. URL: <https://link.springer.com/book/10.1007/978-3-030-32177-2>.
- [Luo+18] L. Luo, W. Gu, S. Zhou, H. Huang, S. Gao, J. Han, Z. Wu, and X. Dou. “Optimal planning of electric vehicle charging stations comprising multi-types of charging facilities”. In: *Applied Energy* 226 (2018), pp. 1087–1099. ISSN: 0306-2619. DOI: <https://doi.org/10.1016/j.apenergy.2018.06.014>. URL: <https://www.sciencedirect.com/science/article/pii/S0306261918308663>.
- [MN13] W. S. G. M. and D. Neumann. “Optimal location of charging stations in smart cities: A points of interest based approach.” In: (2013). URL: <http://aisel.aisnet.org/icis2013/proceedings/BreakthroughIdeas/12/>.
- [Met+22] M. Metais, O. Jouini, Y. Perez, J. Berrada, and E. Suomalainen. “Too much or not enough? Planning electric vehicle charging infrastructure: A review of modeling options”. In: *Renewable and Sustainable Energy Reviews* 153 (2022), p. 111719. ISSN: 1364-0321. DOI: <https://doi.org/10.1016/j.rser.2021.111719>. URL: <https://www.sciencedirect.com/science/article/pii/S136403212100993X>.
- [Mor+22] B. J. Mortimer, C. Hecht, R. Goldbeck, D. U. Sauer, and R. W. De Doncker. “Electric Vehicle Public Charging Infrastructure Planning Using Real-World Charging Data”. In: *World Electric Vehicle Journal* 13.6 (2022). ISSN: 2032-6653. DOI: [10.3390/wevj13060094](https://doi.org/10.3390/wevj13060094). URL: <https://www.mdpi.com/2032-6653/13/6/94>.
- [MMA17] M. R. Mozafar, M. H. Moradi, and M. H. Amini. “A simultaneous approach for optimal allocation of renewable energy sources and electric vehicle charging stations in smart grids based on improved GA-PSO algorithm”. In: *Sustainable Cities and Society* 32 (2017), pp. 627–637. ISSN: 2210-6707. DOI: <https://doi.org/10.1016/j.scs.2017.05.007>. URL: <https://www.sciencedirect.com/science/article/pii/S2210670716306035>.

## Bibliography

---

- [Pow+22] S. Powell, G. V. Cezar, L. Min, I. M. L. Azevedo, and R. Rajagopal. “Charging infrastructure access and operation to reduce the grid impacts of deep electric vehicle adoption”. In: *Nature Energy* 7.10 (Oct. 2022), pp. 932–945. ISSN: 2058-7546. DOI: [10.1038/s41560-022-01105-7](https://doi.org/10.1038/s41560-022-01105-7). URL: <https://doi.org/10.1038/s41560-022-01105-7>.
- [QOB18] J. Quiros-Tortos, L. Ochoa, and T. Butler. “How Electric Vehicles and the Grid Work Together: Lessons Learned from One of the Largest Electric Vehicle Trials in the World”. In: *IEEE Power and Energy Magazine* 16.6 (2018), pp. 64–76. DOI: [10.1109/MPE.2018.2863060](https://doi.org/10.1109/MPE.2018.2863060).
- [Rub18] P. A. Rubin. “Choosing "Big M" Values”. In: (Sept. 2018). DOI: [10.1109/CJECE.2014.2377653](https://doi.org/10.1109/CJECE.2014.2377653). URL: <https://orinanobworld.blogspot.com/2018/09/choosing-big-m-values.html>.
- [Sha+15] N. Shahraki, H. Cai, M. Turkay, and M. Xu. “Optimal locations of electric public charging stations using real world vehicle travel patterns”. In: *Transportation Research Part D: Transport and Environment* 41 (2015), pp. 165–176. ISSN: 1361-9209. DOI: <https://doi.org/10.1016/j.trd.2015.09.011>. URL: <https://www.sciencedirect.com/science/article/pii/S1361920915001352>.
- [SDR09] A. Shapiro, D. Dentcheva, and A. Ruszczyski. *Lectures on stochastic programming. Modeling and theory*. Jan. 2009. DOI: [10.1137/1.9780898718751](https://doi.org/10.1137/1.9780898718751).
- [Sha03] A. Shapiro. “Monte Carlo Sampling Methods”. In: *Stochastic Programming*. Vol. 10. Handbooks in Operations Research and Management Science. Elsevier, 2003, pp. 353–425. DOI: [https://doi.org/10.1016/S0927-0507\(03\)10006-0](https://doi.org/10.1016/S0927-0507(03)10006-0). URL: <https://www.sciencedirect.com/science/article/pii/S0927050703100060>.
- [SA13] H. D. Sherali and W. P. Adams. *A reformulation-linearization technique for solving discrete and continuous nonconvex problems*. Apr. 2013. URL: <https://link.springer.com/book/10.1007/978-1-4757-4388-3>.
- [Tru19a] E. S. Trust. *Minimising the costs of street works and grid connections for electric vehicle charging infrastructure*. Aug. 2019. URL: <https://energysavingtrust.org.uk/service/resources-for-local-authorities-on-electric-vehicle-chargepoints/>.
- [Tru19b] E. S. Trust. *Procuring electric vehicle charging infrastructure as a local authority*. Sept. 2019. URL: <https://energysavingtrust.org.uk/service/resources-for-local-authorities-on-electric-vehicle-chargepoints/>.

- 
- [UK10] C. Upchurch and M. Kuby. “Comparing the p-median and flow-refueling models for locating alternative-fuel stations”. In: *Journal of Transport Geography* 18.6 (2010). Special Section on Alternative Fuels and Vehicles, pp. 750–758. ISSN: 0966-6923. DOI: <https://doi.org/10.1016/j.jtrangeo.2010.06.015>. URL: <https://www.sciencedirect.com/science/article/pii/S0966692310000967>.
- [WL13] Y.-W. Wang and C.-C. Lin. “Locating multiple types of recharging stations for battery-powered electric vehicle transport”. In: *Transportation Research Part E: Logistics and Transportation Review* 58 (2013), pp. 76–87. ISSN: 1366-5545. DOI: <https://doi.org/10.1016/j.tre.2013.07.003>. URL: <https://www.sciencedirect.com/science/article/pii/S1366554513001403>.
- [War+13] R. A. Waraich, M. D. Galus, C. Dobler, M. Balmer, G. Andersson, and K. W. Axhausen. “Plug-in hybrid electric vehicles and smart grids: Investigations based on a microsimulation”. In: *Transportation Research Part C: Emerging Technologies* 28 (2013). Euro Transportation: selected paper from the EWGT Meeting, Padova, September 2009, pp. 74–86. ISSN: 0968-090X. DOI: <https://doi.org/10.1016/j.trc.2012.10.011>. URL: <https://www.sciencedirect.com/science/article/pii/S0968090X12001337>.
- [Wil13] H. P. Williams. *Model building in Mathematical Programming, 5th Edition*. Mar. 2013. URL: <https://www.wiley.com/en-us/Model+Building+in+Mathematical+Programming%5C%2C+5th+Edition-p-9781118443330>.
- [WS17] F. Wu and R. Sioshansi. “A stochastic flow-capturing model to optimize the location of fast-charging stations with uncertain electric vehicle flows”. In: *Transportation Research Part D: Transport and Environment* 53 (2017), pp. 354–376. ISSN: 1361-9209. DOI: <https://doi.org/10.1016/j.trd.2017.04.035>. URL: <https://www.sciencedirect.com/science/article/pii/S136192091630102X>.